

AEROSOL PROFILING AND ATMOSPHERIC BOUNDARY LAYER

Dr. Juan Luis Guerrero-Rascado
University of Granada

Andalusian Institute for Earth System Research (IISTA-CEAMA)



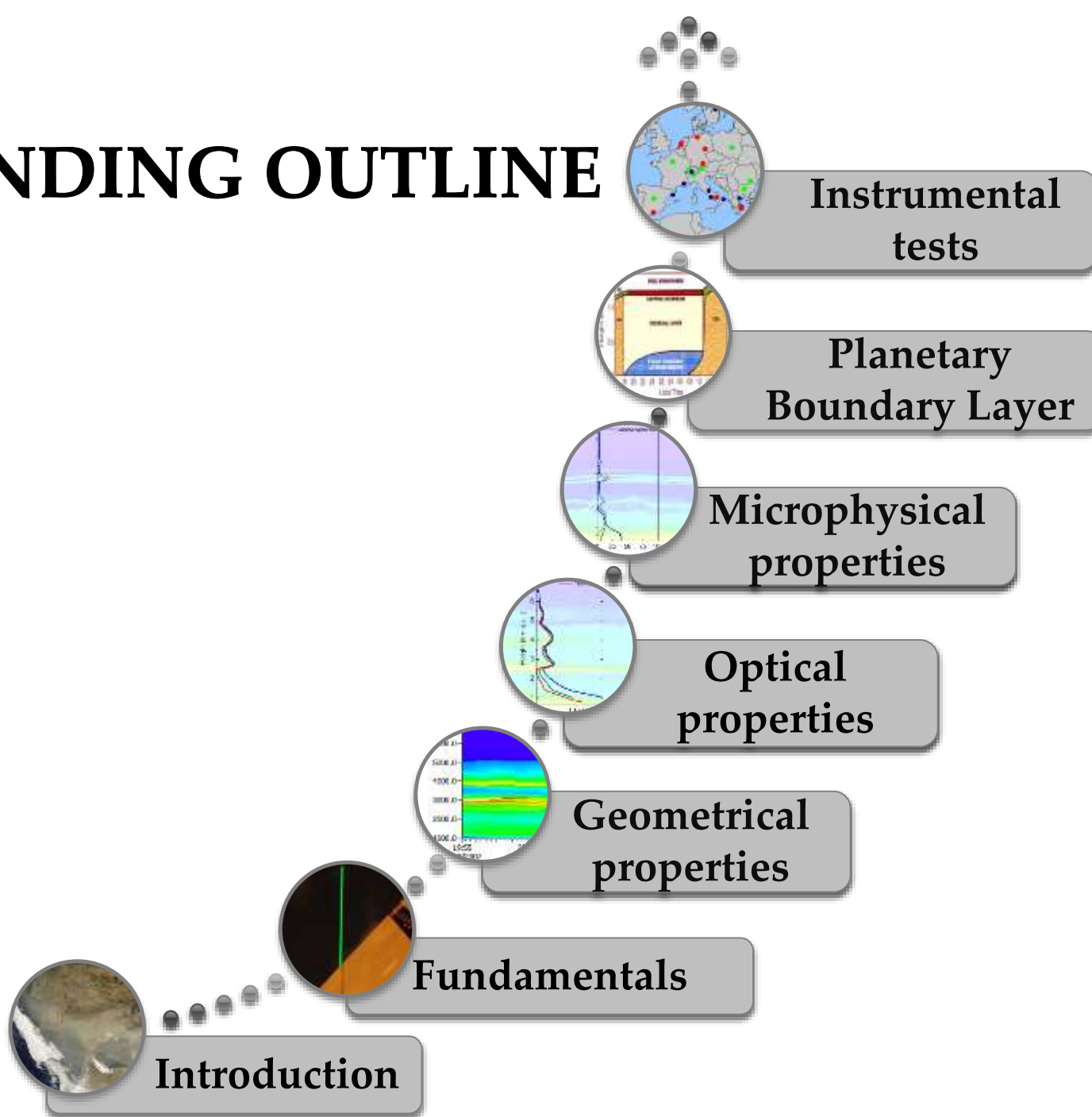
IISTA

Instituto Interuniversitario de Investigación
del Sistema Tierra en Andalucía

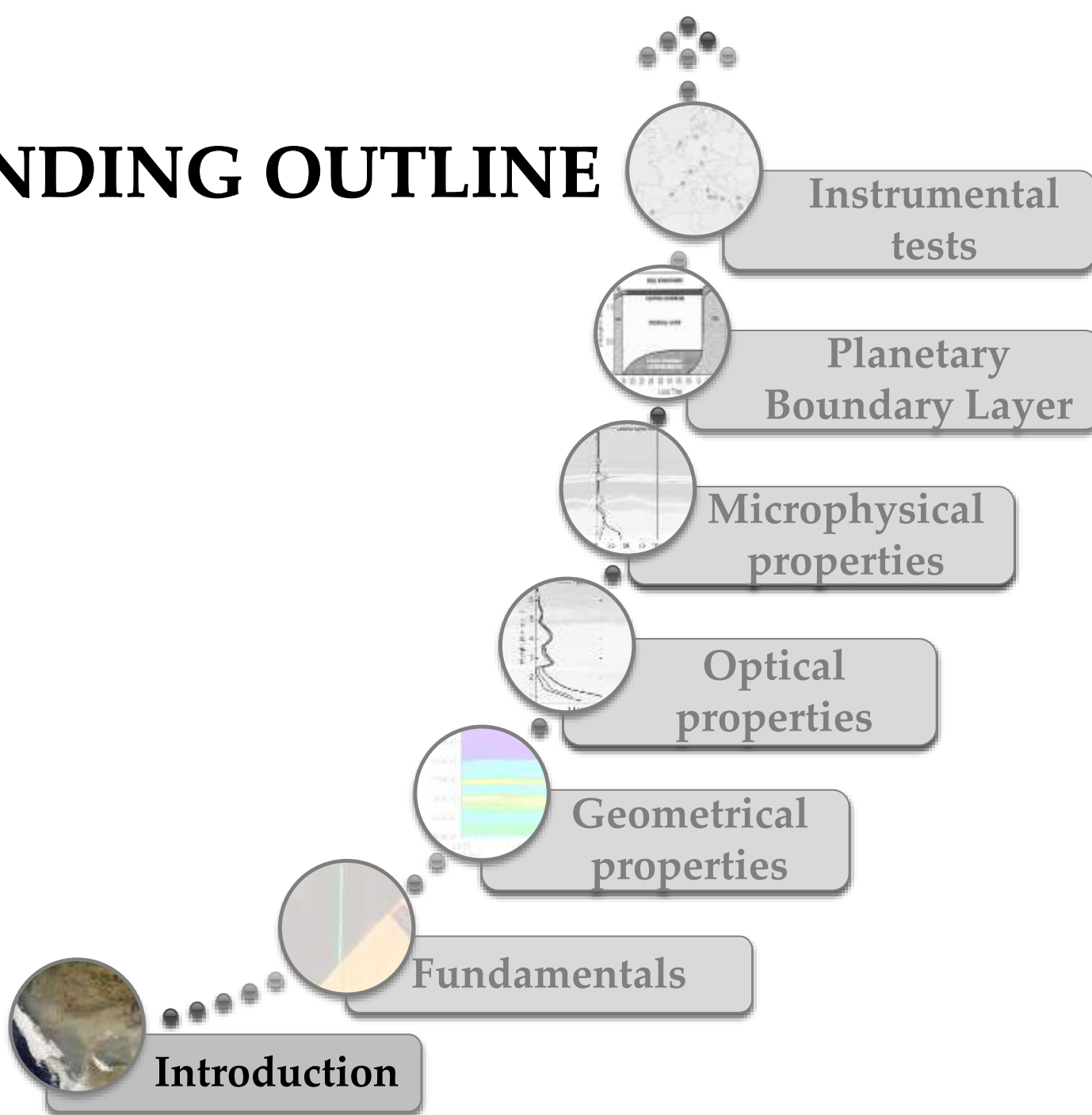


SHORT SUMMER SCHOOL ON
ATMOSPHERIC PHYSICS

ASCENDING OUTLINE



ASCENDING OUTLINE



INTRODUCTION

WHAT IS REMOTE SENSING?

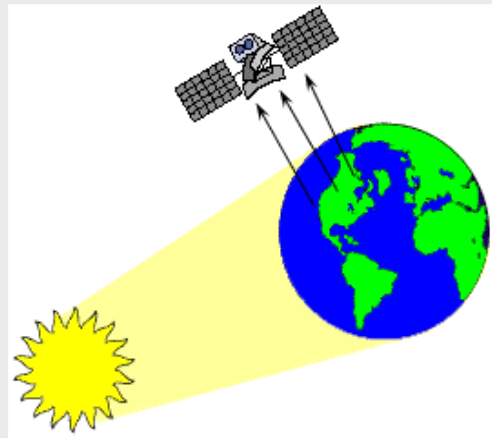


Process of obtaining information about properties of a target without contact.

This information is propagated by means of electromagnetic radiation interacting with the target.

INTRODUCTION

Passive remote sensing



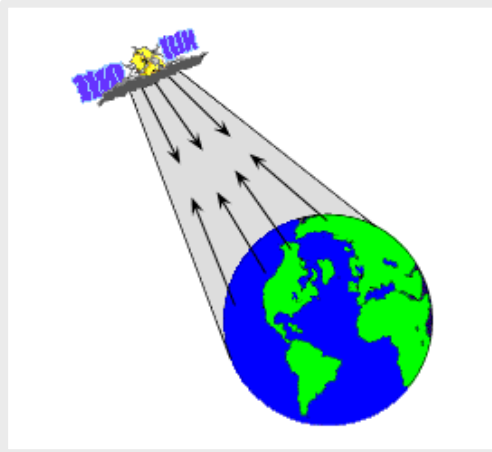
Based on “**uncontrolled illumination**”:

- Sun
- terrestrial emission

Passive methods:

- extinction
- scattering
- longwave emission

Active remote sensing



Based on “**controled illumination**” and measurement of backscattering

Active methods:

- lidar
- radar

Lidar (light detection and ranging) is an active remote sensing technology that measures distance by illuminating a target with a laser and analyzing the reflected light

INTRODUCTION

There are a wide variety of fields of applications for lidar:

- * Geology
- * Archaeology
- * Biology (vegetation)
- * Society
- * Astronomy
- * Energy
- * Conservation (Monuments)
- * Atmosphere



INTRODUCTION

Archaeology: aiding in the planning of field campaigns, mapping features beneath forest canopy, and providing an overview of broad, continuous features that may be indistinguishable on the ground, creating high-resolution digital elevation models (DEMs) of archaeological sites that can reveal micro-topography that are otherwise hidden by vegetation

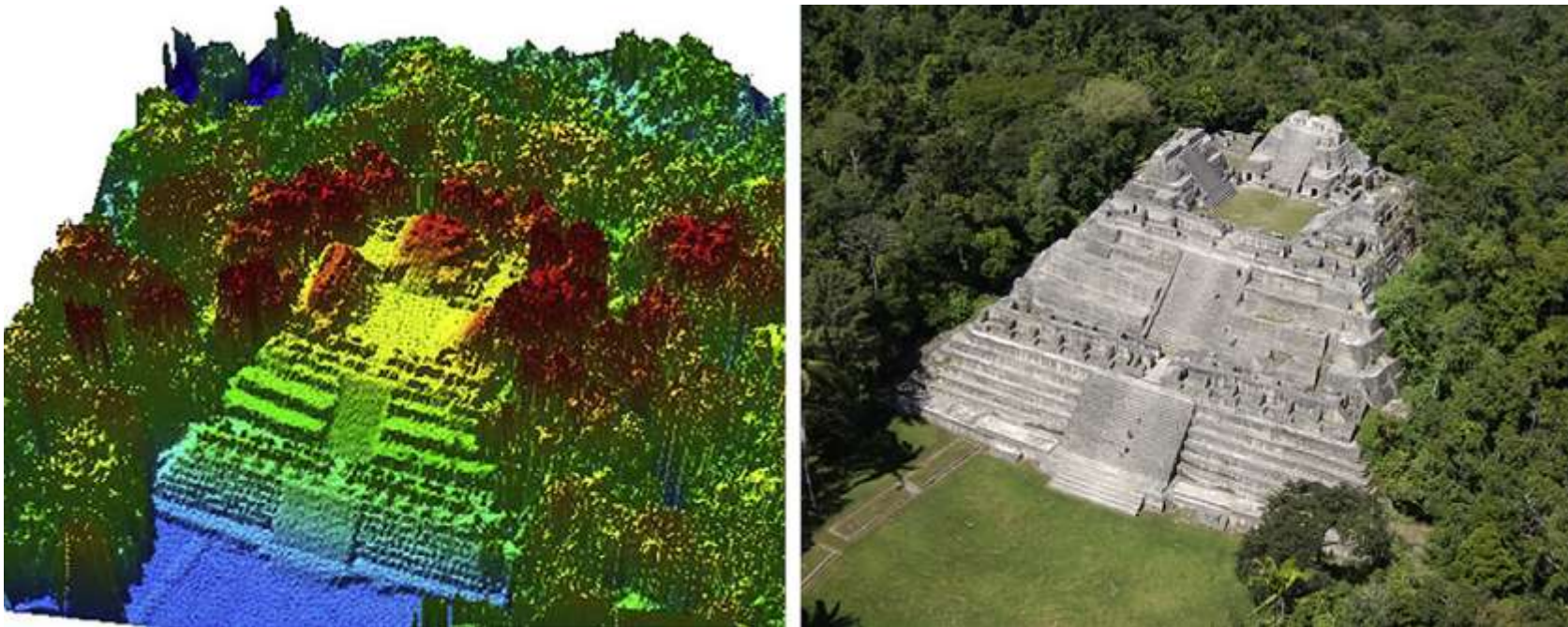


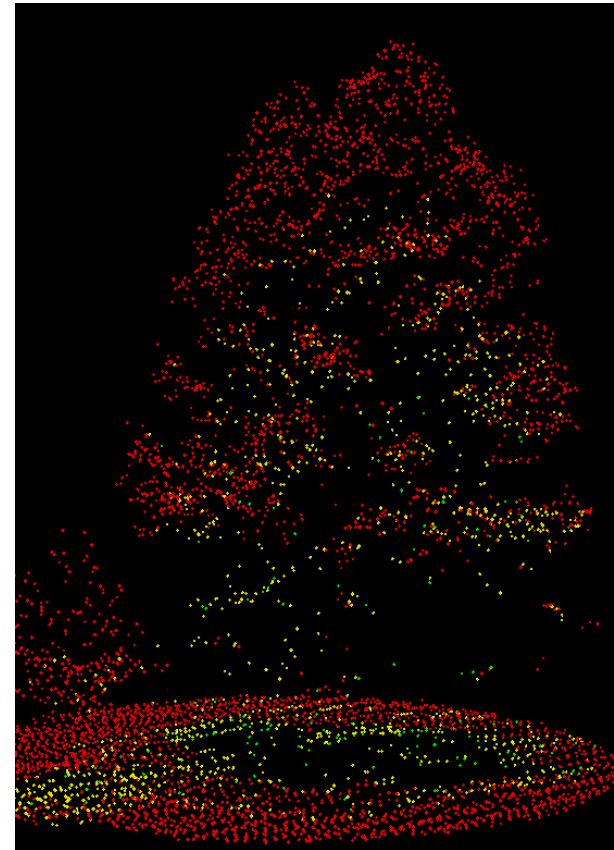
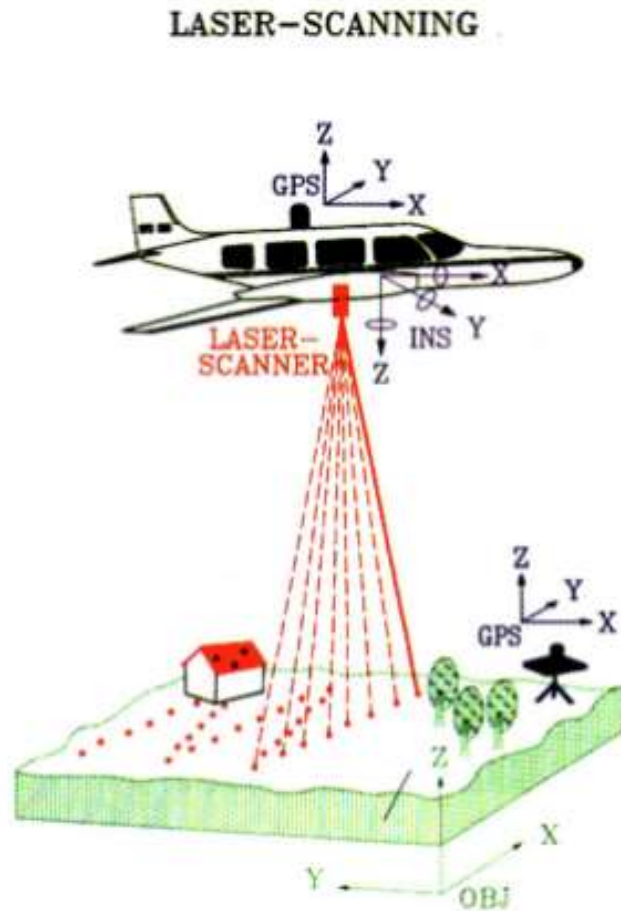
Image taken from: Chase et al., 2011, *Journal of Archeological Science*, 38, 387-398

Maya Site of Caracol (Belize)



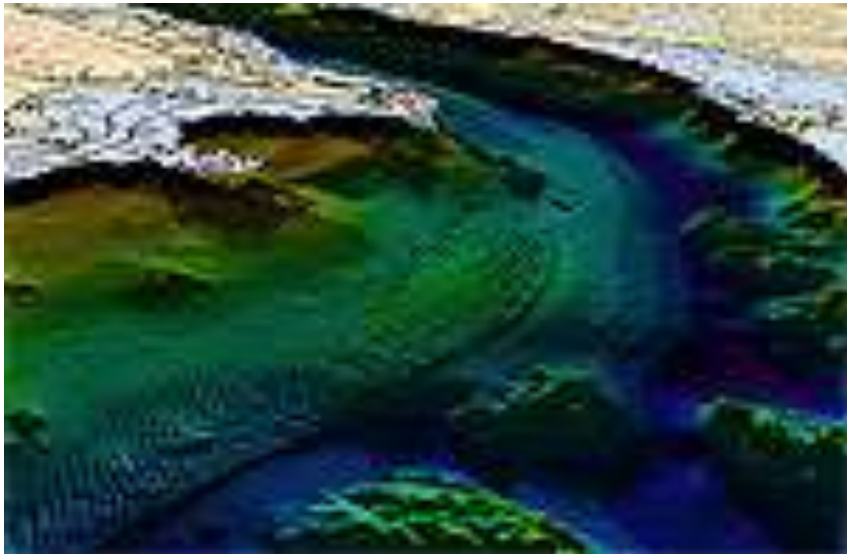
INTRODUCTION

Biology (vegetation): lidar has also found many applications in forestry. Canopy height and biomass measurements can be all be studied using airborne lidar systems. Tree height strongly correlated to other properties (as woody biomass, age, etc)



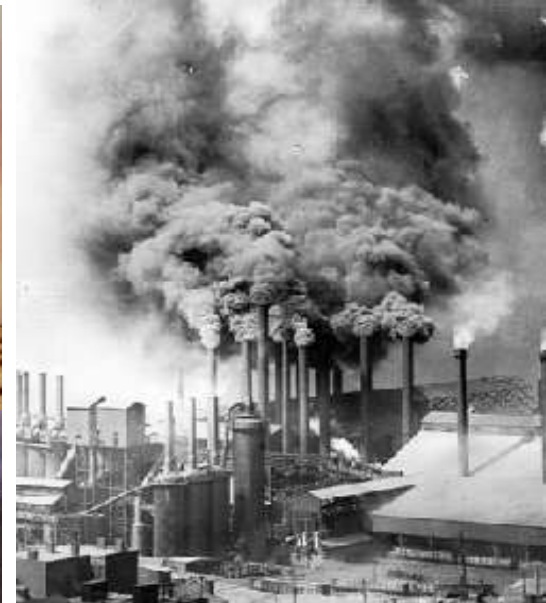
INTRODUCTION

Geology: In geophysics and tectonics, a combination of aircraft-based lidar and GPS has evolved into an important tool for detecting faults and for measuring uplift. The output of the two technologies can produce extremely accurate elevation models for terrain and enables surveys to be taken of the coastline. It is also used extensively to monitor glaciers and perform coastal change analysis



INTRODUCTION

- Aerosol particles: liquid or solid particles suspended in a gaseous medium (several types)
- Atmospheric aerosols play an important role in the Earth's climate system:
 1. they interact with solar and thermal radiation, modulating the Earth radiation budget
 2. they modify clouds microphysical properties by acting as cloud condensation nuclei and ice forming nuclei

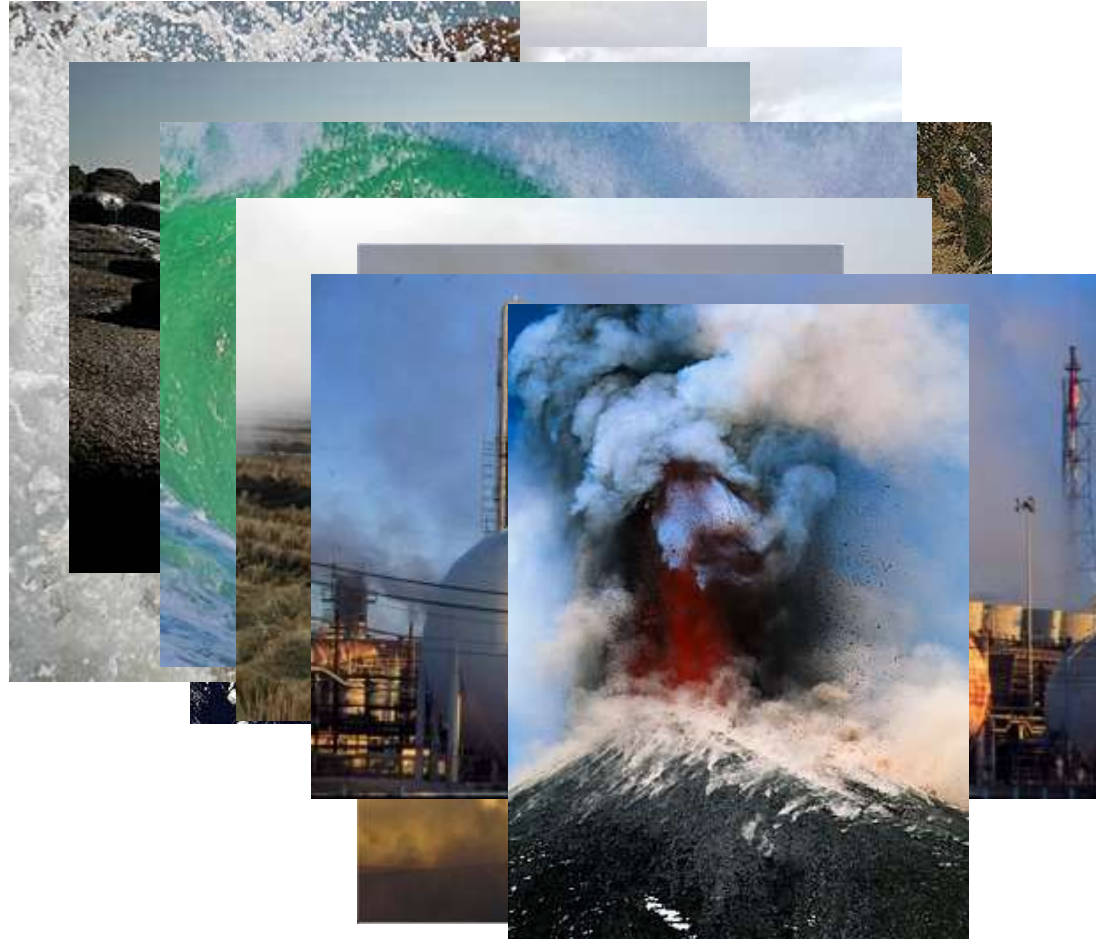


INTRODUCTION

- Aerosol particles: cooling/warming effect
depending on vertical distribution and types (among other factors)

- Classification:

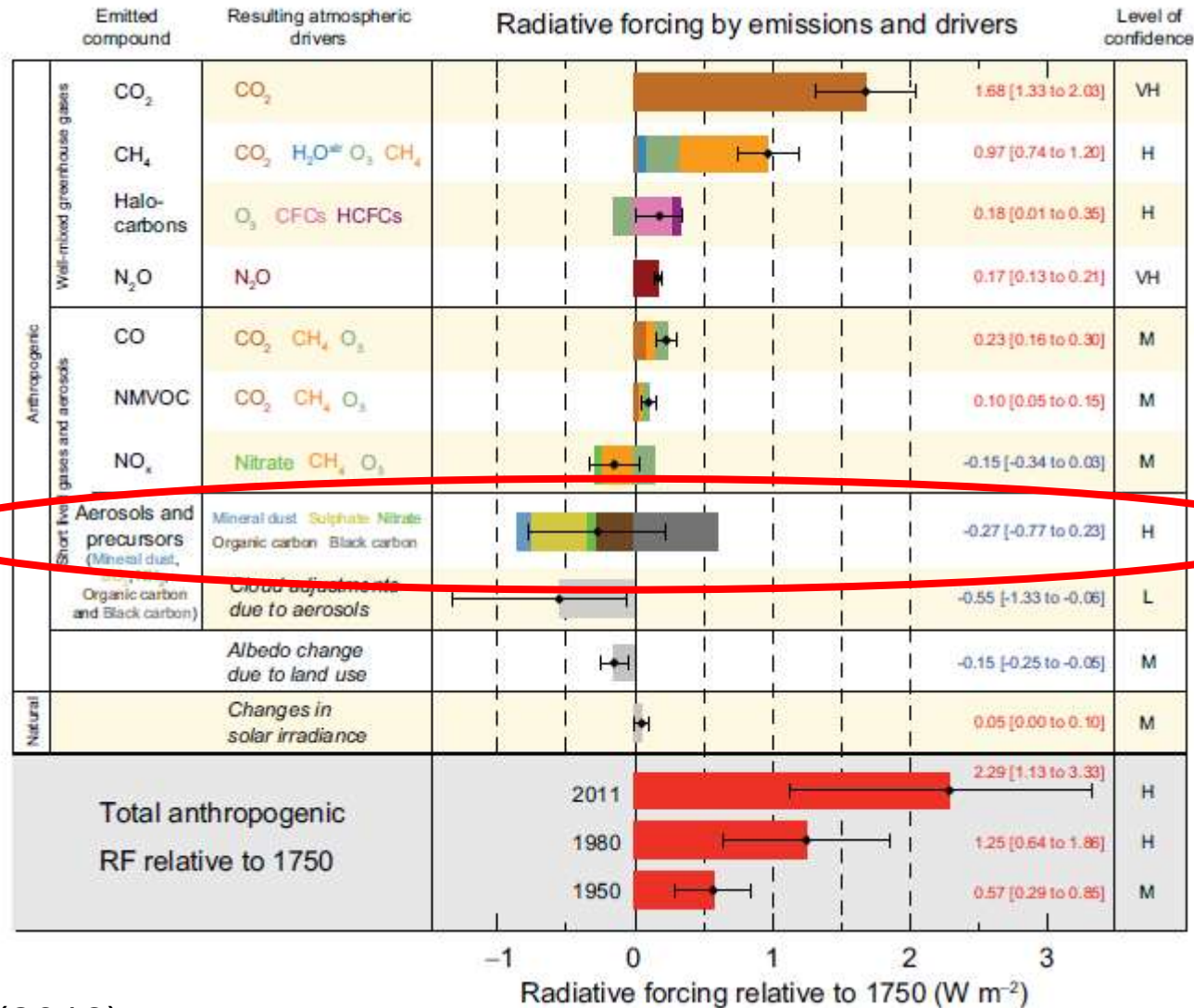
- ✓ Mineral particles
- ✓ Marine particles
- ✓ Carbon particles
- ✓ Sulfates, nitrates and organic compounds



Sulfates have both natural origin (volcanism) and anthropogenic origin (pollution) and are transported by wind as aerosols. Carbon particles are created by wind erosion of soil and biomass burning.

INTRODUCTION

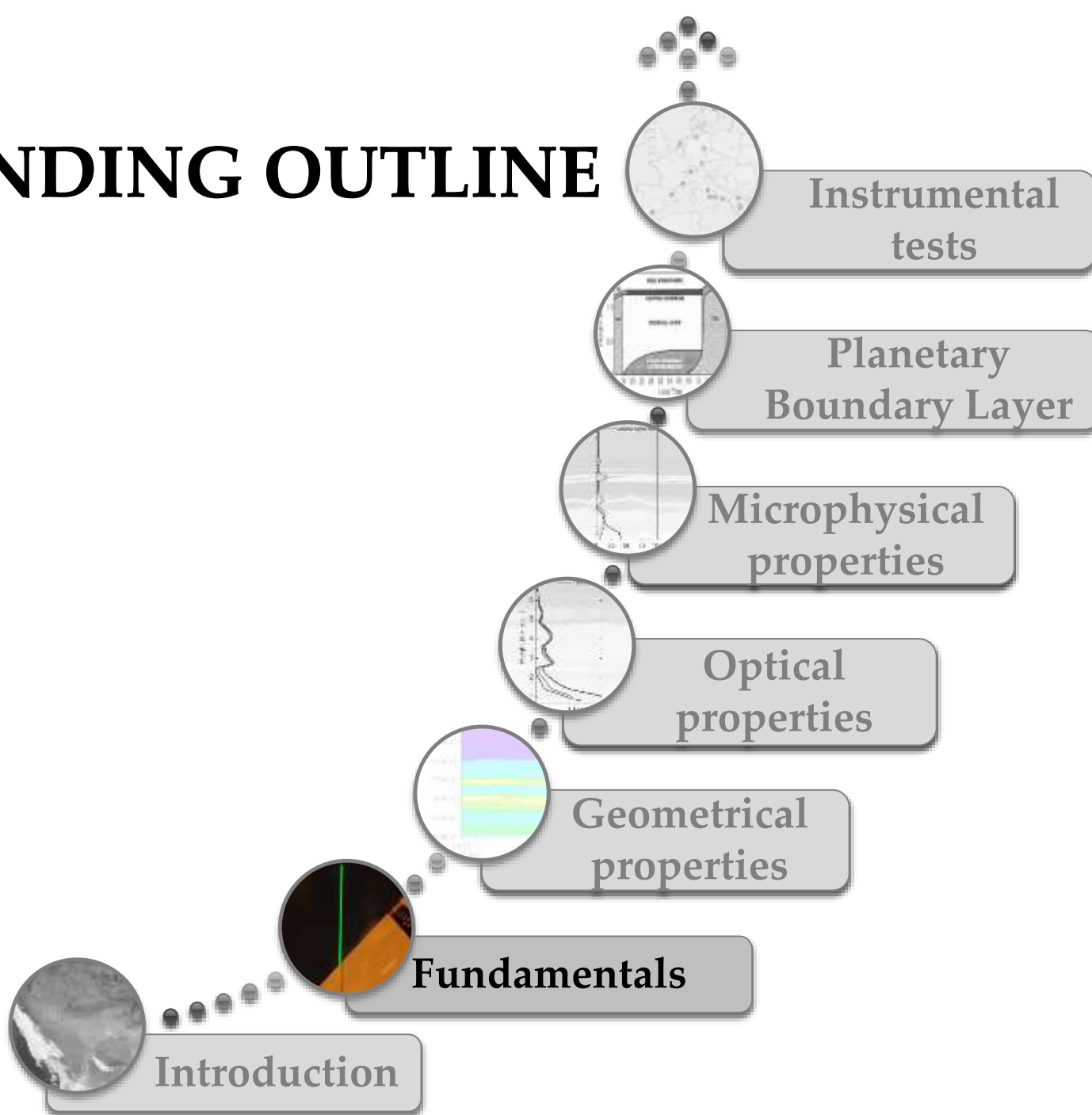
Radiative forcing by components



IPCC (2013)

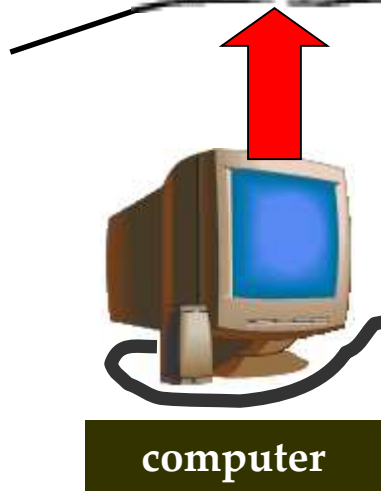
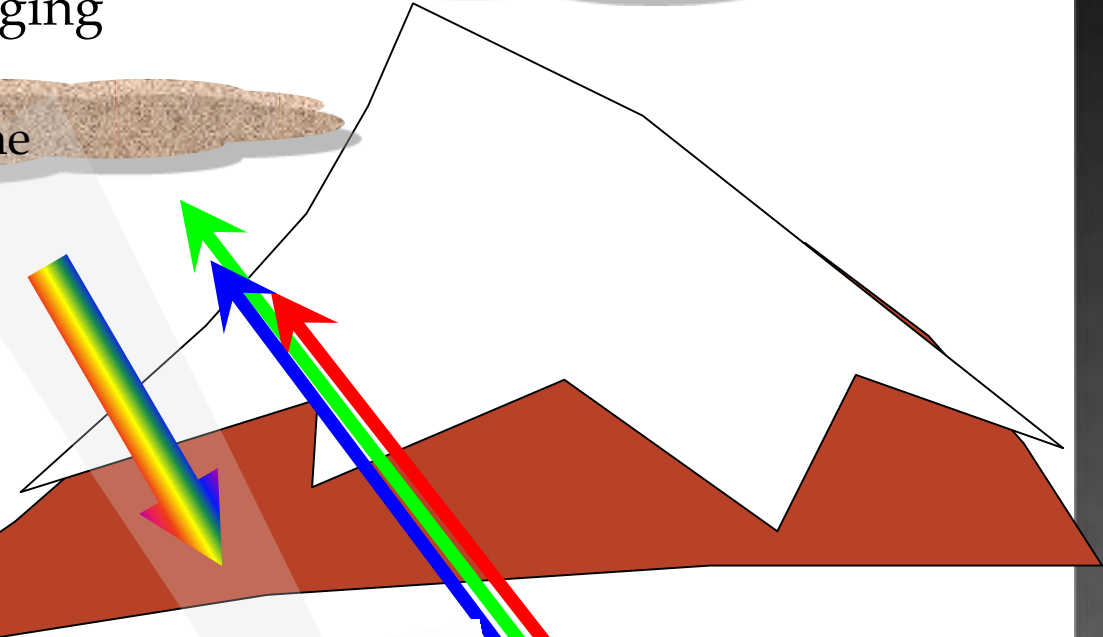
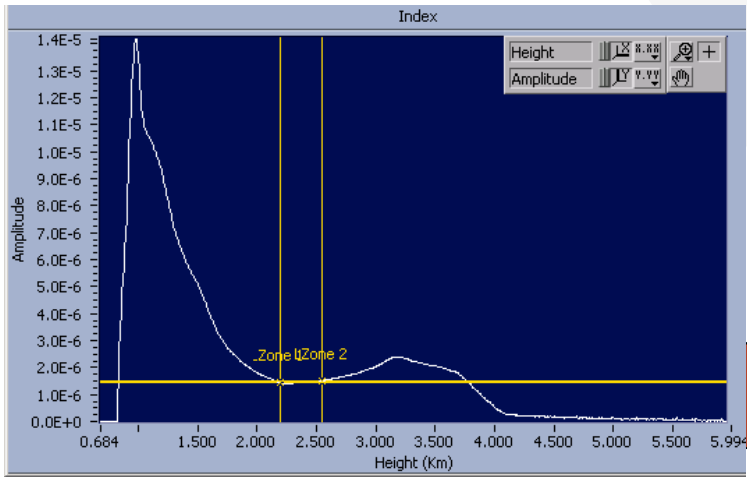


ASCENDING OUTLINE



LIDAR TECHNIQUE

Lidar: Light detection and ranging



transient recorder

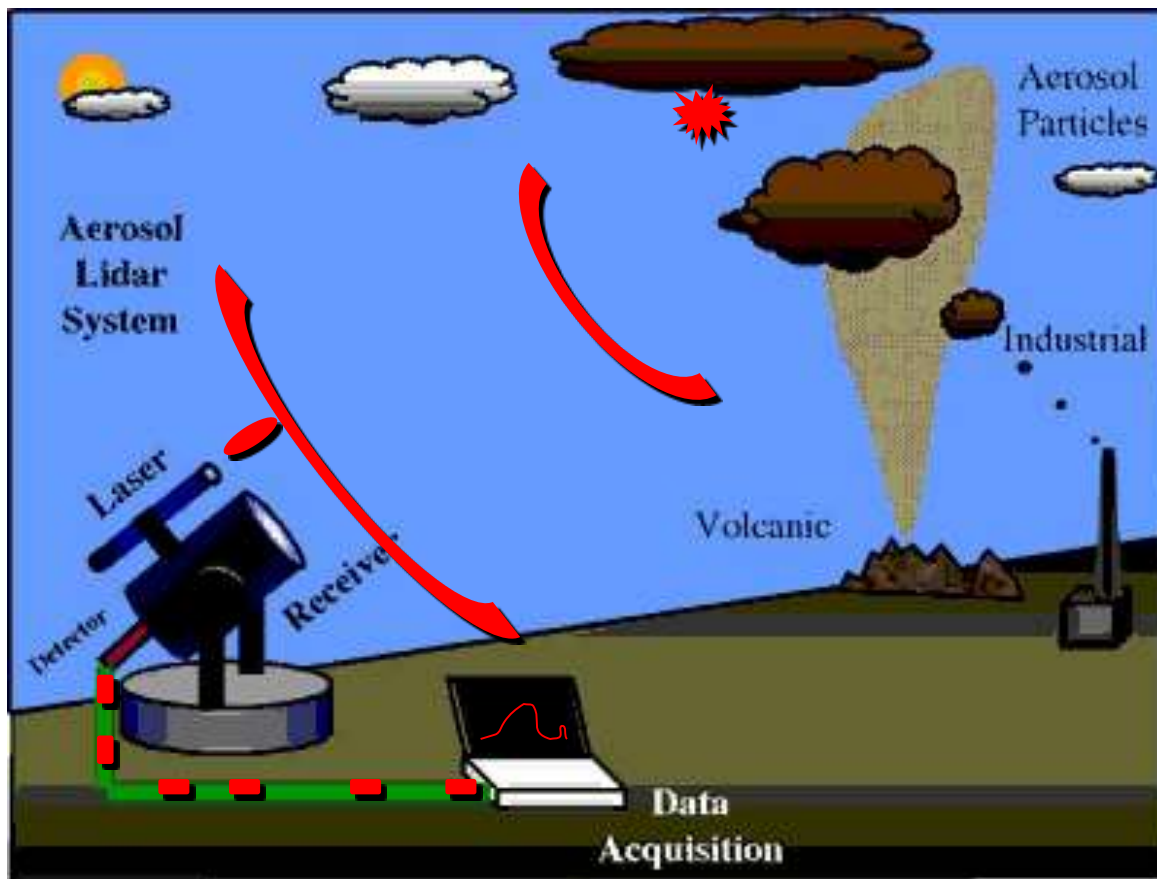
Licel

receiver

emitter

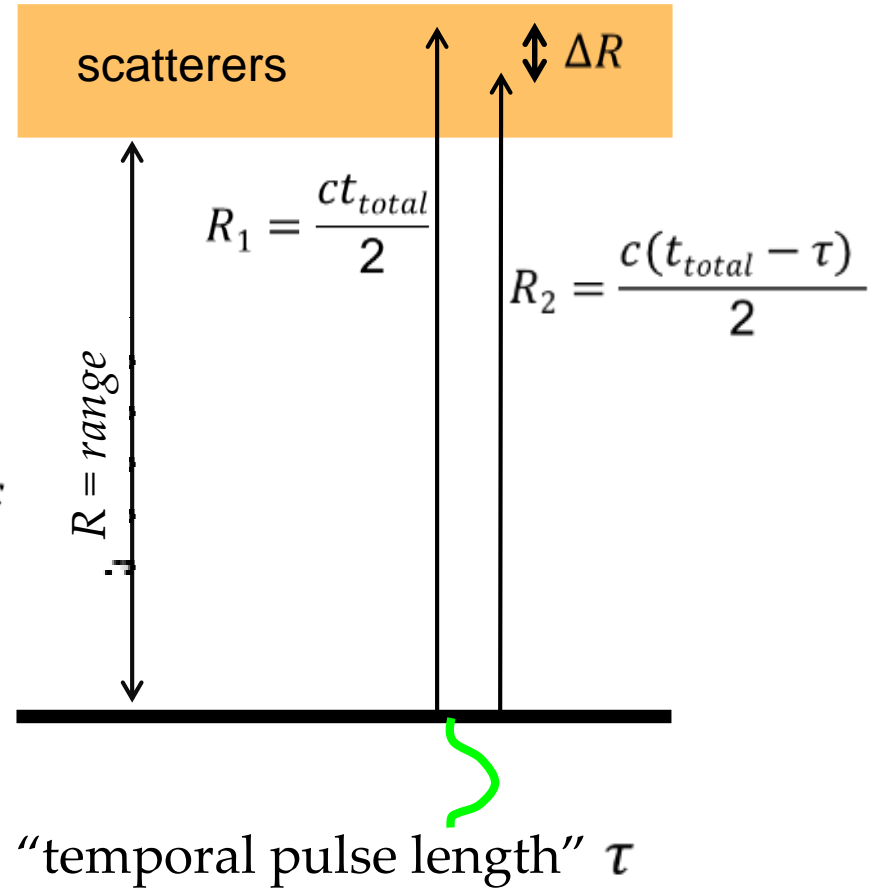
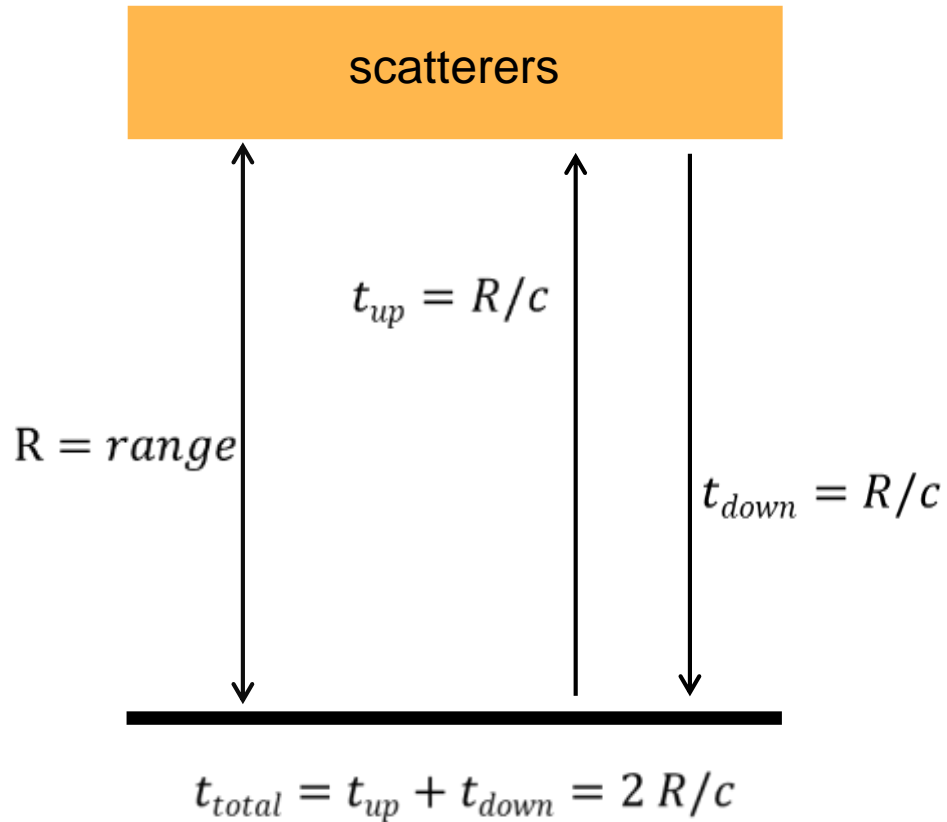


LIDAR TECHNIQUE



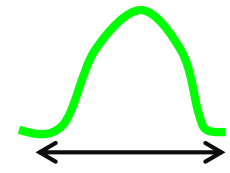
The key of this technique is the use of pulsed lasers, which allow for obtaining range-resolved information from the delay between emitted and received pulses

RANGING (BASED ON TIMING)



$$\Delta R = R_1 - R_2 = \frac{c\tau}{2}$$

“effective (spatial) pulse length”



RANGING (BASED ON TIMING)

$$\Delta R = R_1 - R_2 = \frac{c\tau}{2}$$

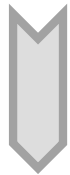
“effective (spatial) pulse length”

(**potential** spatial lidar resolution)

Spatial resolution example:

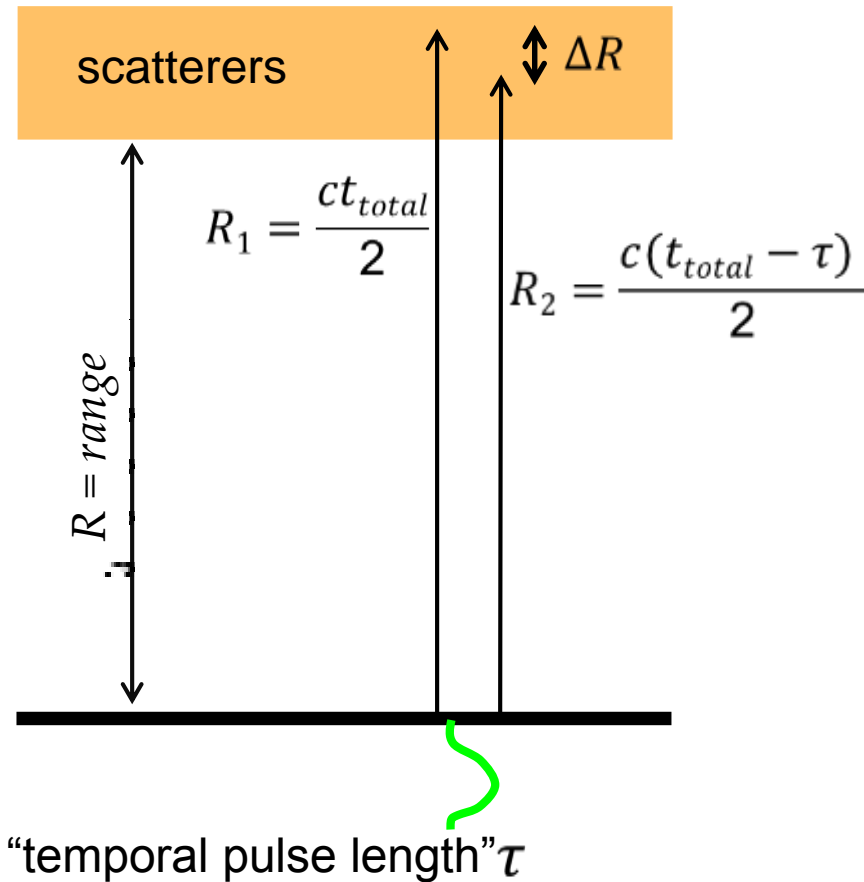
Nd:YAG Laser (1064 nm)

Q-switch pulsed: $\tau \sim 10$ ns

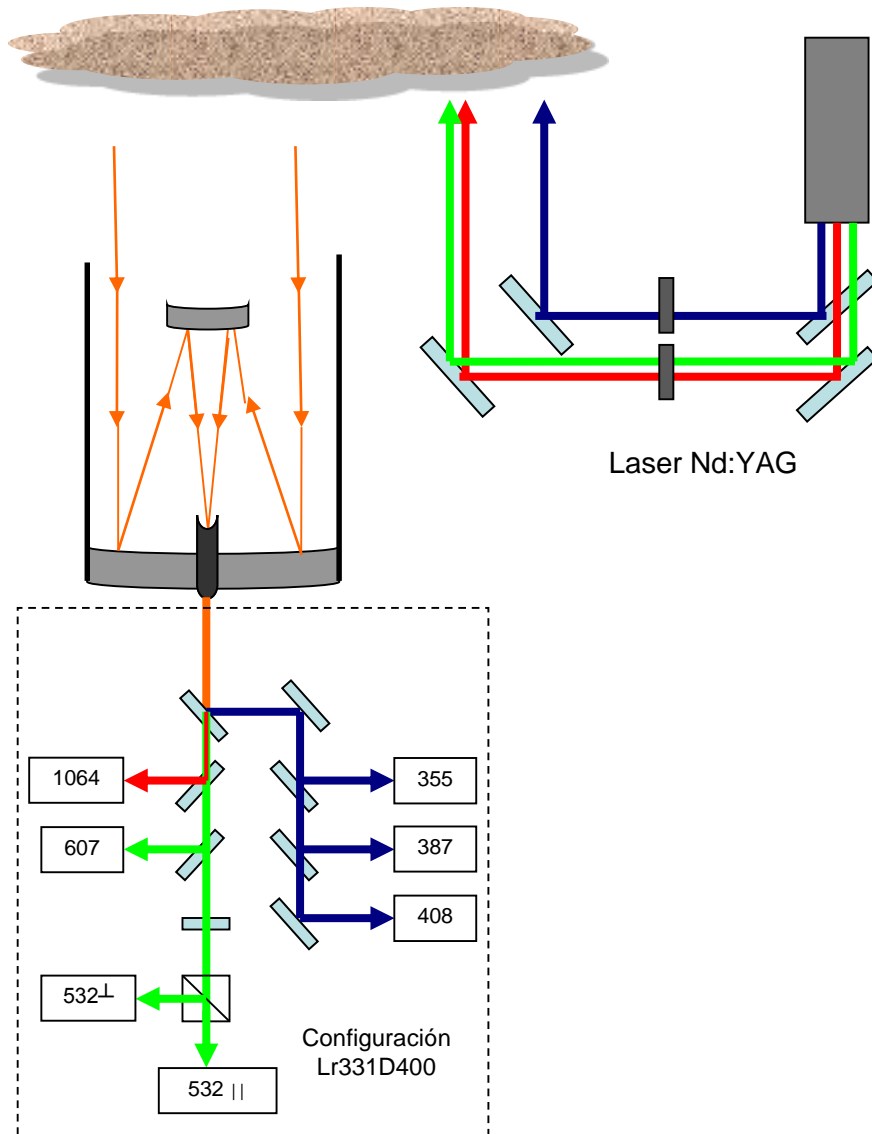


$$\Delta R \approx 1.5 \text{ m}$$

In practice there are additional limitations like the sampling frequency of the acquisition system or the finite bandwidth of the detector...



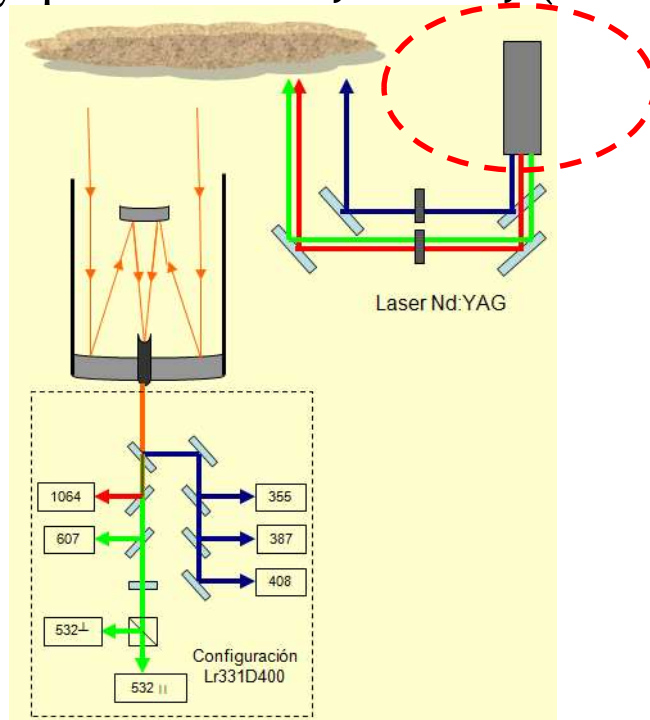
LIDAR SETUP



- Transmitter system
- Receiver system

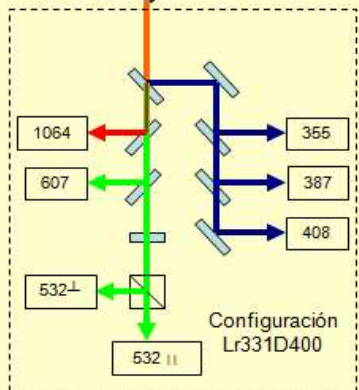
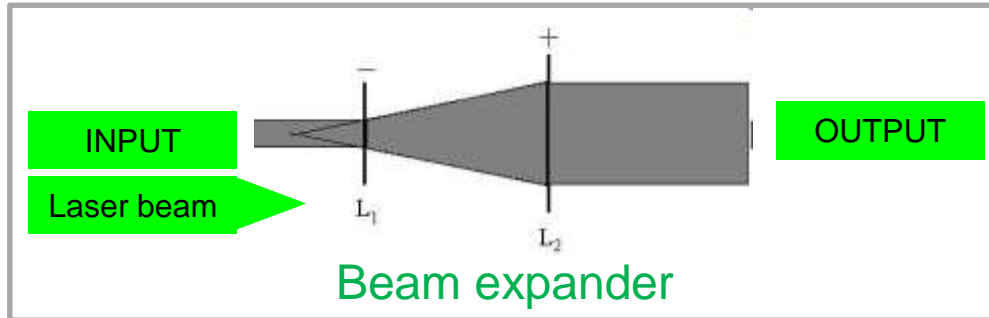
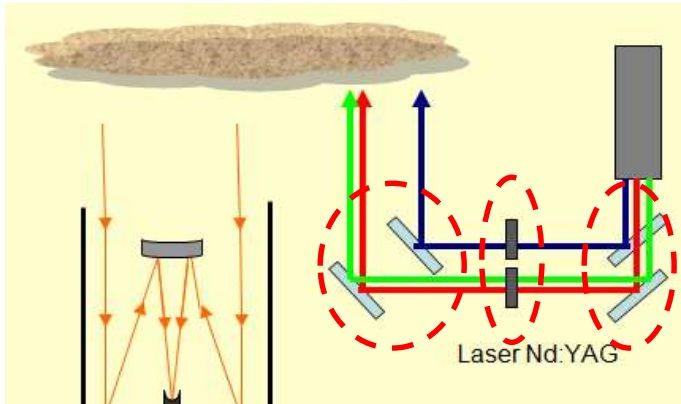
LIDAR SETUP: LASER SOURCE

- 1960's: nitrogen laser (337 nm) and ruby laser (694nm→347nm): relatively low average power, limited to 2 km
- 1980's: pulsed lasers with high average power as UV excimer laser (XeCl at 308nm and XeF at 351 nm) and Nd:YAG laser
- currently Nd:YAG (Neodymium-doped Yttrium Aluminum Garnet):
1064 nm → 532 nm → 355 nm
repetition frequency : 1-50 Hz
energy/pulse: 100 mJ to 1.5 J (at 1064 nm)

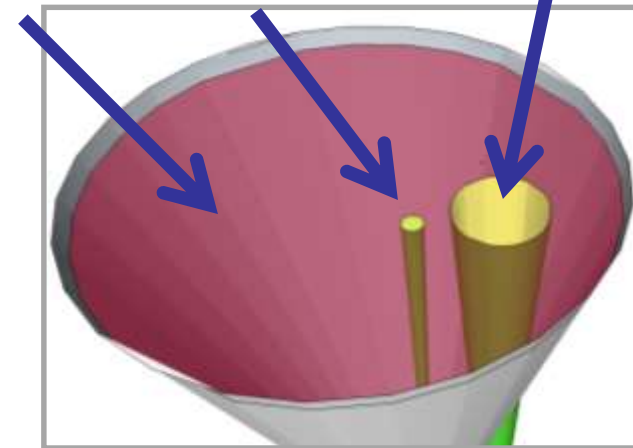


LIDAR SETUP: TRANSMITTER OPTICS

- Mirrors to transmit the laser beam (high reflectivity / high transmissivity)
- Beam expander made of lenses (anti-reflection coated) allows for:
 - a beam expansion by a factor $\sim x4 - x10$
 - reducing background light
 - increasing SNR
 - reducing divergence ($\sim 1\text{mrad}$)

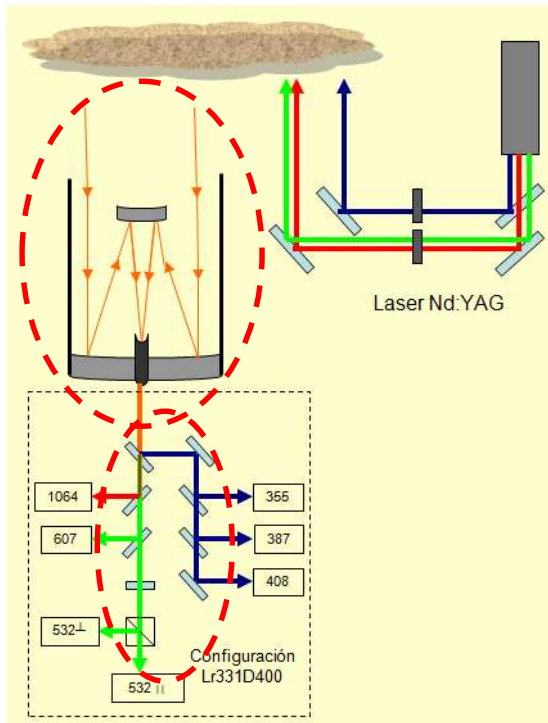


Background light Non-expanded beam Expanded beam

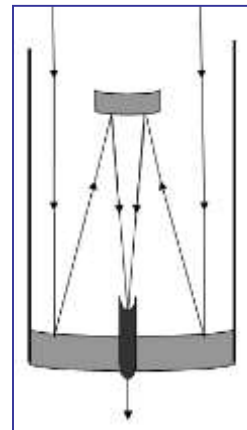


LIDAR SETUP: RECEIVER OPTICS

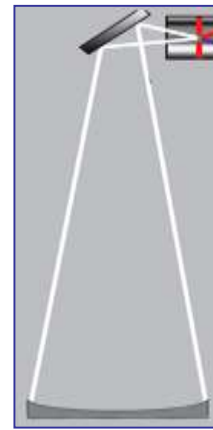
- φ_{primary} : 30 cm – 1 m and $\varphi_{\text{secondary}}$: ~ 1cm
- compromise between a small FOV necessary for high background suppression and a large FOV for a sufficient signal intensity from short distances (FOV a factor of ~2-10 larger than the laser divergence)
- receiver optics behind telescope must be optimized for high transmission of the Raman signals
- dichroic beam splitters: reflect light of a certain λ and transmit others
- interference filters: typically FWHM < 0.5 nm, suppression factor 10^8 - 10^{10}



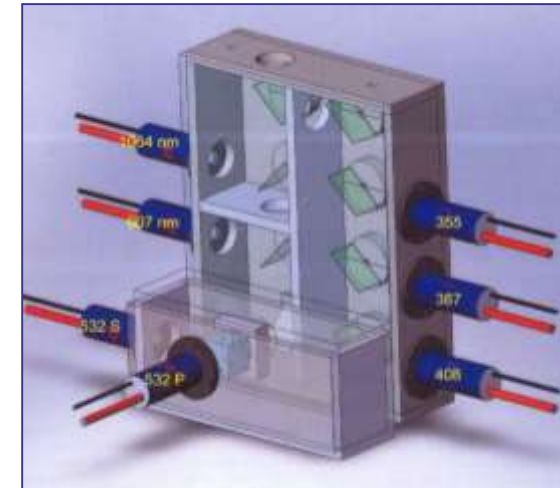
Telescopes



Cassegrainian



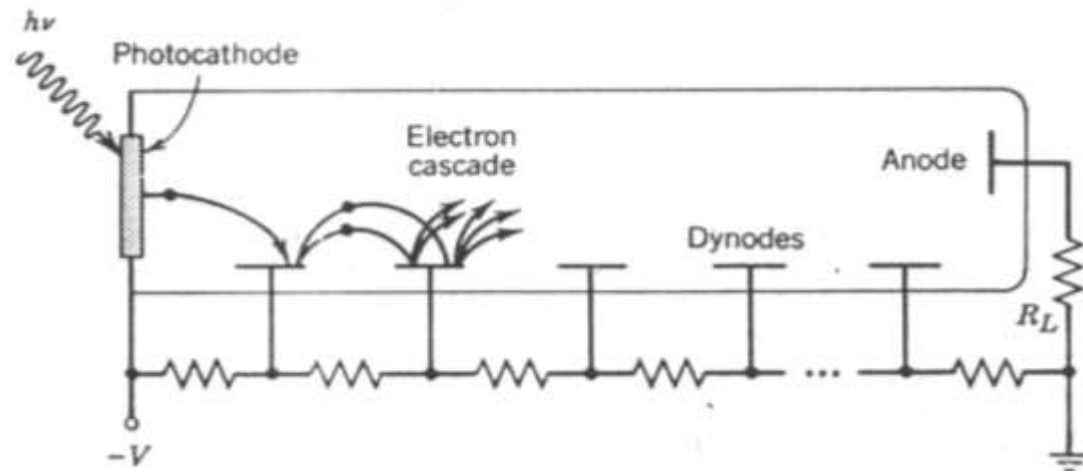
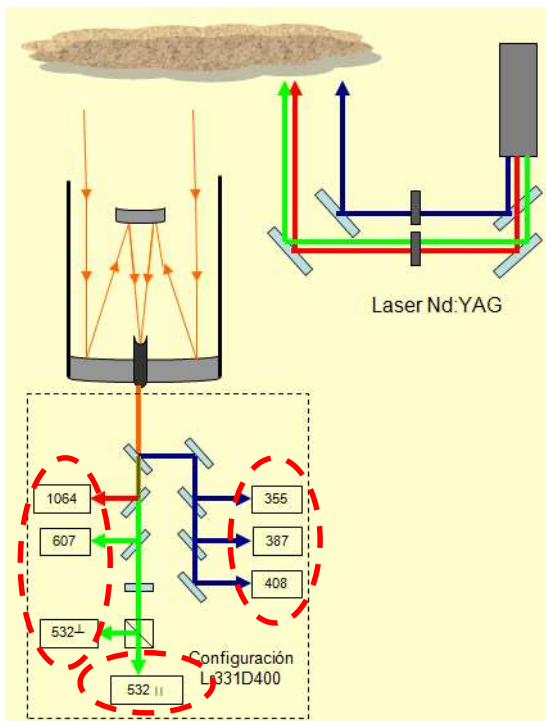
Newtonian





LIDAR SETUP: DETECTORS AND DATA ACQUISITION

- photomultipliers in An and PC mode are typically used (PMTs)
- high quantum efficiency (in UV ~ 25%) and low noise
- detector outputs can be preamplified before registration
- time resolution (or window length) is ~ 100 ns, (7.5 – 15 m)
- averaging time for the raw signals is 10- 60 s
- signals are usually further averaged in time and space during data evaluation



ELASTIC LIDAR FOR AEROSOLS

Generally consists of a non-tunable high-power pulsed laser and intensity of the received signal is measured

A narrow beam is transmitted into the atmosphere and backscattered by the atmosphere to a receiver telescope and detector

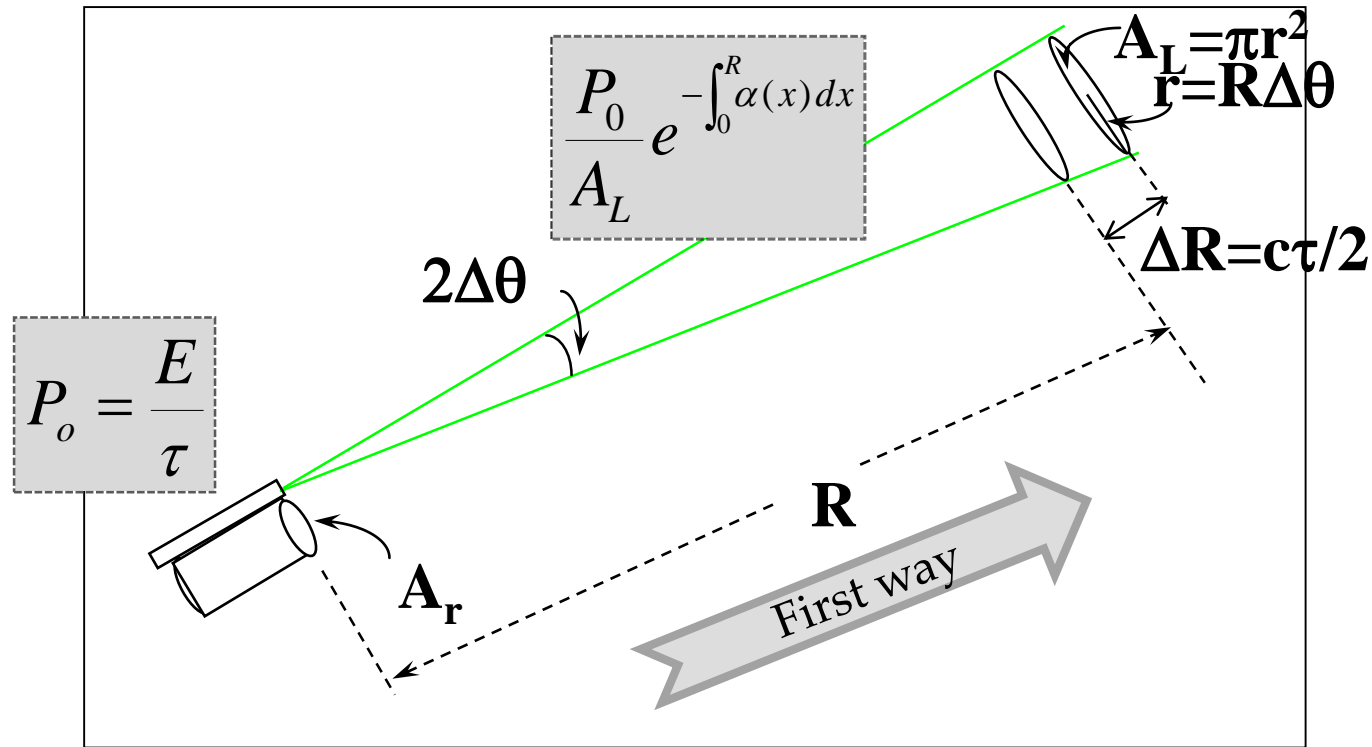
The nature of the backscattering is determined by the properties of the volume of the atmosphere that contains the Rayleigh (molecules) and Mie (particles) scatterers

The combination of the short laser pulse (~ 10 ns) and the small beam divergence ($\sim 10^{-3}$ to 10^{-4} radians) results in volumes of a few cubic meters at ranges of tens of km

The primary properties measured are the intensity and polarization of the signal, and these are used to retrieve particle properties



LIDAR EQUATION



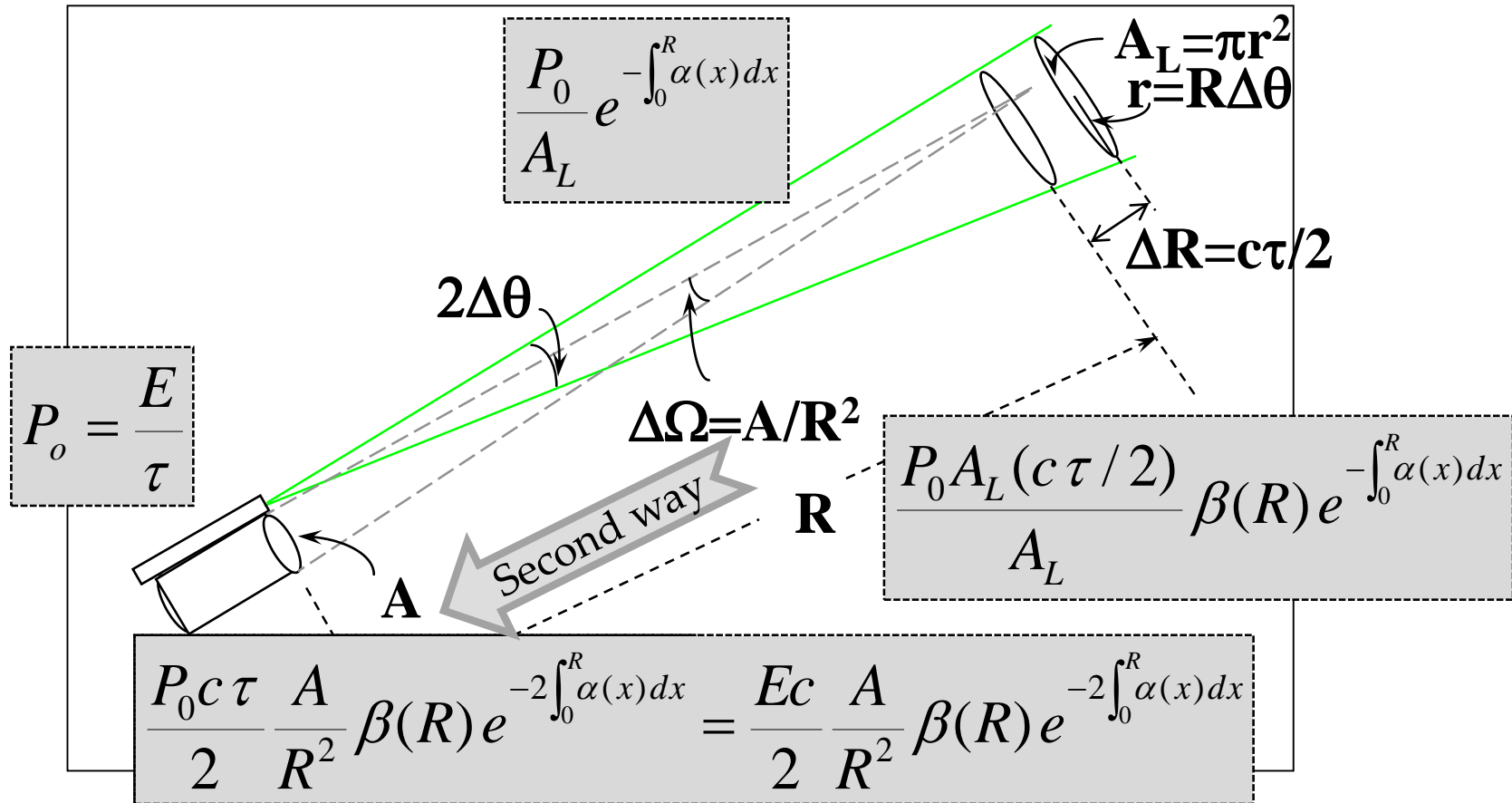
P_o average power of single laser pulse, τ temporal pulse length

$E_o = P_o \tau$ pulse energy

The propagation through distance R implies an attenuation $e^{-\int_0^R \alpha(x) dx}$

and $(P_o / A_L) e^{-\int_0^R \alpha(x) dx}$ represent the power per unit area that illuminates a volume of atmosphere at distance R

LIDAR EQUATION



The illuminated volume $c(\tau/2)A_L$ produces a backscattered signal proportional to the backscatter coefficient

This signal travels back to the detector suffering an additional attenuation and thus the signal collected by the detector system of surface A is:

$$\frac{P_0 c \tau}{2} \frac{A}{R^2} \beta(R) e^{-2\int_0^R \alpha(x) dx}$$

LIDAR EQUATION

$$P(R, \lambda) = P_o(\lambda) \frac{C}{R^2} \beta(R, \lambda) e^{-2 \int_0^R \alpha(x, \lambda) dx} = P_o(\lambda) \frac{C}{R^2} \beta(R, \lambda) T(R, \lambda)^2$$

$P(R, \lambda)$ = power received by the system after backscattering from range R

$P_o(\lambda)$ = power transmitted

C = lidar calibration constant

$\beta(R, \lambda)$ = backscatter coeff. ($\text{length}^{-1}\text{sr}^{-1}$)

$\alpha(R, \lambda)$ = volume extinction coeff. (length^{-1})

The term $\beta(R, \lambda)$ is the backscatter coefficient at distance R, it stands for the ability of the atmosphere to scatter light back into the direction from which it comes

$T(R, \lambda)$ is the transmission term and describes how much light gets lost on the way from the lidar to distance R and back

Most of the information about atmospheric properties derived from backscatter lidar measurements is based on extinction, $\alpha(R, \lambda)$, and backscatter coefficients, $\beta(R, \lambda)$





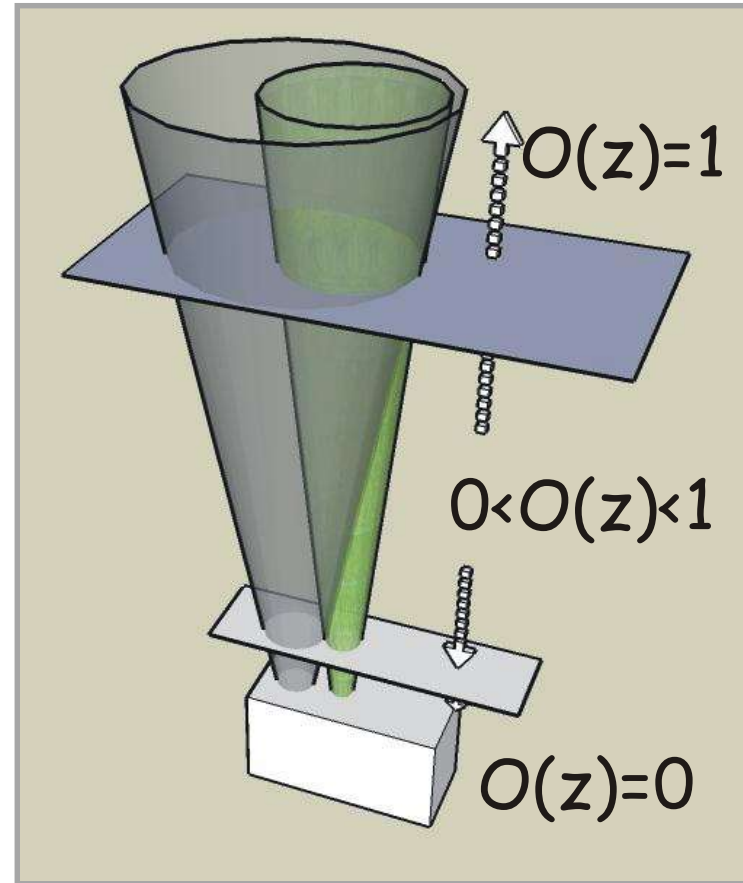
... MORE ON LIDAR EQUATION

Overlap function $O(R)$:
geometrical overlap between laser
beam and telescope field of view

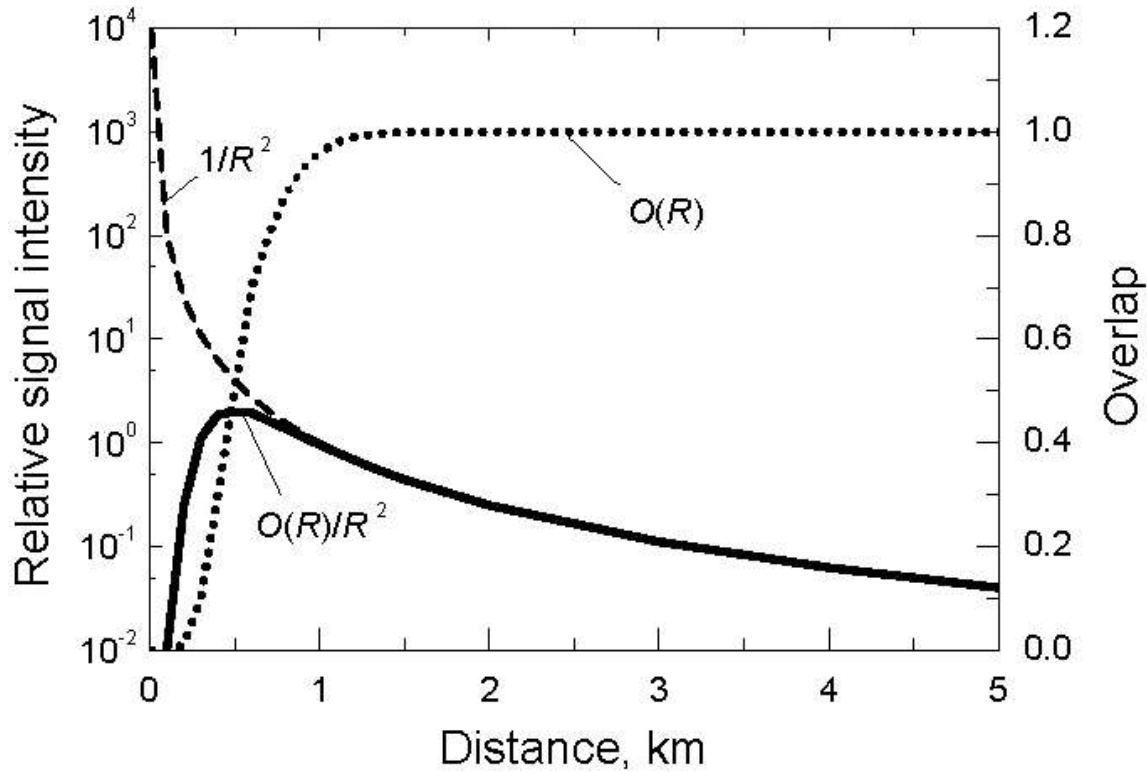
$O(R)$ accounts for the partial
overlap in the near height-range
and tends to stabilize (ideally to 1)
in the far height-range

Elastic lidar equation including overlap:

$$P(R, \lambda) = P_o(\lambda) \frac{C}{R^2} O(R) \beta(R, \lambda) e^{-2 \int_0^R \alpha(x, \lambda) dx}$$



... MORE ON LIDAR EQUATION



Elastic lidar equation including overlap:

$$P(R, \lambda) = P_o(\lambda) \frac{C}{R^2} O(R) \beta(R, \lambda) e^{-2 \int_0^R \alpha(x, \lambda) dx}$$

LIDAR EQUATION

$$P(R, \lambda) = P_o(\lambda) \frac{C}{R^2} O(R) \beta(R, \lambda) e^{-2 \int_0^R \alpha(x, \lambda) dx}$$

measured signal

instrumental features

atmospheric properties

$\beta(R, \lambda)$ = backscatter coeff. ($\text{length}^{-1}\text{sr}^{-1}$)

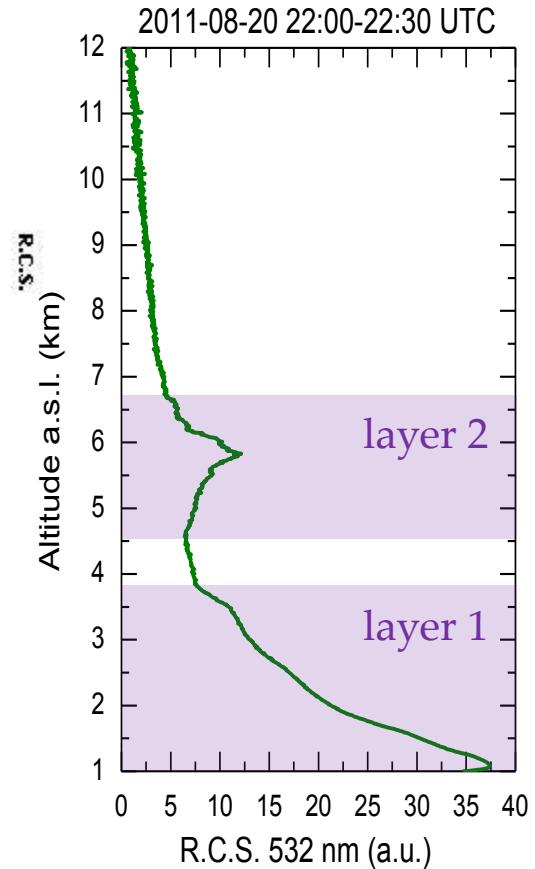
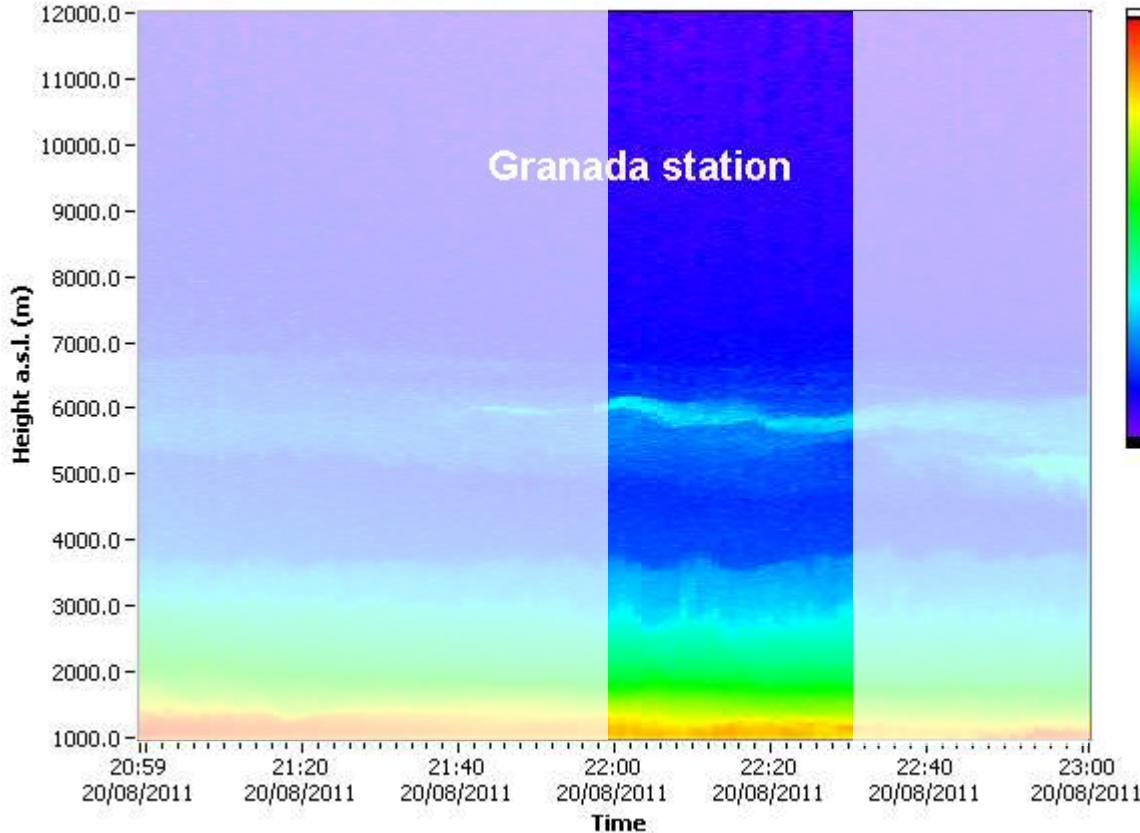
$\alpha(R, \lambda)$ = volume extinction coeff. (length^{-1})

Depend on the particle properties as size, shape, composition, concentration, etc.



FIRST STEPS USING LIDAR EQUATION

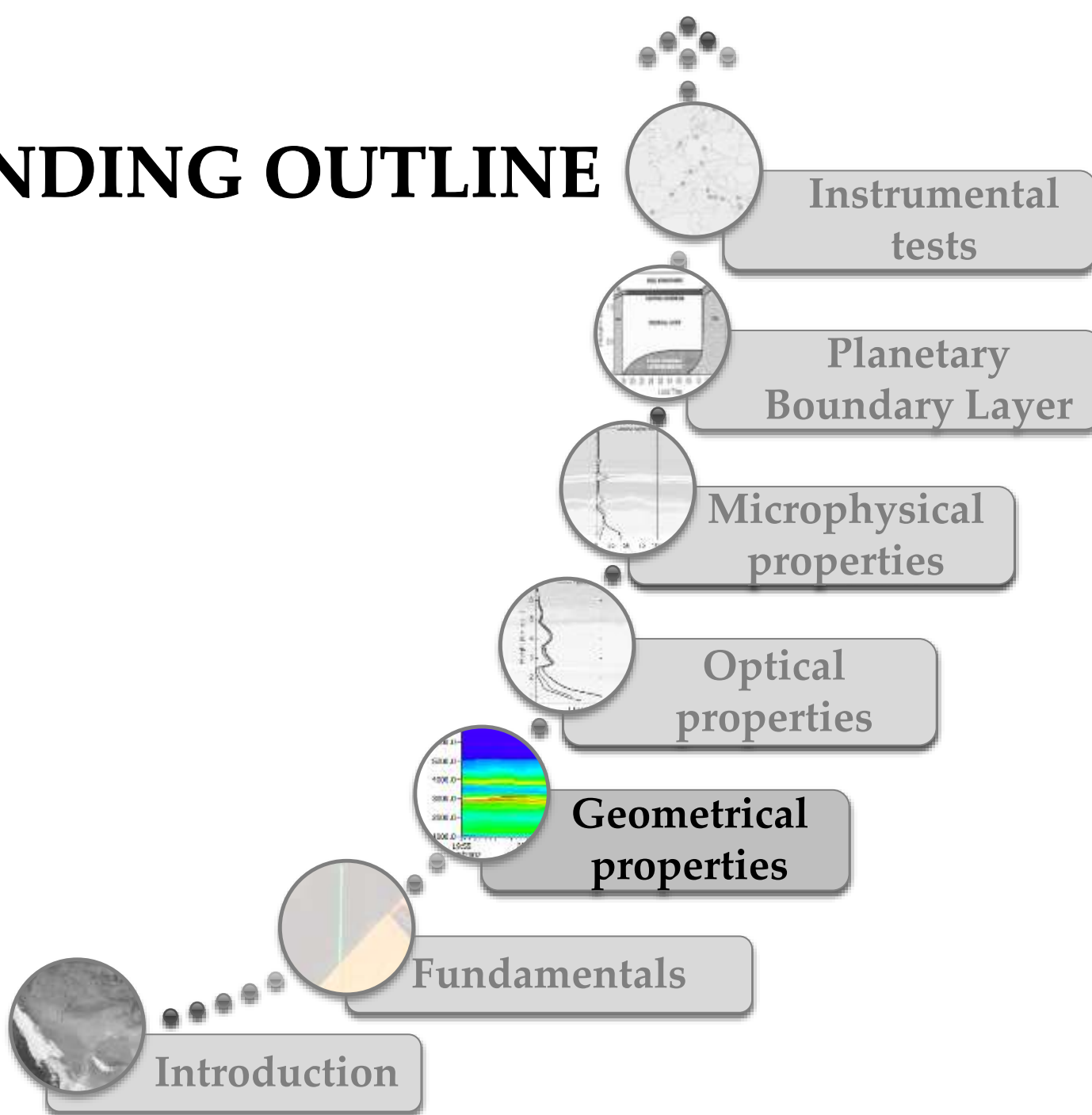
...performing a basic calculation (range corrected signal) on the lidar equation, a first idea of the behavior of the atmosphere can be obtained...



$$R.C.S.(R, \lambda) \equiv P(R, \lambda) \cdot R^2 = P_o(\lambda) \cdot C \cdot O(R) \cdot \beta(R, \lambda) \cdot e^{-2 \int_0^R \alpha(x, \lambda) dx}$$

$$R.C.S.(R, \lambda) \propto \beta(R, \lambda) \cdot T(R, \lambda)^2$$

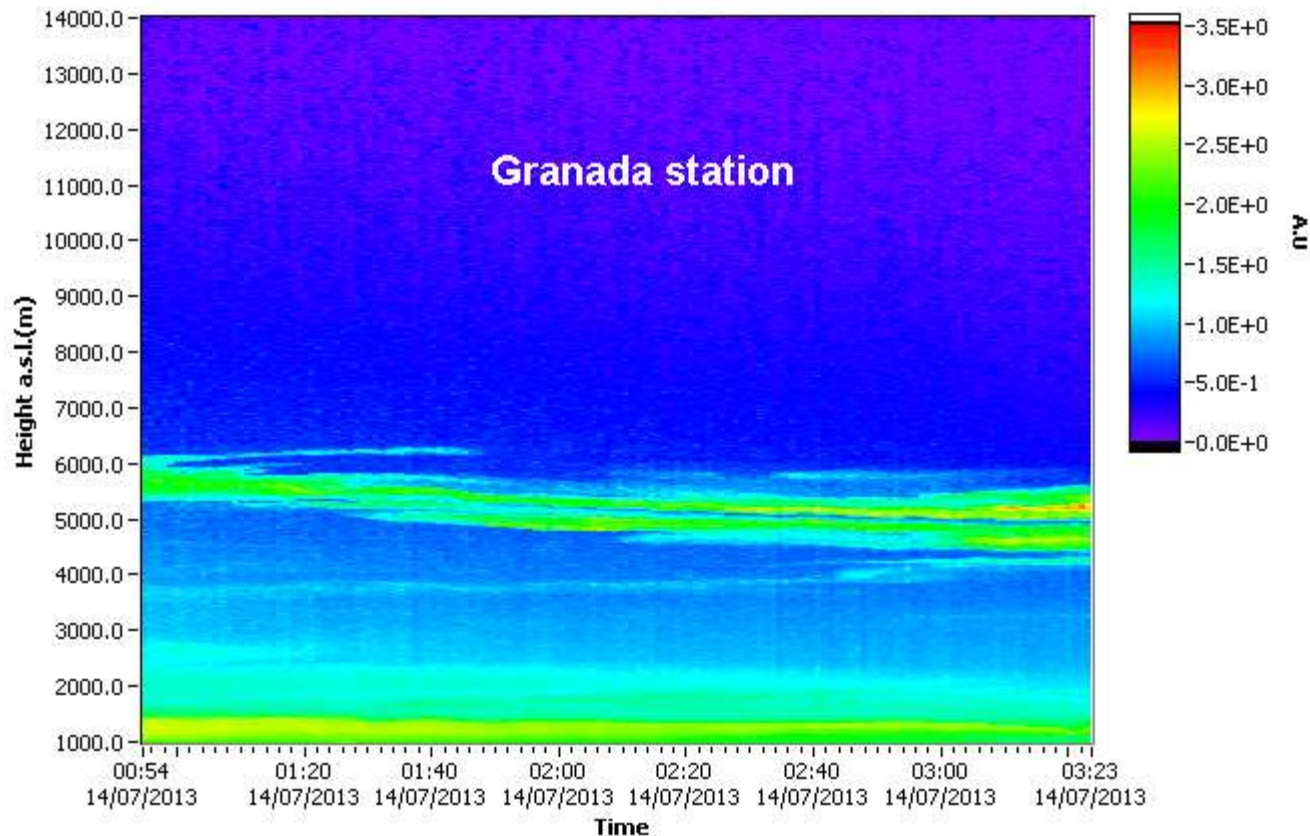
ASCENDING OUTLINE



GEOMETRICAL PROPERTIES

Geometrical properties:

- base height
- top height
- geometrical thickness



Quicklooks can provide a rough estimate of geometrical properties but quantitative information is needed

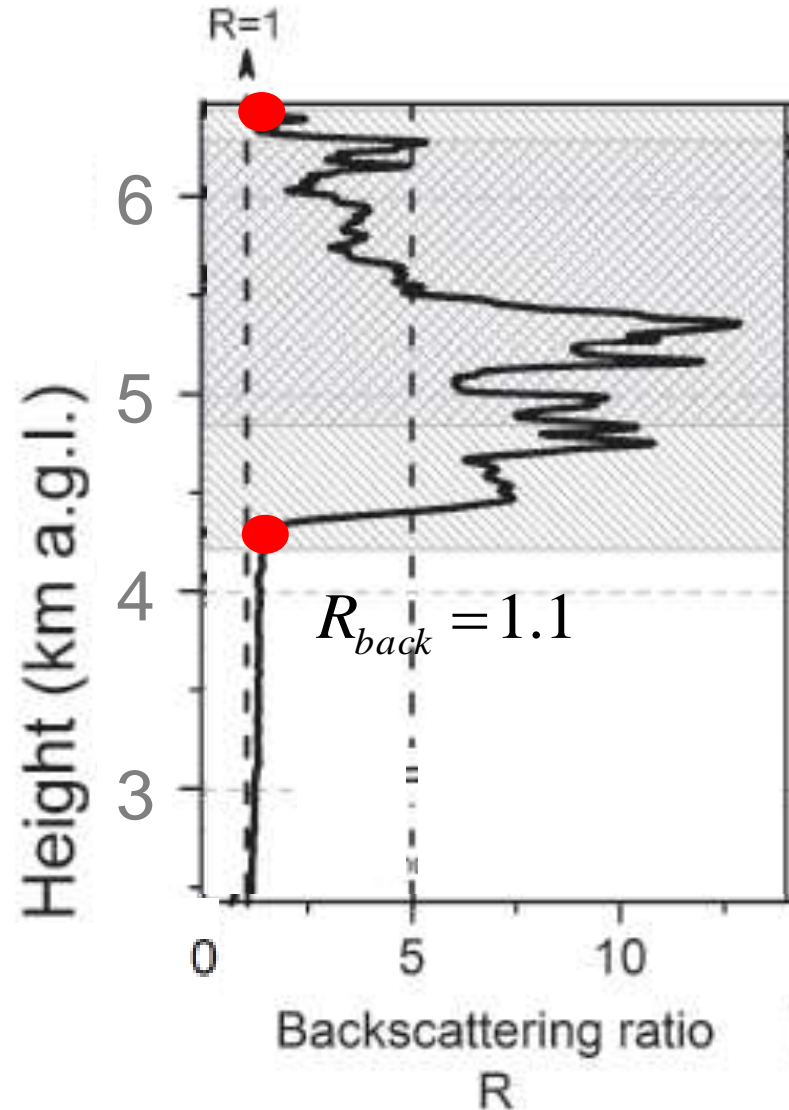
Forest fire smoke layers on 14/07/2013

GEOMETRICAL PROPERTIES

To quantify geometrical properties two groups of algorithms: threshold methods and derivative methods

Threshold methods: processed profiles are needed. Typically, this threshold is established in terms of the backscattering ratio:

$$R_{back}(R) = \frac{\beta_{part}(R) + \beta_{mol}(R)}{\beta_{mol}(R)} = 1 + \frac{\beta_{part}(R)}{\beta_{mol}(R)}$$



GEOMETRICAL PROPERTIES

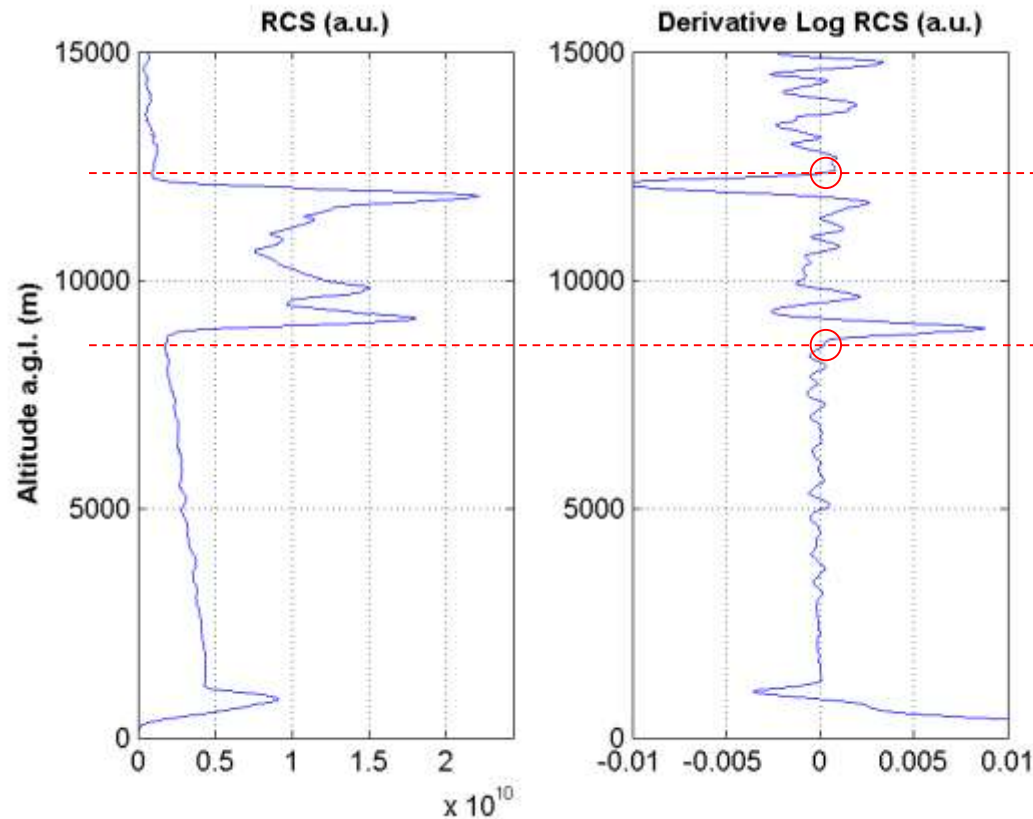
Derivative methods:

- advantage of the derivative methods: applied directly to uncalibrated raw lidar data, i.e., no additional measurements, models or assumptions are required
- first derivate method, second derivate method, logarithm derivate method
- logarithmic derivate method because it mostly quantifies the relative change of the signal, instead of an absolute change as other derivative methods



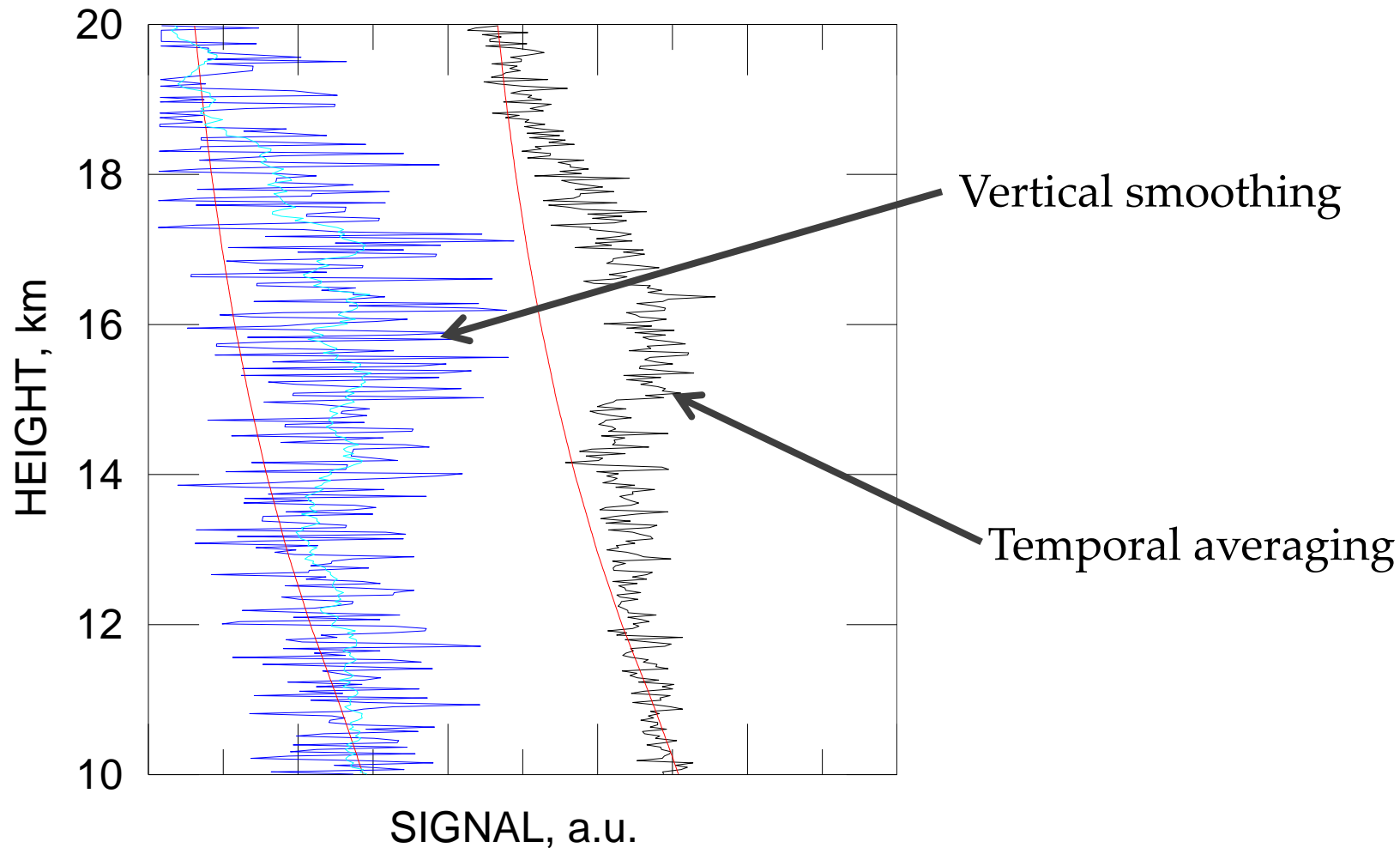
GEOMETRICAL PROPERTIES

- the backscattered lidar signal of a clear atmosphere decreases monotonically with altitude (derivative is always negative)
- aerosol layer implies an abrupt increase in the signal values, such that around the layer base and layer top the sign of this derivative changes
- the change from negative to positive is identified as layer boundaries

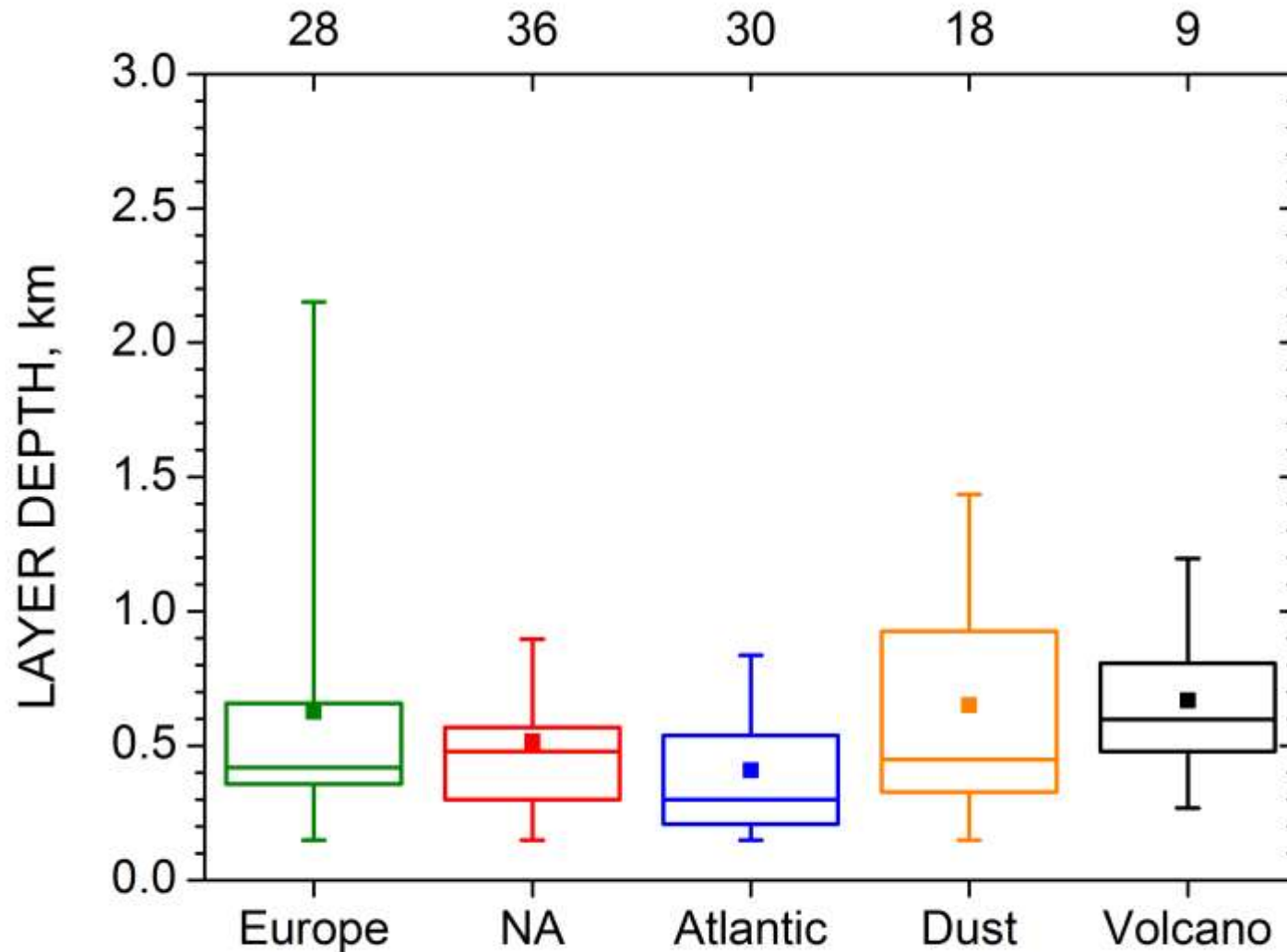


GEOMETRICAL PROPERTIES

Signal-to-noise ratio (SNR) is a critical issue when geometrical properties are computed. To improve SNR, two methods are possible:



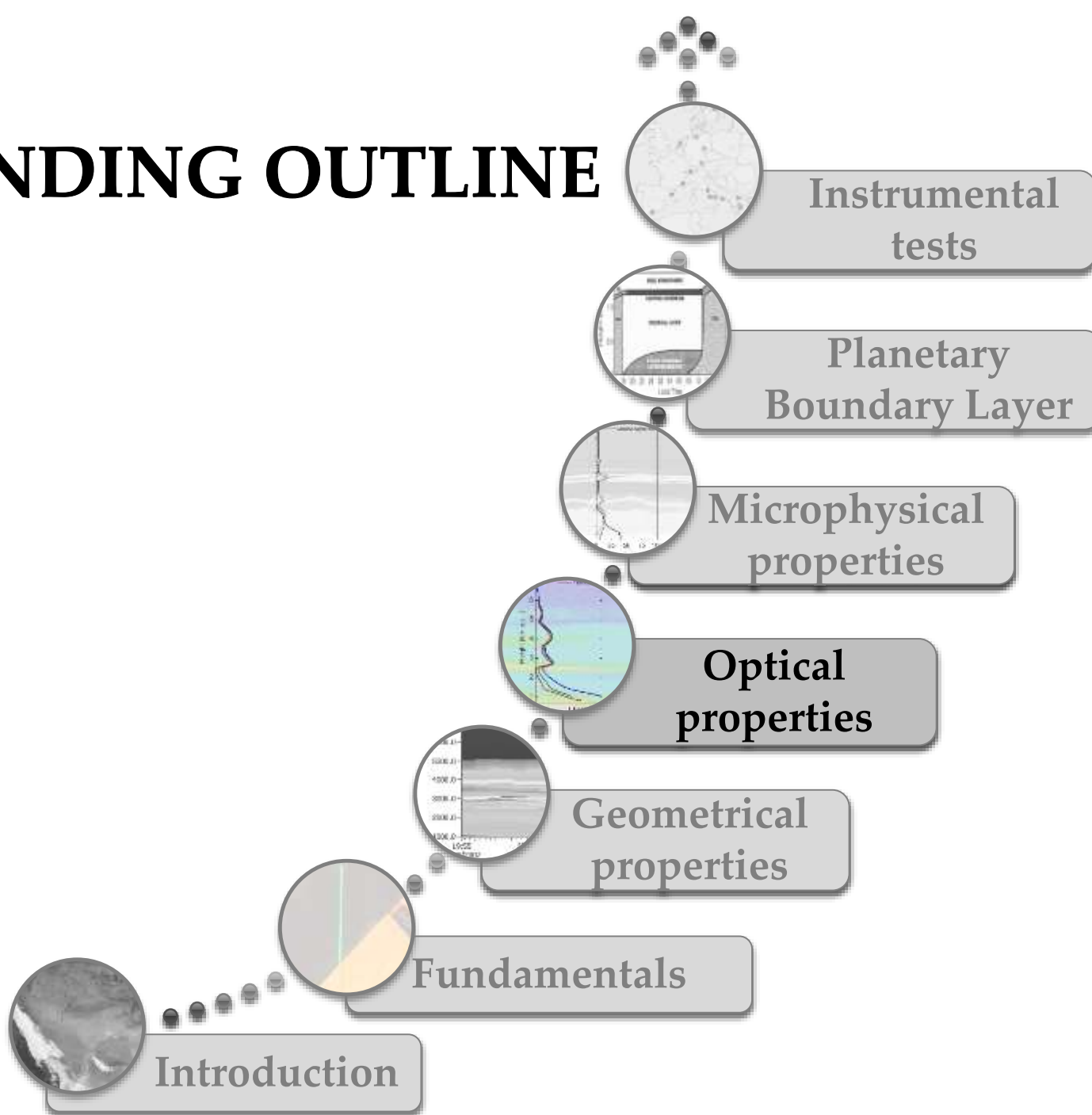
GEOMETRICAL PROPERTIES



Two-year analysis of layer depth in Portugal (Preissler et al., JGR 2013)



ASCENDING OUTLINE





LIDAR OPTICAL ALGORITHMS

ELASTIC METHOD

First we will describe the technique used to compute the particle backscatter coefficient from return signals measured with the widely used elastic standard backscatter lidar

The main drawback of this method is that trustworthy profiles of the climate relevant volume extinction coefficient of the particles cannot be obtained. The extinction profile must be estimated from the determined backscatter coefficient profile

RAMAN METHOD

By applying the so-called Raman lidar technique, the profile of the particle extinction and backscatter coefficients can be independently determined

An aerosol Raman lidar measures two signal profiles, which permit the separation of particle and molecular backscatter contributions

KLETT-FERNALD METHOD

Starting point: lidar equation

$$P(R, \lambda) = P_o(\lambda) \frac{C}{R^2} O(R) \beta(R, \lambda) e^{-2 \int_0^R \alpha(x, \lambda) dx} =$$
$$= P_o(\lambda) \frac{C}{R^2} O(R) \beta(R, \lambda) T(R, \lambda)^2$$

$\beta(R, \lambda)$ ($\text{km}^{-1}\text{sr}^{-1}$) and $\alpha(R, \lambda)$ (km^{-1}) are the backscatter and extinction coefficients in the atmosphere

Remembering the definition of lidar range corrected signal:

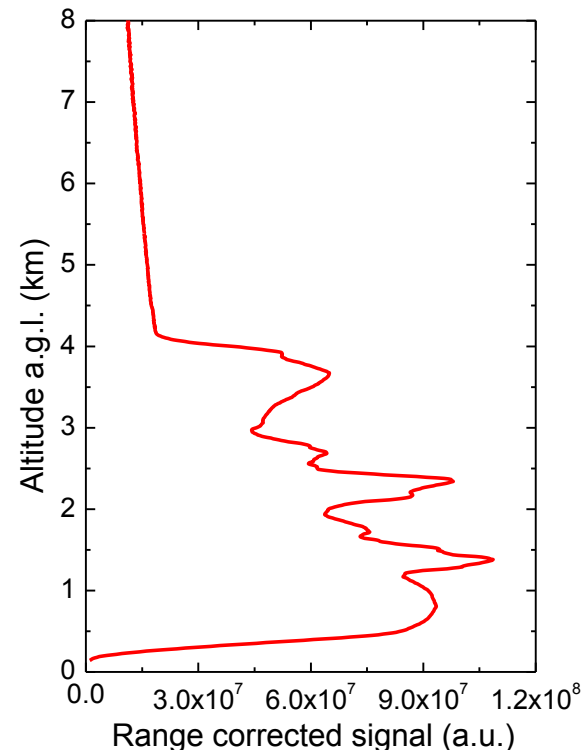
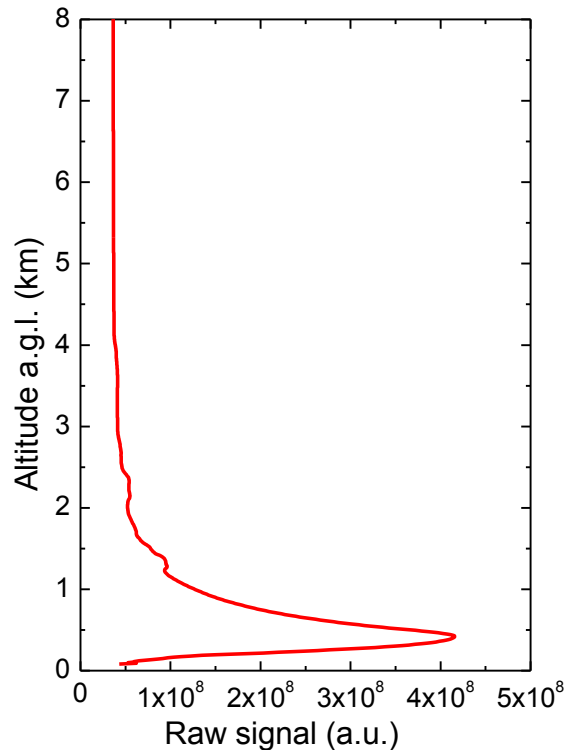
$$R.C.S.(R, \lambda) \equiv P(R, \lambda) \cdot R^2 = P_o(\lambda) \cdot C \cdot O(R) \cdot \beta(R, \lambda) \cdot e^{-2 \int_0^R \alpha(x, \lambda) dx}$$



KLETT-FERNALD METHOD

$$R.C.S.(R, \lambda) \equiv P(R, \lambda) \cdot R^2 = P_o(\lambda) \cdot C \cdot O(R) \cdot \beta(R, \lambda) \cdot e^{-2 \int_0^R \alpha(x, \lambda) dx}$$

The conversion of lidar signal into range corrected lidar signal causes a change in appearance:



KLETT-FERNALD METHOD

$$R.C.S.(R, \lambda) \equiv P(R, \lambda) \cdot R^2 = P_o(\lambda) \cdot C \cdot O(R) \cdot \beta(R, \lambda) \cdot e^{-2 \int_0^R \alpha(x, \lambda) dx}$$

... some considerations:

- the overlap is assumed to be complete, $O(R) = 1 \rightarrow R \geq R_{\min}$
- we drop the wavelength dependence

$$R.C.S.(R) \equiv P(R) \cdot R^2 = P_o \cdot C \cdot \beta(R) \cdot e^{-2 \int_0^R \alpha(x) dx}$$

- $\beta(R)$ ($\text{km}^{-1}\text{sr}^{-1}$) and $\alpha(R)$ (km^{-1}) are caused by particles and molecules:

$$\beta(R) = \beta_{mol}(R) + \beta_{part}(R)$$

$$\alpha(R) = \sigma_{mol}^{scat}(R) + \cancel{\sigma_{mol}^{abs}(R)} + \sigma_{part}^{scat}(R) + \sigma_{part}^{abs}(R)$$

$\approx 0 \text{ km}^{-1}$ at lidar wavelengths



KLETT-FERNALD METHOD

Taking into account molecular absorption effects are ignored:

$$\alpha(R) = \sigma_{mol}^{scat}(R) + \sigma_{part}^{scat}(R) + \sigma_{part}^{abs}(R) = \alpha_{mol}(R) + \alpha_{part}(R)$$

Therefore, the range corrected signal is:

$$\underline{R.C.S.(R)} = P_o \cdot C \cdot \left[\underline{\beta_{mol}(R)} + \underline{\beta_{part}(R)} \right] \cdot e^{-2 \int_0^R [\alpha_{mol}(x) + \underline{\alpha_{part}(x)}] dx}$$

measurement **unknowns**

The molecular properties, $\beta_{mol}(R)$ and $\alpha_{mol}(R)$, can be determined from the Rayleigh theory using the best available meteorological data of temperature and pressure or approximated from appropriate standard atmospheres so that only the aerosol scattering and absorption properties, $\beta_{part}(R)$ and $\alpha_{part}(R)$, remain to be determined



KLETT-FERNALD METHOD

Shortcoming: 1 measurement versus 2 unknowns

$$\underline{R.C.S.(R)} = P_o \cdot C \cdot \left[\beta_{mol}(R) + \underline{\beta_{part}(R)} \right] \cdot e^{-2 \int_0^R [\alpha_{mol}(x) + \underline{\alpha_{part}(x)}] dx}$$

measurement **unknowns**

How to solve?: definition of the particle and molecular lidar ratio (extinction-to-backscatter ratio)

$$Lr_{part}(R, \lambda) = \frac{\alpha_{part}(R, \lambda)}{\beta_{part}(R, \lambda)}$$

dependent on range and wavelength because depends on:

- size distribution
- shape
- composition (refractive index)

$$Lr_{mol}(\cancel{R}, \lambda) = \frac{\alpha_{mol}(R, \lambda)}{\beta_{mol}(R, \lambda)} = \frac{8\pi}{3} sr$$

independent on range and wavelength



KLETT-FERNALD METHOD

In the next step:

- lidar ratio definitions are included
- the equation is reorganized
- the resulting Bernoulli equation is solved

Solution:

$$\beta_{part}(R) = -\beta_{mol}(R) + \frac{R.C.S.(R) \cdot \exp\left\{-2 \int_{R_0}^R [Lr_{part}(x) - Lr_{mol}] \beta_{mol}(x) dx\right\}}{\beta_{part}(R_0) + \beta_{mol}(R_0)} - 2 \int_{R_0}^R Lr_{part}(x') \cdot R.C.S.(x') \cdot \exp\left(-2 \int_{R_0}^{x'} [Lr_{part}(x) - Lr_{mol}] \beta_{mol}(x) dx\right) dx'$$

...many things ... but they are known (almost)



KLETT-FERNALD METHOD

$$\beta_{part}(R) = -\beta_{mol}(R) +$$

$$R.C.S.(R) \exp \left\{ -2 \int_{R_0}^R [Lr_{part}(x) - Lr_{mol}] \beta_{mol}(x) dx \right\}$$

$$+ \frac{R.C.S.(R_0)}{\beta_{part}(R_0) + \beta_{mol}(R_0)} - 2 \int_{R_0}^R Lr_{part}(x') \cdot R.C.S.(x') \exp \left(-2 \int_{R_0}^{x'} [Lr_{part}(x) - Lr_{mol}] \beta_{mol}(x) dx \right) dx'$$

- lidar range corrected signal (R.C.S.) is known
- molecular properties are known from meteorological data of temperature and pressure or approximated from appropriate standard atmospheres
- particle lidar ratio is an input parameter
- boundary condition at R_0 ... how to choose it?



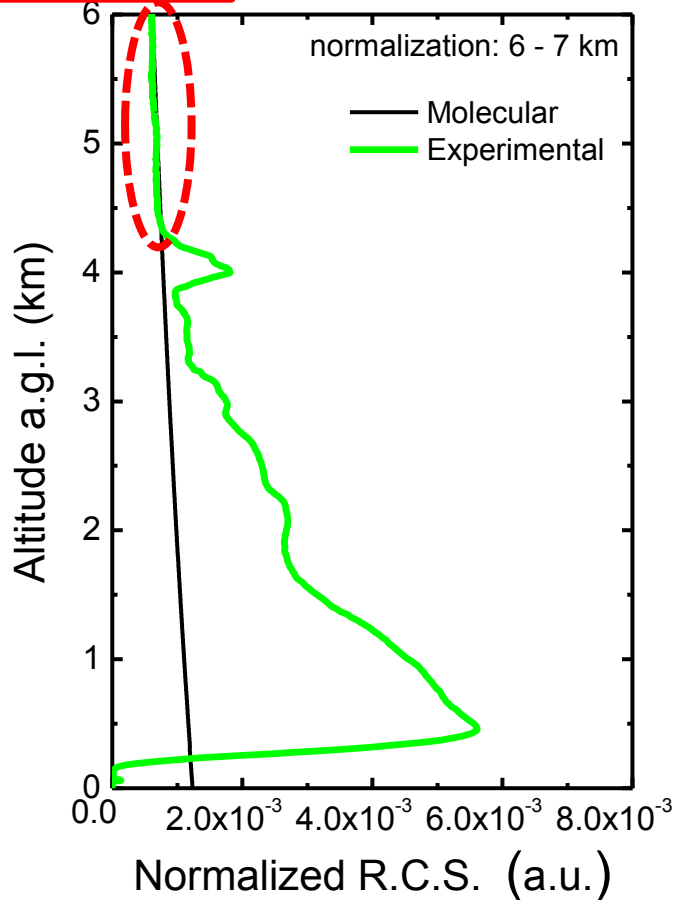
KLETT-FERNALD METHOD



$$\beta_{part}(R) = -\beta_{mol}(R) +$$

$$R.C.S.(R) \cdot \exp \left\{ -2 \int_{R_0}^R [Lr_{part}(x) - Lr_{mol}] \beta_{mol}(x) dx \right\}$$

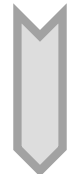
$$+ \frac{R.C.S.(R_0)}{\beta_{part}(R_0) + \beta_{mol}(R_0)} - 2 \int_{R_0}^R Lr_{part}(x') \cdot R.C.S.(x') \cdot \exp \left(-2 \int_{R_0}^{x'} [Lr_{part}(x) - Lr_{mol}] \beta_{mol}(x) dx \right) dx'$$



at R_0 : $\beta_{part}(R_0) \ll \beta_{mol}(R_0)$

$$\beta_{part}(R_0) + \beta_{mol}(R_0) \approx \beta_{mol}(R_0)$$

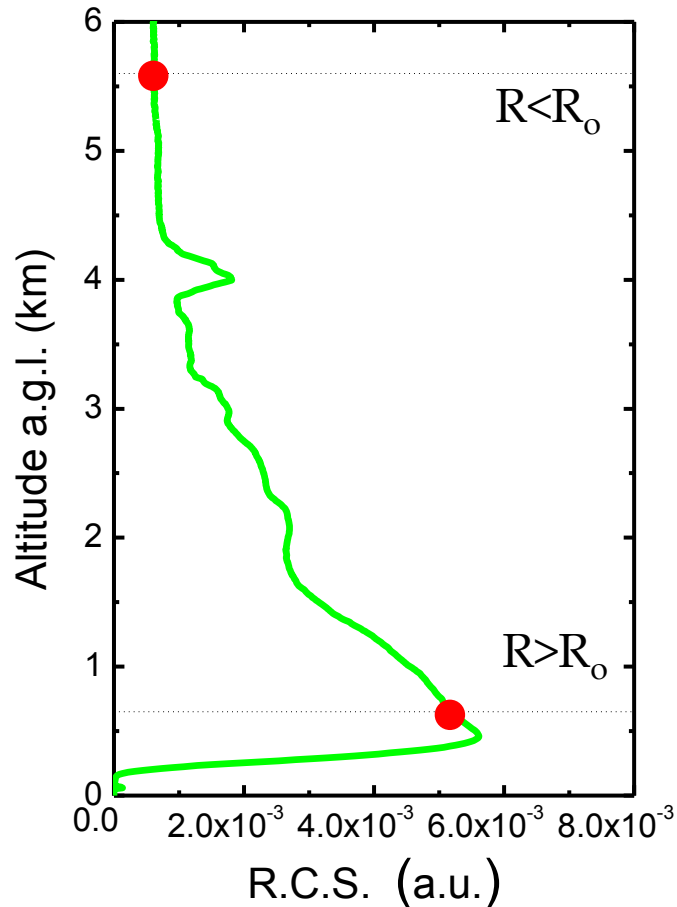
(clean air conditions are normally given in the middle and upper troposphere)



Now, the boundary condition term is also known

KLETT-FERNALD METHOD

In principle, the solution for $\beta_{\text{part}}(R)$ can be integrated by starting from the reference range R_0 , which may be either the near end ($R > R_0$, "forward integration") or the remote end ($R < R_0$, "backward integration") of the measuring range



Forward integration	Backward integration
bad $\beta_{\text{part}}(R_0)$	good $\beta_{\text{part}}(R_0)$ (clean atmosphere)
numerically unstable	numerically stable
good SNR for R.C.S. at R_0	worse SNR for R.C.S. at R_0 (easily solved)

Backward integration method is preferred

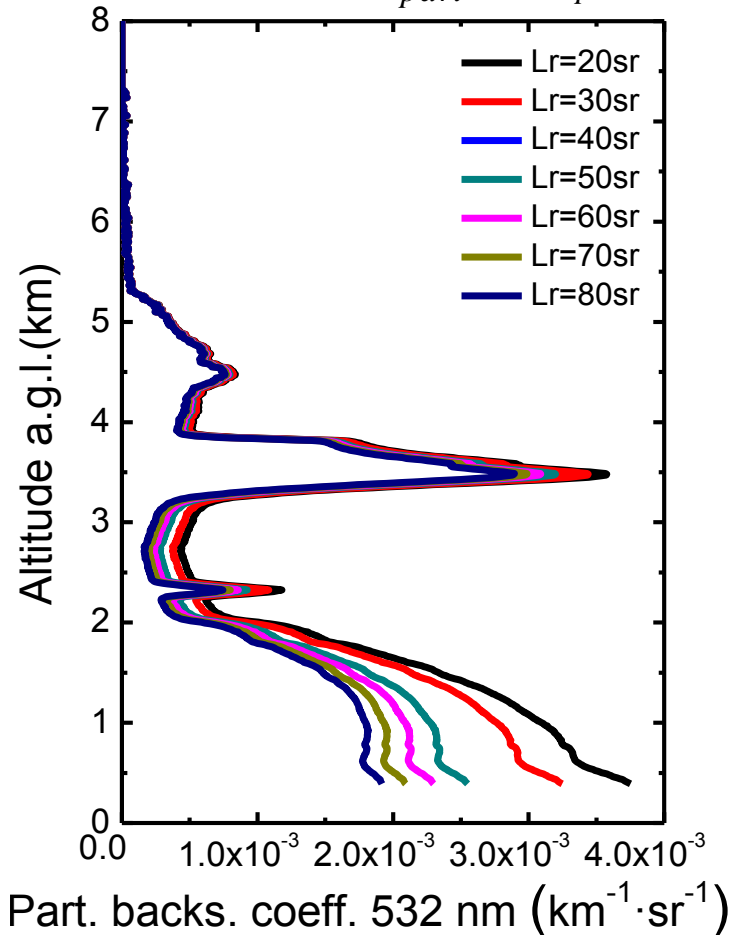


KLETT-FERNALD METHOD

The most critical parameter in this method is the selection of a particle lidar ratio

$$Lr_{part}(R, \lambda) \equiv \frac{\alpha_{part}(R, \lambda)}{\beta_{part}(R, \lambda)}$$

Effect of Lr_{part} on β_{part} :



Lr_{part} values independent of altitude are typically used

Some values of particle lidar ratio:

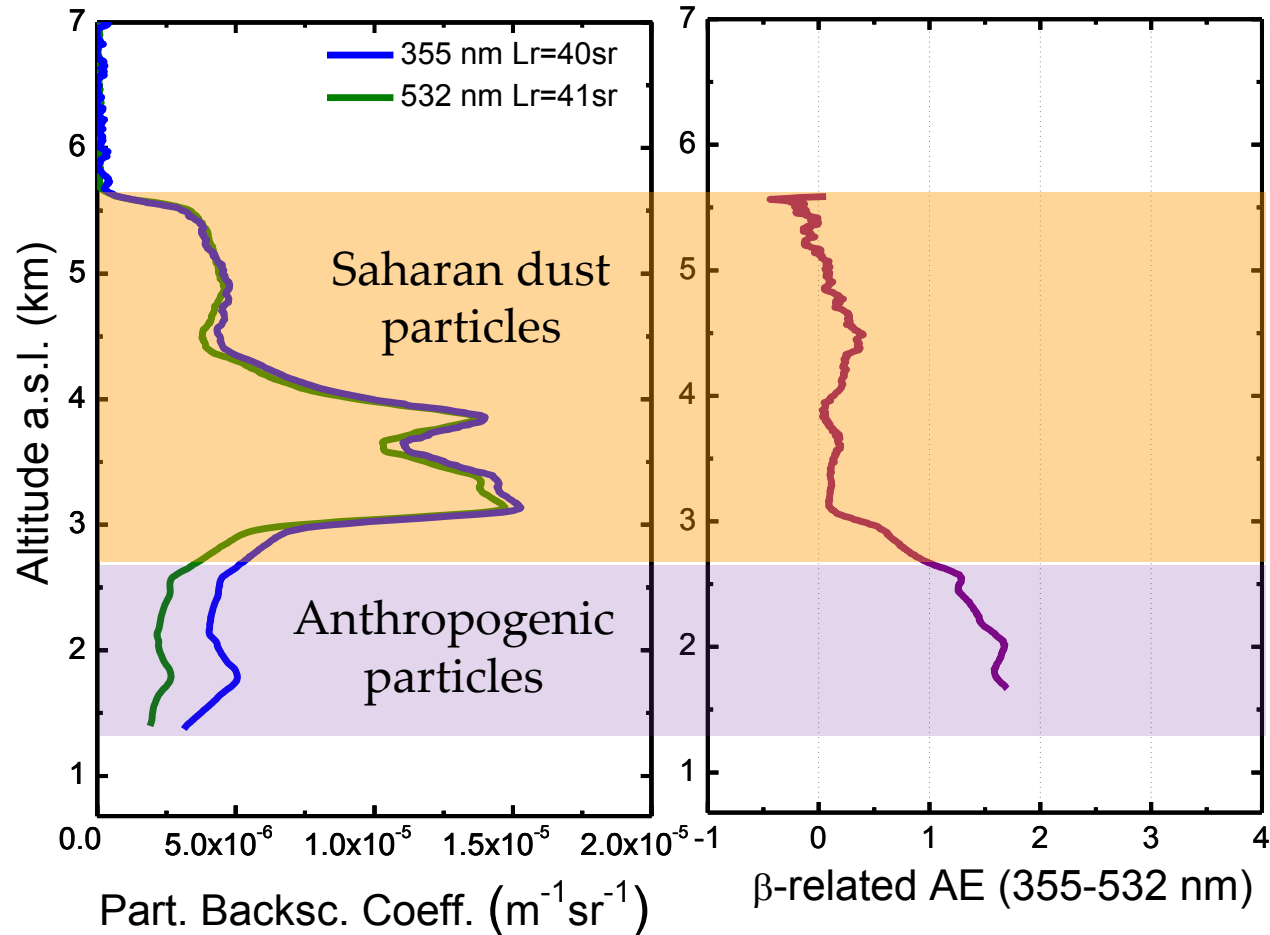
Type	Lr (at 532 nm)
Marine particles	20-35 sr
Saharan dust	40-70 sr
Biomass burning	70-100 sr
Urban/continental	45-75 sr



KLETT-FERNALD METHOD

The spectral dependence of β_{part} is strongly dependent on particle size: commonly used for the qualitative description of particle size

$$a_{\beta}(R) = - \frac{\ln\left(\frac{\beta_{part}(R, \lambda_1)}{\beta_{part}(R, \lambda_2)}\right)}{\ln\left(\frac{\lambda_1}{\lambda_2}\right)}$$

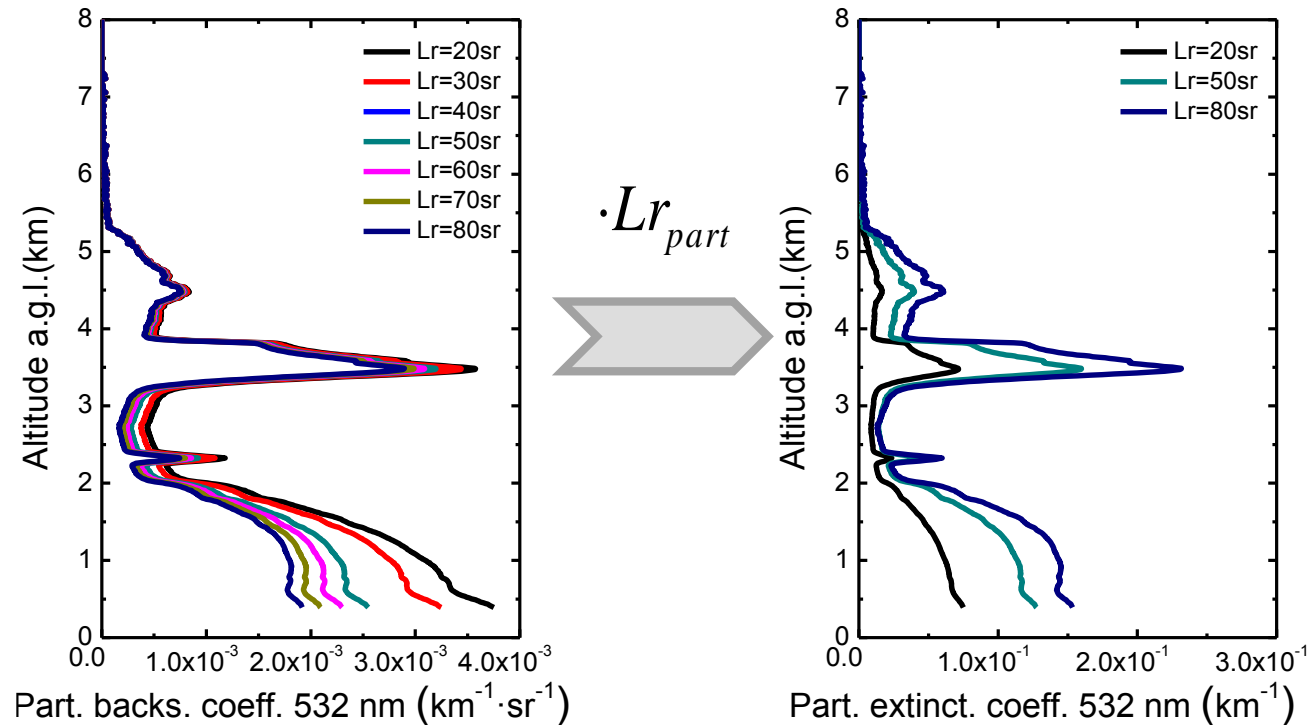


KLETT-FERNALD METHOD

In this way we obtain the profile of the particle backscatter coefficient and from this the profile of particle extinction coefficient can be estimated by:

$$\alpha_{part}(R) = Lr_{part}(R)\beta_{part}(R)$$

An example:



$$AOD = \int_0^{\infty} \alpha_{part}(R) dR$$

Lr	AOD
20 sr	0.17
50 sr	0.33
80 sr	0.44

KLETT-FERNALD METHOD

Improvement : K-F method constrained by $AOD_{\text{photometer}}$

1 – Application of K-F method with an initial value of Lr_{part}

2 – Computation of aerosol extinction profile and AOD from lidar:

$$\alpha_{\text{part}}(R) = Lr_{\text{part}}\beta_{\text{part}}(R) \Rightarrow AOD_{\text{lidar}} = \int_0^{\infty} \alpha_{\text{part}}(R)dR = Lr_{\text{part}} \int_0^{\infty} \beta_{\text{part}}(R)dR$$

3 – Comparison of AOD from lidar and photometer:

$$\left| AOD_{\text{photometer}} - AOD_{\text{lidar}} \right| \leq \varepsilon$$

4 – Modification of Lr_{part} if necessary (go to 1)

This column-related Lr_{part} must be considered as an effective Lr_{part} :

the true Lr_{part} profile remains unknown



SUMMARY ON K-F METHOD

- The K-F method allows for determining the β_{part} profile
- Numerical stability is given in the backward integration
- The reference range R_0 is usually chosen such that β_{part} at R_0 is negligible compared to the known β_{mol}
- The most critical input parameter is the $L_{\text{part}}(R)$. This quantity depends on the microphysical, chemical and morphological properties of the particles, and can vary strongly with height, specially when the atmospheric aerosols present a layered structure.
- The application of the K-F method constrained by $\text{AOD}_{\text{photometer}}$ allows for obtaining an an effective L_{part} , but the true L_{part} profile remains unknown
- Variations between 20 and 100 sr make it practically impossible to estimate trustworthy particle extinction profiles from backscatter ones



MOLECULAR COMPONENT

As previously mentioned, the K-F method (and others that will be shown later) needs the molecular component

β_{mol} profile can be computed from the Rayleigh theory and ideal gas law:

$$\beta_{mol}(R) = \frac{9\pi^2(n_s^2 - 1)^2}{\lambda^4 N_s^2 (n_s^2 + 2)^2} \left(\frac{6 + 3\rho}{6 - 7\rho} \right) N_s \frac{T_0}{P_0} \frac{P(R)}{T(R)}$$

n_s refractive index

ρ depolarization factor (0.0301, 0.0284 and 0.0273 at 355, 532 and 1064 nm respectively)

$N_s = 2.547 \cdot 10^{19} \text{ cm}^{-3}$ molecular number density for conditions of a standard atmosphere at sea level

$$P_0 = 1013.25 \text{ hPa}$$

$$T_0 = 15^\circ \text{ C}$$

Only pressure and temperature profile are needed



MOLECULAR COMPONENT

How to obtain T and P profiles?

Option 1: download radiosounding observations from...

University of Wyoming
College of Engineering
Department of Atmospheric Science

<http://weather.uwyo.edu/upperair/sounding.html>

Region	Type of plot	Year	Month	From	To	Station Number
South America ▼	Text: List ▼	2014 ▼	Jul ▼	26/12Z ▼	26/12Z ▼	80222

Click on the image to request a sounding at that location or enter the station number above.



80222 Bogota/Eldorado (SKBO)



MOLECULAR COMPONENT

How to obtain T and P profiles?

Option 2: if no radiosoundings nearby, use model data from NOAA

online:

<http://www.ready.noaa.gov/READYamet.php>



Air Resources Laboratory - x

www.ready.noaa.gov/READYamet.php

Conducting research and development in the fields of air quality, atmospheric dispersion, climate, and boundary layer

Enter search term(s)

ARL site only All NOAA

READY Archived Meteorology

Archived Model Graphics

Choose a forecast location by entering a 3 or 4-character station identifier or a 6-digit WMO index number or a latitude/longitude pair and then click the Continue button, or by clicking on the location in the map. You will be taken to the model products section. Information on ARL's data archive is available at <http://ready.arl.noaa.gov/archives.php>.

Select a Location

Using a Code Identifier **OR By Selecting a U.S. or World City**

OR by Latitude & Longitude

Latitude (degrees) [Convert Deg/Min/Sec into Decimal Degrees](#)

Longitude (West < 0)

OR click a location on the map below.

MOLECULAR COMPONENT

How to obtain T and P profiles?

Option 2: if no radiosoundings nearby, use model data from NOAA

online:

<http://www.ready.noaa.gov/READYamet.php>

READY -
www.ready.noaa.gov/ready2-bin/mainarc.pl

ARL
Air Resources Laboratory
Conducting research and development in the fields of air quality, atmospheric dispersion, climate, and boundary layer

ARL Home > READY > Archived Meteorology > READY Program Options Menu

READY Program Options Menu

READY PRODUCTS FOR LOCATION: 37.16 -3.61

DISPLAY PROGRAM What is UTC, GMT, Z time?	METEOROLOGICAL DATA Information on archived datasets
METEOROGRAM	-----Choose An Archived Dataset----- <input type="button" value="Go"/>
WINDGRAM	-----Choose An Archived Dataset----- <input type="button" value="Go"/>
WINDROSE	-----Choose An Archived Dataset----- <input type="button" value="Go"/>
SOUNDING	GDAS (1 deg, 3 hourly, Global) <input type="button" value="Go"/>
STABILITY TIME-SERIES	-----Choose An Archived Dataset----- <input type="button" value="Go"/>
2D MAP (NCAR GRAPHICS)	-----Choose An Archived Dataset----- <input type="button" value="Go"/>
2D MAP (PSPLOT)	-----Choose An Archived Dataset----- <input type="button" value="Go"/>



MOLECULAR COMPONENT

How to obtain T and P profiles?

Option 2: if no radiosoundings nearby, use model data from NOAA

online:

<http://www.ready.noaa.gov/READYamet.php>

READY -

www.ready.noaa.gov/ready2-bin/listarcfile.pl?product=profile1a&userid=3846&metdata=GDAS1&mdatacfg=GDAS1

ARL
Air Resources Laboratory
Conducting research and development in the fields of air quality, atmospheric dispersion, climate, and boundary layer

ARL Home > READY > Archived Meteorology > Choose Archive File

Select the GDAS1 File for the Period of Interest

GDAS1 Meteorological File: current7days Next>>

For data availability (what's missing) view [archives.php web page](#).

FILE FORMAT OF THE ARCHIVE DATA:

If available, the current 7 days of data are located in the file called:

current7days

otherwise,

gdas1.mmmyy.w#

where,

mmm = 3 letter month (jan=January)

yy = 2 number year (05=2005)

w# = w1 for the first 7 days of the month



MOLECULAR COMPONENT

How to obtain T and P profiles?

Option 2: if no radiosoundings nearby, use model data from NOAA

online:

<http://www.ready.noaa.gov/READYamet.php>

Change Default Model Parameters and Display Options

Time to plot (start time for animation)	Month: 07	Day: 22	Hour: 12		
Animation:	<input type="radio"/> None	<input type="radio"/> GIF	<input type="radio"/> Flash	<input type="radio"/> Javascript	Duration: 24 hours
Type:	<input checked="" type="radio"/> Full Sounding	<input type="radio"/> Only to 400 mb			
Output Options:	<input type="radio"/> Graphic and text	<input checked="" type="radio"/> Text only			
Graphics:	<input type="radio"/> Text Listing	<input checked="" type="radio"/> Skew-T Log-P	<input type="radio"/> Theta	<input type="radio"/> All	
Profile graphic size (dpi):	<input type="radio"/> 72	<input type="radio"/> 84	<input checked="" type="radio"/> 96	<input type="radio"/> 120	
Create PDF?	<input type="radio"/> Yes	<input checked="" type="radio"/> No			

Type your access code (displayed at right) into the text box. This code is an image that cannot be read by a computer. This access code prevents automated programs from requesting access to READY products, which have saturated the system denying others from obtaining products in a timely manner.

[READY Use Agreement](#)

Enter the access code from the box above to request product (case insensitive):



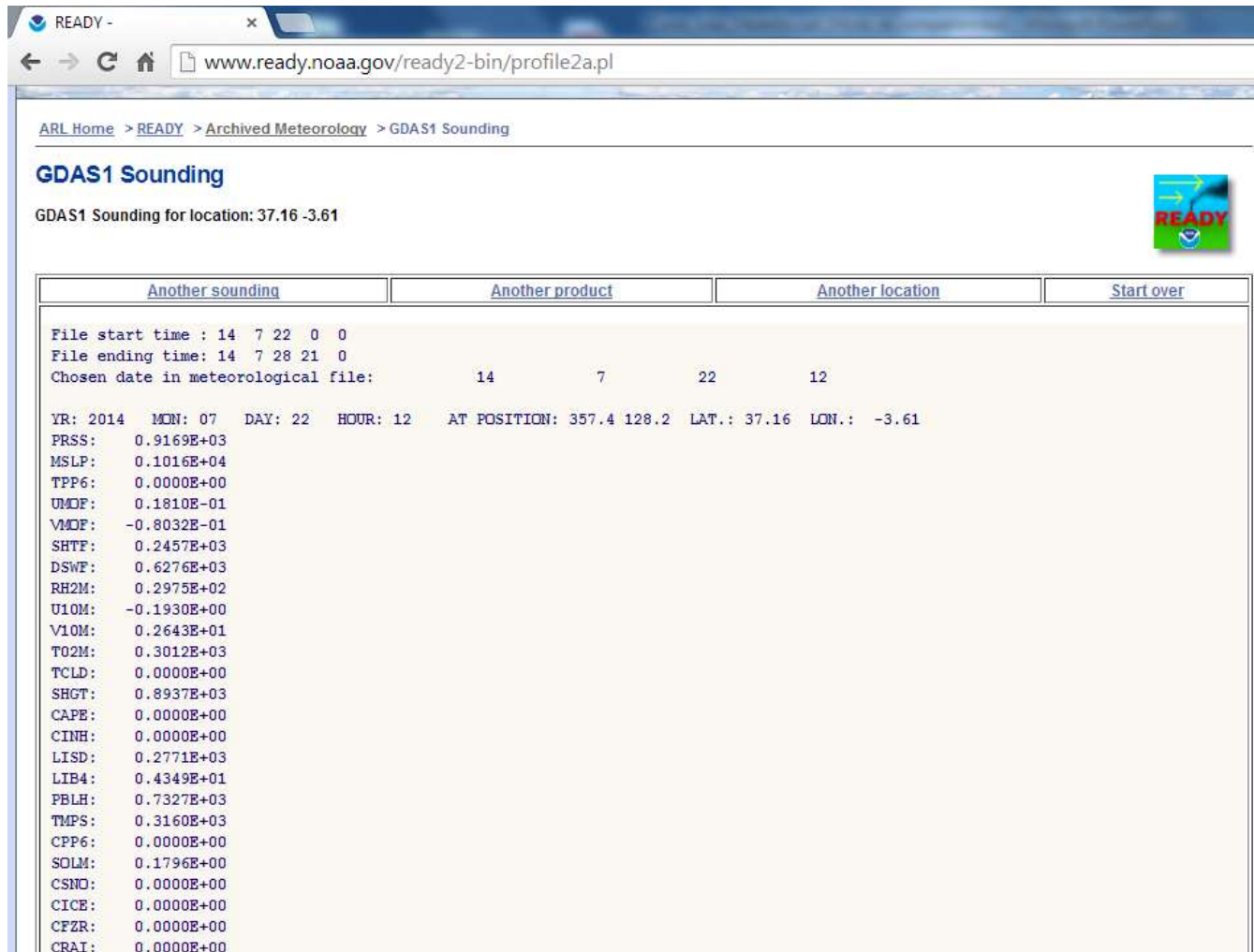
MOLECULAR COMPONENT

How to obtain T and P profiles?

Option 2: if no radiosoundings nearby, use model data from NOAA

online:


<http://www.ready.noaa.gov/READYamet.php>



ARL Home > READY > Archived Meteorology > GDAS1 Sounding

GDAS1 Sounding

GDAS1 Sounding for location: 37.16 -3.61



Another sounding	Another product	Another location	Start over
----------------------------------	---------------------------------	----------------------------------	----------------------------

File start time : 14 7 22 0 0
File ending time: 14 7 28 21 0
Chosen date in meteorological file: 14 7 22 12

YR: 2014 MON: 07 DAY: 22 HOUR: 12 AT POSITION: 357.4 128.2 LAT.: 37.16 LON.: -3.61

PRSS: 0.9169E+03
MSLP: 0.1016E+04
TPP6: 0.0000E+00
UMDF: 0.1810E-01
VMDF: -0.8032E-01
SHTF: 0.2457E+03
DSWF: 0.6276E+03
RH2M: 0.2975E+02
U10M: -0.1930E+00
V10M: 0.2643E+01
TQ2M: 0.3012E+03
TCLD: 0.0000E+00
SHGT: 0.8937E+03
CAPE: 0.0000E+00
CINH: 0.0000E+00
LISD: 0.2771E+03
LIB4: 0.4349E+01
PBLH: 0.7327E+03
TMPS: 0.3160E+03
CPP6: 0.0000E+00
SOLM: 0.1796E+00
CSND: 0.0000E+00
CICE: 0.0000E+00
CFZR: 0.0000E+00
CRAI: 0.0000E+00



MOLECULAR COMPONENT

How to obtain T and P profiles?

Option 2: if no radiosoundings nearby, use model data from NOAA
off-line

Download HYSPLIT software from:

<https://ready.arl.noaa.gov/HYSPLIT.php>

Download GDAS meteorological data from:

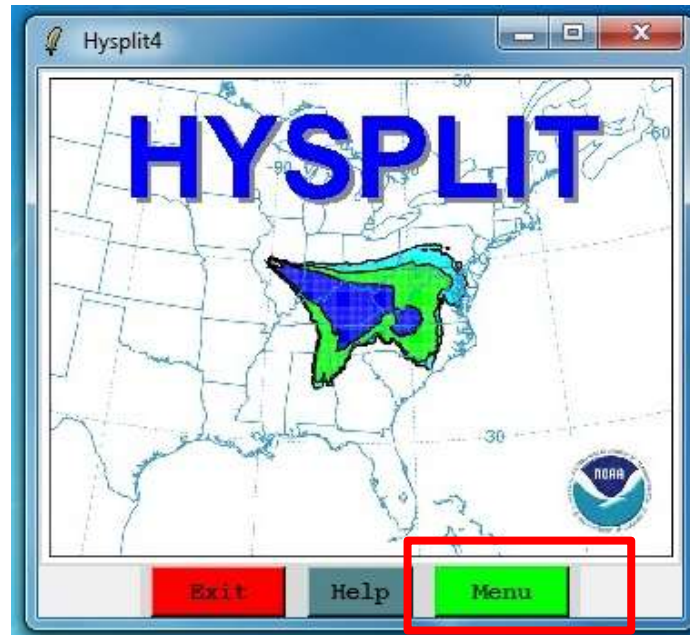
<ftp://arlftp.arlhq.noaa.gov/pub/archives/gdas1/>



MOLECULAR COMPONENT

How to obtain T and P profiles?

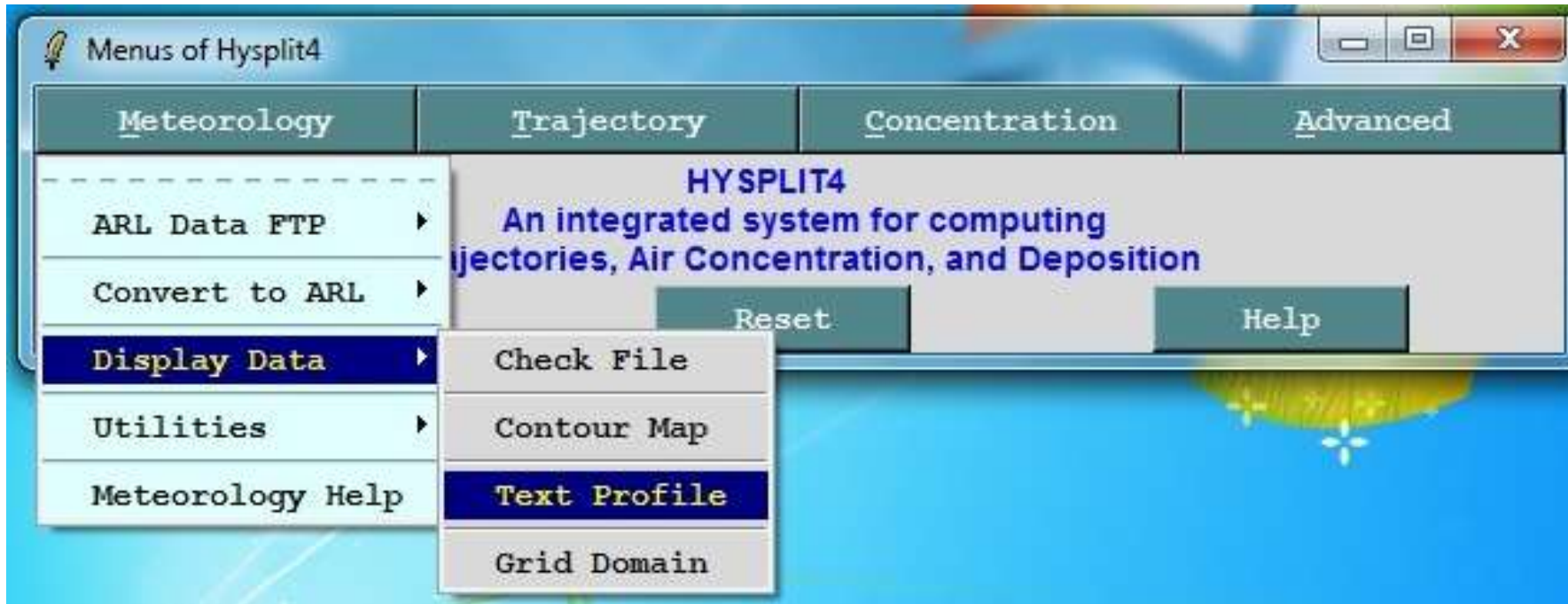
Option 2: if no radiosoundings nearby, use model data from NOAA
off-line



MOLECULAR COMPONENT

How to obtain T and P profiles?

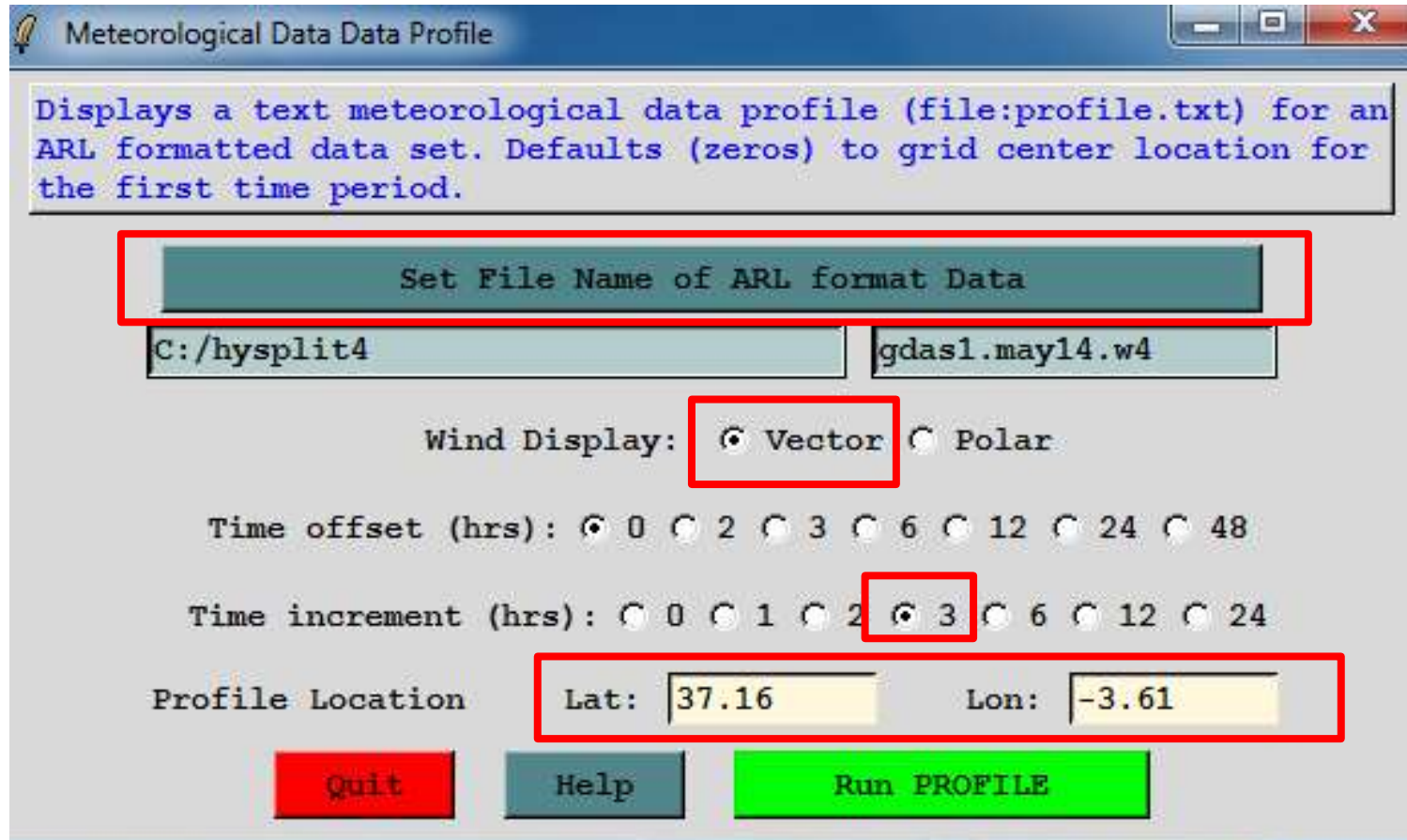
Option 2: if no radiosoundings nearby, use model data from NOAA
off-line



MOLECULAR COMPONENT

How to obtain T and P profiles?

Option 2: if no radiosoundings nearby, use model data from NOAA
off-line



Meteorological Data Data Profile

Displays a text meteorological data profile (file:profile.txt) for an ARL formatted data set. Defaults (zeros) to grid center location for the first time period.

Set File Name of ARL format Data

C:/hysplit4 gdas1.may14.w4

Wind Display: Vector Polar

Time offset (hrs): 0 2 3 6 12 24 48

Time increment (hrs): 0 1 2 3 6 12 24

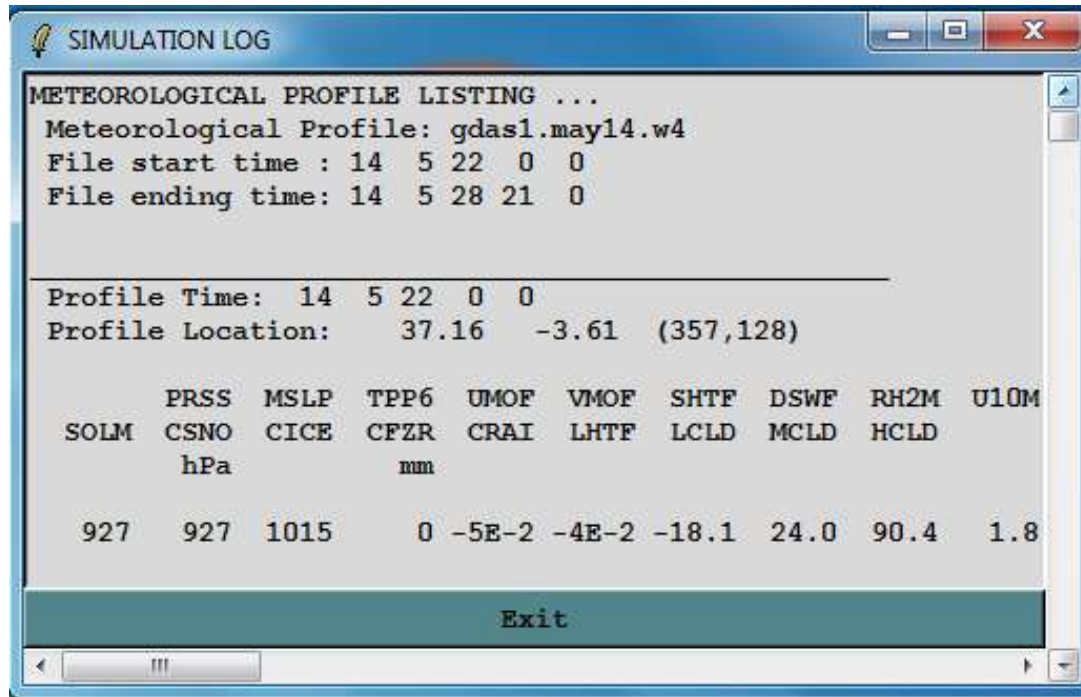
Profile Location Lat: 37.16 Lon: -3.61

Quit Help Run PROFILE

MOLECULAR COMPONENT

How to obtain T and P profiles?

Option 2: if no radiosoundings nearby, use model data from NOAA
off-line



```
SIMULATION LOG
METEOROLOGICAL PROFILE LISTING ...
Meteorological Profile: gdas1.may14.w4
File start time : 14  5 22  0  0
File ending time: 14  5 28 21  0

Profile Time: 14  5 22  0  0
Profile Location:  37.16  -3.61  (357,128)

PRSS  MSLP  TPP6  UMOF  VMOF  SHTF  DSWF  RH2M  U10M
SOLM  CSNO  CICE  CFZR  CRAI  LHTF  LCLD  MCLD  HCLD
      hPa          mm

927   927  1015    0 -5E-2 -4E-2 -18.1  24.0  90.4  1.8

Exit
```

Radiosoundings for the whole week each 3 h are computed

Go to folder: `.../hysplit4/working` to find your file "profile.txt"

MOLECULAR COMPONENT

How to obtain T and P profiles?

Option 3: if no radiosoundings nearby, use standard atmosphere scaled to your surface temperature and pressure

Example: U. S. Standard Atmosphere, 1976

Atmospheric layer(km)	dT/dz (K/km)
0-11	-6.5
11-20	0
20-32	1.0
32-47	2.8
47-51	0
51-71	-2.8
71-86	-2

$$P = P_0 \cdot \exp\left[-\frac{G \cdot (z_g - z_0)}{T_0}\right] \quad \text{if } dT/dz = 0$$

$$P = P_0 \cdot \left[\frac{T_0}{T}\right]^{\frac{G}{dT/dz}} \quad \text{if } dT/dz \neq 0$$

$$G = g \cdot M / R \quad \left\{ \begin{array}{l} g \text{ gravity at sea level} \\ M \text{ mean molecular mass of air} \\ R = 8.31432 \text{ J} \cdot \text{K}^{-1} \cdot \text{mol}^{-1} \end{array} \right.$$

T_0 P_0 z_0 temperature, pressure and height of the layer base

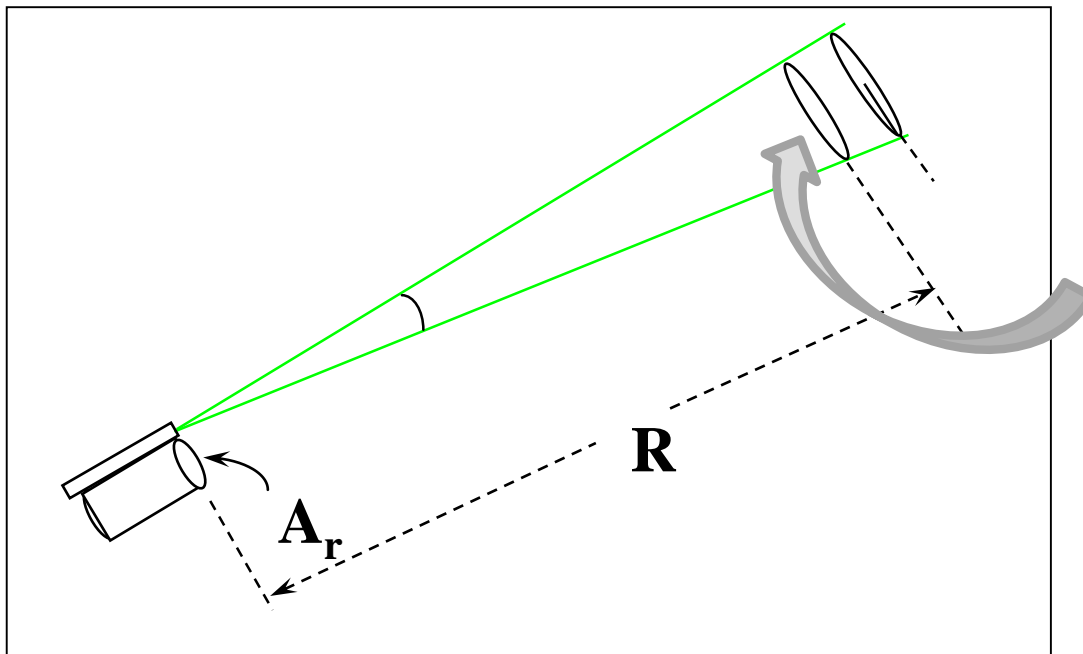
$z_g = z \cdot R_E / (z + R_E)$ geopotential height with Earth's radius: $R_E = 6372795 \text{ m}$



RAMAN METHOD

To solve the problems associated with the elastic backscatter lidar several solutions have been proposed

The Raman lidar measures lidar return signals elastically backscattered by air molecules and particles and inelastically (Raman) backscattered by nitrogen and/or oxygen molecules

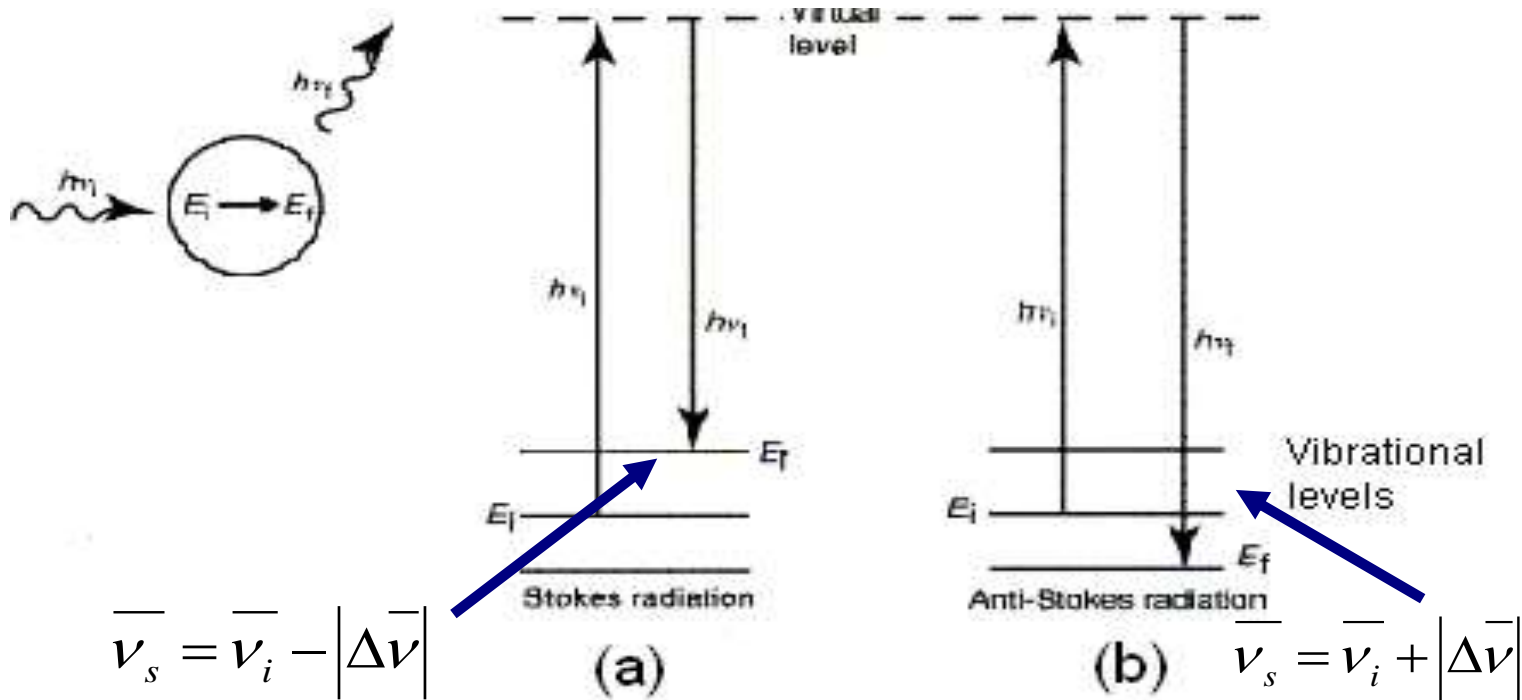


Raman lidar systems detect the wavelength-shifted molecular return produced by rotational and vibrational Raman scattering from the chosen molecule

RAMAN SCATTERING

Elastic scattering : scattered frequency equal to incident one

Raman scattering: scattered frequency shifted in a known amount depending on the scatterers



$$\Delta\bar{\nu} = \bar{\nu}_i - \bar{\nu}_s = \frac{\Delta E}{hc_0}$$

Key: this shift characterizes each molecule

RAMAN SCATTERING

Shifts for N₂ molecule:

Excitation wavelength (nm)	Shifted wavelength (nm)
355	387
488	551
532	607

The strength of Raman signals is a factor of 20 (rotational Raman lines) to 500 (vibration-rotational Raman lines) lower than the one of Rayleigh signals

The Raman lidar is mainly used during nighttime in absence of the strong daylight sky background



RAMAN LIDAR EQUATION

$$P(R, \lambda_{Raman}) = P_0(\lambda_L) \frac{C}{R^2} O(R) \beta_{Raman}(R, \lambda_{Raman}) e^{-\int_0^R [\alpha(x, \lambda_L) + \alpha(x, \lambda_{Raman})] dx}$$

$P(R, \lambda_{Raman})$ = power received by the system after backscattering from range R

$P_0(\lambda_L)$ = power transmitted

C = lidar calibration constant

$\beta_{Raman}(R, \lambda_{Raman})$ ($\text{km}^{-1}\text{sr}^{-1}$) is the Raman molecular backscatter coefficient

$\beta_{part}(R, \lambda_L)$ does not appear in the equation

The only particle scattering effect on the signal strength is the attenuation

$\alpha(R, \lambda_L)$ describes the extinction on the way up to the backscatter region and $\alpha(R, \lambda_{Raman})$ the extinction on the way back to the lidar

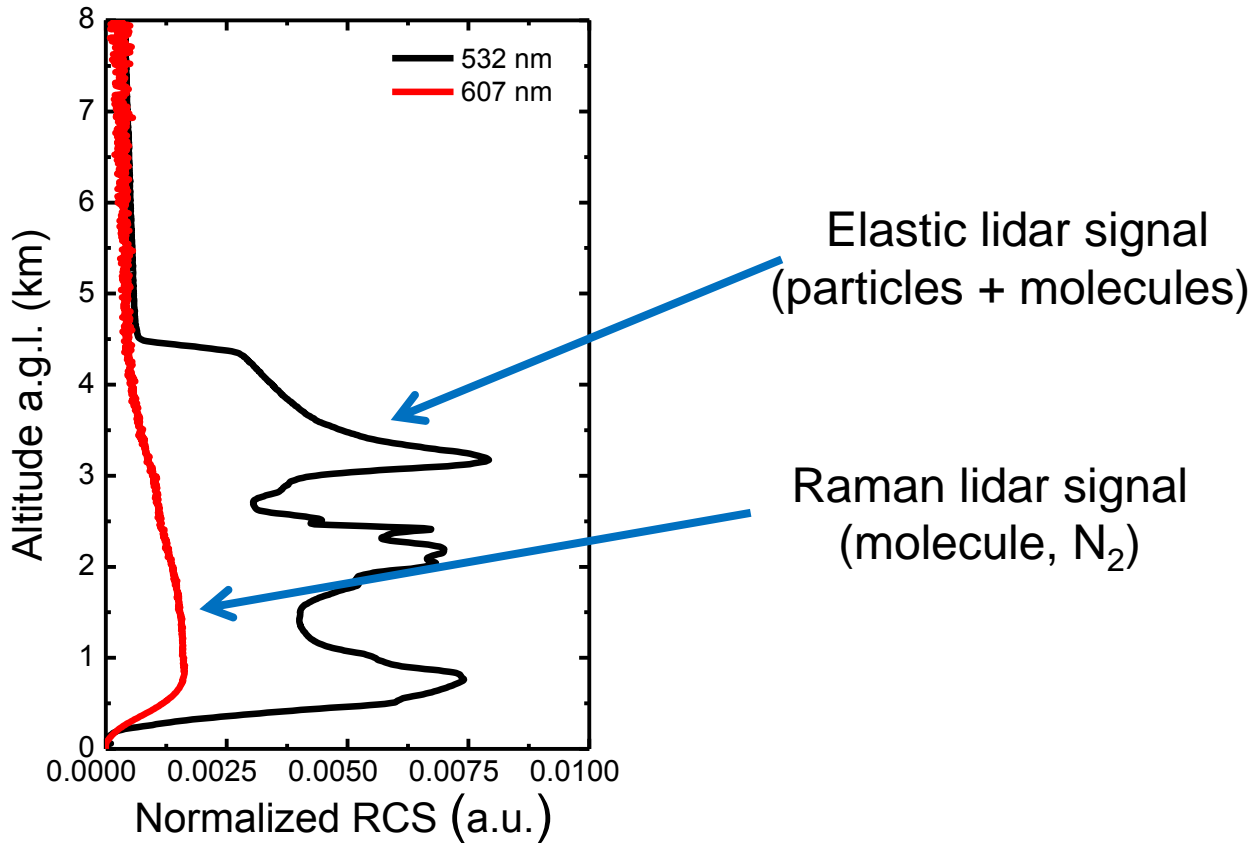




ELASTIC VS. RAMAN LIDAR EQUATION

$$P(R, \lambda_{Raman}) = P_0(\lambda_L) \frac{C_R}{R^2} O(R) \beta_{Raman}(R, \lambda_{Raman}) e^{-\int_0^R [\alpha(x, \lambda_L) + \alpha(x, \lambda_{Raman})] dx}$$

$$P(R, \lambda_L) = P_0(\lambda_L) \frac{C}{R^2} O(R) [\beta_{part}(R, \lambda_L) + \beta_{mol}(R, \lambda_L)] e^{-2 \int_0^R \alpha(x, \lambda_L) dx}$$



RAMAN METHOD: PARTICLE EXTINCTION

Starting point: Raman lidar equation

$$P(R, \lambda_{Raman}) = P_0(\lambda_L) \frac{C}{R^2} O(R) \beta_{Raman}(R, \lambda_{Raman}) e^{-\int_0^R [\alpha(x, \lambda_L) + \alpha(x, \lambda_{Raman})] dx}$$

... some considerations:

- the overlap is assumed to be complete, $O(R) = 1 \rightarrow R \geq R_{min}$
- $\beta_{Raman}(R, \lambda_{Raman})$ is calculated from the molecular number density N_{Raman} which is the N_2 or O_2 molecule number density and the Raman backscatter cross section:

$$\beta_{Raman}(R, \lambda_{Raman}) = N_{Raman}(R) \cdot \frac{d\sigma_{Raman}}{d\Omega}(\pi, \lambda_{Raman})$$

- $N_{Raman}(R)$ is calculated from actual radio-sounding observations or standard atmosphere temperature and pressure profiles



RAMAN METHOD: PARTICLE EXTINCTION

After some operation on the Raman lidar equation that include the use of the Raman backscatter coefficient and the logarithm derivation of the equation, we obtain:

$$\alpha(R, \lambda_L) + \alpha(R, \lambda_{Raman}) = \frac{d}{dR} \ln \left[\frac{N_{Raman}(R)}{R.C.S.(R, \lambda_{Raman})} \right]$$

Total extinction coefficients are caused by particles and molecules. Therefore, the particle extinction coefficient is:

$$\begin{aligned} \alpha_{part}(R, \lambda_L) + \alpha_{part}(R, \lambda_{Raman}) &= \\ &= \frac{d}{dR} \ln \left[\frac{N_{Raman}(R)}{R.C.S.(R, \lambda_{Raman})} \right] - \alpha_{mol}(R, \lambda_L) - \alpha_{mol}(R, \lambda_{Raman}) \end{aligned}$$



RAMAN METHOD: PARTICLE EXTINCTION

To obtain the particle extinction coefficient at the transmitted wavelength we have to introduce the k-exponent which describes the wavelength dependence of the particle extinction coefficient for this spectral range:

$$\alpha_{part}(\lambda) \propto \lambda^{-k} \Rightarrow \alpha_{part}(\lambda_L) = \alpha_{part}(\lambda_{Raman}) \left(\lambda_L / \lambda_{Raman} \right)^{-k}$$

$k \approx 1$ for particles at these “small” spectral ranges $[\lambda_L, \lambda_{Raman}]$

[355, 387] nm

[532, 607] nm

Solution:

$$\alpha_{part}(R, \lambda_L) = \frac{\frac{d}{dR} \ln \left[\frac{N_{Raman}(R)}{R.C.S.(R, \lambda_{Raman})} \right] - \alpha_{mol}(R, \lambda_L) - \alpha_{mol}(R, \lambda_{Raman})}{1 + \left(\frac{\lambda_L}{\lambda_{Raman}} \right)^k}$$

(without any assumption on Lr_{part})



RAMAN METHOD: PARTICLE BACKSCATTER

Because now $\alpha_{\text{part}}(R)$ is known, $\beta_{\text{part}}(R)$ can also be calculated using the elastic lidar equation

Elastic lidar equation:

$$P(R, \lambda_L) = P_0(\lambda_L) \frac{C}{R^2} O(R) [\beta_{\text{part}}(R, \lambda_L) + \beta_{\text{mol}}(R, \lambda_L)] e^{-2 \int_0^R \alpha(x, \lambda_L) dx}$$

Raman lidar equation:

$$P(R, \lambda_{\text{Raman}}) = P_0(\lambda_L) \frac{C_R}{R^2} O(R) \beta_{\text{Raman}}(R, \lambda_{\text{Raman}}) e^{-\int_0^R [\alpha(x, \lambda_L) + \alpha(x, \lambda_{\text{Raman}})] dx}$$

where
$$\beta_{\text{Raman}}(R, \lambda_{\text{Raman}}) = N_{\text{Raman}}(R) \cdot \frac{d\sigma_{\text{Raman}}}{d\Omega}(\pi, \lambda_{\text{Raman}})$$

By forming the ratio:
$$\frac{P(R, \lambda_L) P(R_0, \lambda_{\text{Raman}})}{P(R_0, \lambda_L) P(R, \lambda_{\text{Raman}})}$$



RAMAN METHOD: PARTICLE BACKSCATTER

Inserting the respective lidar equations and rearranging the resulting equation, the solution is:

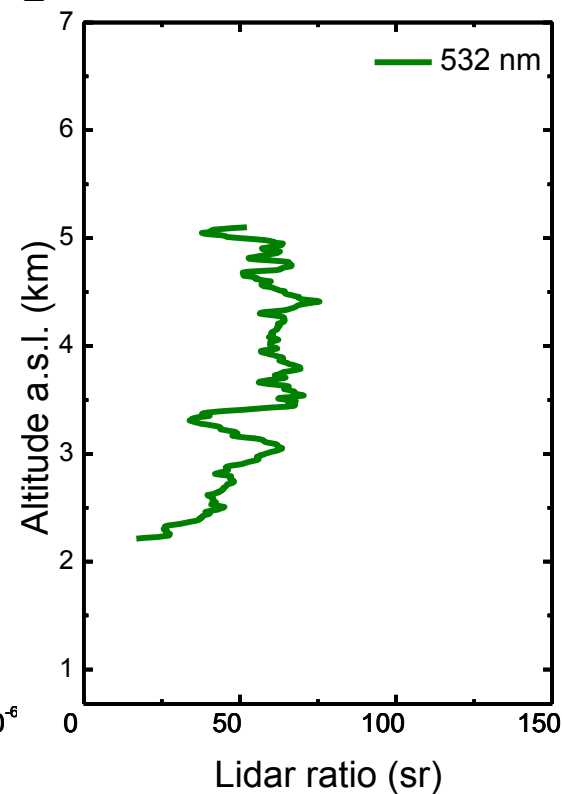
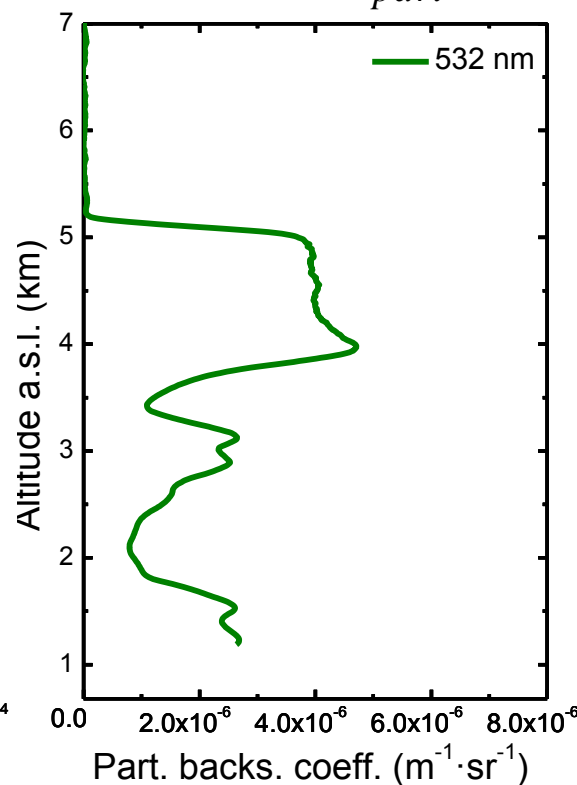
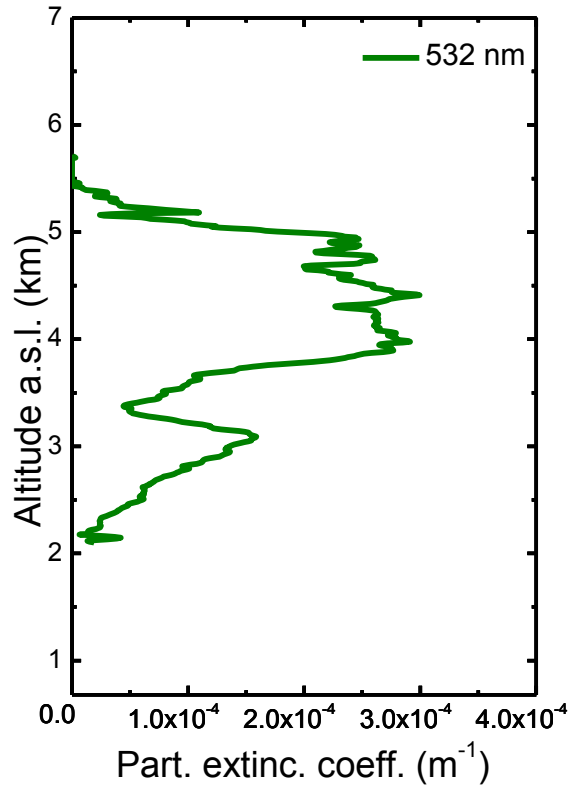
$$\beta_{part}(R, \lambda_L) = -\beta_{mol}(R, \lambda_L) + \left\{ \beta_{part}(R_0, \lambda_L) + \beta_{mol}(R_0, \lambda_L) \right\} \frac{P(R, \lambda_L) P(R_0, \lambda_{Raman}) N_{Raman}(R)}{P(R_0, \lambda_L) P(R, \lambda_{Raman}) N_{Raman}(R_0)} \frac{\exp \left\{ - \int_{R_0}^R [\alpha_{part}(x, \lambda_{Raman}) + \alpha_{mol}(x, \lambda_{Raman})] dx \right\}}{\exp \left\{ - \int_{R_0}^R [\alpha_{part}(x, \lambda_L) + \alpha_{mol}(x, \lambda_L)] dx \right\}}$$

- overlap effects cancel out because β_{part} is determined from the ratio of two lidar equations: β_{part} is determined even at R very close to the lidar
- the air density, β_{mol} and α_{mol} must be estimated from measured or standard atmosphere profiles of pressure and temperature
- lidar signals are measured by the instrument
- as in the Klett method, a reference value for β_{part} at R_0 must be estimated. It is recommended to choose R_0 in the upper troposphere where particle scattering is negligible compared to Rayleigh scattering

RAMAN METHOD: LIDAR RATIO

Finally, the height profile of the particle lidar ratio can be derived through the independent determination of α_{part} and β_{part} :

$$L_{part}(R, \lambda_L) = \frac{\alpha_{part}(R, \lambda_L)}{\beta_{part}(R, \lambda_L)}$$



SUMMARY ON RAMAN METHOD

- The Raman method allows for independently determining the $\alpha_{\text{part}}(R)$ and $\beta_{\text{part}}(R)$, and therefore also $L_{\text{part}}(R)$
- Lidar ratio assumptions or other critical assumptions are not needed
- The reference range R_0 is usually chosen such that β_{part} at R_0 is negligible compared to the known β_{mol}
- β_{part} can be obtained even at altitudes very close to the lidar, due to overlap effects are canceled out because β_{part} is determined from the ratio of two lidar equations
- Multiwavelength Raman lidar provides this information at several wavelengths. The “multiwavelength” information allows obtaining particle microphysical properties



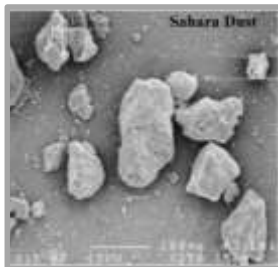
LIDAR DEPOLARIZATION

- A fundamental principle of light is that the electric field **E**-vector of the electromagnetic wave at any instant of time displays some orientation in space
- This orientation can be fixed (linearly polarized light), rotating with time (circularly or elliptically polarized light) and randomly changing with time (natural light). Importantly, any state of polarization can be converted to any other state with the help of a set of optical devices
- Pulsed lasers generally used in lidars produce linearly polarized light
- The lidar depolarization technique involves the transmission of a linearly polarized laser pulse and the detection via a beam splitter of the perpendicular and parallel planes of polarization of the backscattered light



LIDAR DEPOLARIZATION

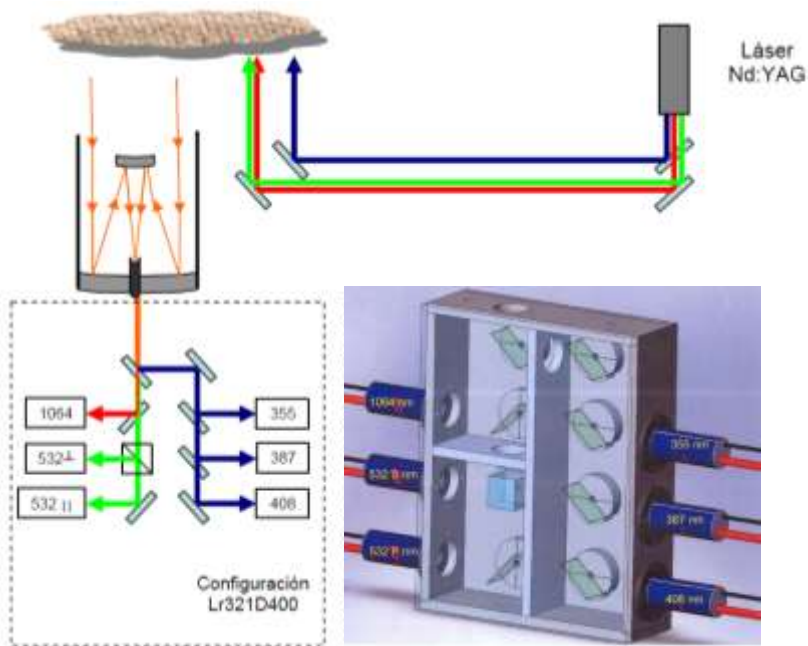
- According to Mie theory, spherical particles always backscatter linearly polarized electromagnetic radiation in the same (incident) plane of polarization. A variety of approximate scattering theories predict that non-spherical particles introduce a depolarized component into the backscattered radiation
- Application of depolarization measurements is discrimination of spherical versus non-spherical aerosol particles and liquid and solid phase clouds



LIDAR DEPOLARIZATION

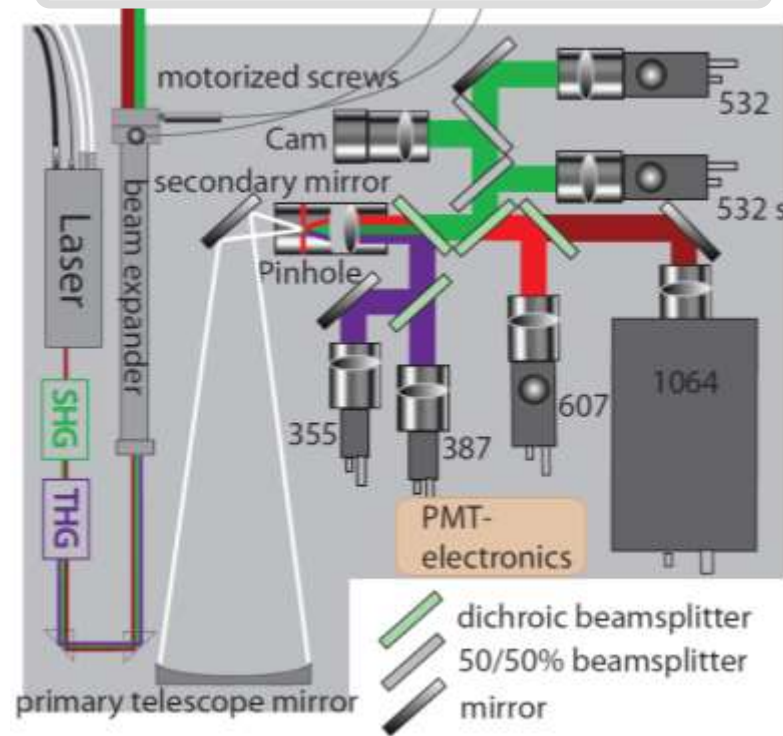
Types of depolarization lidar systems

Detection perpendicular and parallel



Granada lidar (MULHACÉN)

Detection perpendicular and total



Évora lidar (PAOLI)

LIDAR DEPOLARIZATION

Starting point: elastic lidar equation

$$P(R, \lambda) = P_o(\lambda) \frac{C}{R^2} O(R) \beta(R, \lambda) e^{-2 \int_0^R \alpha(x, \lambda) dx}$$

Lidars use polarized light, and many of them are able to discriminate between components. The elastic lidar equations for both components are (dropping the wavelength dependence):

$$P^{\parallel}(R) = P_o \frac{C^{\parallel}}{R^2} O(R) \beta^{\parallel}(R) e^{-2 \int_0^R \alpha^{\parallel}(x) dx}$$

$$P^{\perp}(R) = P_o \frac{C^{\perp}}{R^2} O(R) \beta^{\perp}(R) e^{-\int_0^R [\alpha^{\parallel}(x) + \alpha^{\perp}(x)] dx}$$

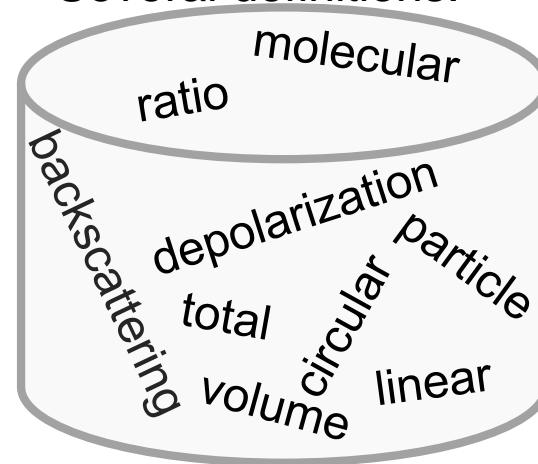
Initial definition of “depolarization ratio”:

$$" \delta(R) " = \frac{C^{\perp} \beta^{\perp}(R) e^{-\int_0^R [\alpha^{\parallel}(x) + \alpha^{\perp}(x)] dx}}{C^{\parallel} \beta^{\parallel}(R) e^{-2 \int_0^R \alpha^{\parallel}(x) dx}} = \frac{\beta^{\perp}(R)}{\beta^{\parallel}(R)} e^{\int_0^R [\alpha^{\parallel}(x) - \alpha^{\perp}(x)] dx} \approx \frac{\beta^{\perp}(R)}{\beta^{\parallel}(R)}$$



LIDAR DEPOLARIZATION

Several definitions:



Mess came from the beginning:

- different instrumental setups
- different research interests



1-. Volume linear depolarization ratio:

$$\delta_v(R) = \frac{\beta^\perp(R)}{\beta^\parallel(R)} = \frac{\beta_{part}^\perp(R) + \beta_{mol}^\perp(R)}{\beta_{part}^\parallel(R) + \beta_{mol}^\parallel(R)} = \frac{C^\parallel}{C^\perp} \frac{P^\perp(R)}{P^\parallel(R)} = K_{cal} \frac{P^\perp(R)}{P^\parallel(R)}$$

Features:

- components: particles and molecules
- signals: cross and parallel
- no processing on raw data
- no overlap effects



LIDAR DEPOLARIZATION

Table of depolarization's parameters

Parameter	Symbol	Features	Formula
volume linear depolarization ratio	δ_v	Part.+mol ; cross and parallel; raw data	-
volume linear depolarization ratio (total)			
particle linear depolarization ratio			
particle linear depolarization ratio (total)			

2-. Volume linear depolarization ratio (total):

$$\delta_v^{total}(R) = \frac{\beta^\perp(R)}{\beta^{total}(R)} = \frac{\beta^\perp(R)}{\beta^\perp(R) + \beta^\parallel(R)} = \frac{\beta_{part}^\perp(R) + \beta_{mol}^\perp(R)}{\beta_{part}^\perp(R) + \beta_{mol}^\perp(R) + \beta_{part}^\parallel(R) + \beta_{mol}^\parallel(R)} =$$

$$= \frac{C^{total}}{C^\perp} \frac{P^\perp(R)}{P^{total}(R)} = K_{cal} \frac{P^\perp(R)}{P^{total}(R)}$$

... definitions of δ_v and δ_v^{total} :

$$\left. \begin{aligned} \delta_v(R) &= \frac{\beta^\perp(R)}{\beta^\parallel(R)} \\ \delta_v^{total}(R) &= \frac{\beta^\perp(R)}{\beta^\perp(R) + \beta^\parallel(R)} \end{aligned} \right\} \rightarrow \delta_v^{total}(R) = \frac{\delta_v(R)}{\delta_v(R) + 1}$$

Features:

- components: part. and mol.
- signals: cross and total
- no processing on raw data
- no overlap effects



LIDAR DEPOLARIZATION

Table of depolarization's parameters

Parameter	Symbol	Features	Formula
volume linear depolarization ratio	δ_v	Part.+mol; cross and parallel; raw data	-
volume linear depolarization ratio (total)	δ_v^{total}	Part.+mol ; cross and total; raw data	$\delta_v^{total}(R) = \frac{\delta_v(R)}{\delta_v(R)+1}$
particle linear depolarization ratio			
particle linear depolarization ratio (total)			

3-. Particle linear depolarization ratio:

$$\delta_{part}(R) = \frac{\beta_{part}^{\perp}(R)}{\beta_{part}^{\parallel}(R)} = \frac{R_{backs} \delta_v (\delta_{mol} + 1) - \delta_{mol} (\delta_v + 1)}{R_{backs} (\delta_{mol} + 1) - (\delta_v + 1)}$$

$$R_{backs} = \frac{\beta_{part} + \beta_{mol}}{\beta_{mol}} \quad \text{backscattering ratio (range dependent)}$$

$$\delta_{mol} = \frac{\beta_{mol}^{\perp}}{\beta_{mol}^{\parallel}} \quad \text{molecular depolarization (range independent)}$$

Features:

- components: particles
- signals: cross and parallel
- retrieved backscatter coeff.
- overlap effects if K-F is used



LIDAR DEPOLARIZATION

Table of depolarization's parameters

Parameter	Symbol	Features	Formula
volume linear depolarization ratio	δ_v	Part.+mol; cross and parallel; raw data	-
volume linear depolarization ratio (total)	δ_v^{total}	Part.+mol ; cross and total; raw data	$\delta_v^{total} = \frac{\delta_v}{\delta_v + 1}$
particle linear depolarization ratio	δ_{part}	Part. ; cross and parallel; retrieved data	$\delta_{part} = \frac{R_{backs} \delta_v (\delta_{mol} + 1) - \delta_{mol} (\delta_v + 1)}{R_{backs} (\delta_{mol} + 1) - (\delta_v + 1)}$
particle linear depolarization ratio (total)			

4-. Particle linear depolarization ratio (total):

$$\delta_{part}^{total}(R) = \frac{\beta_{part}^{\perp}(R)}{\beta_{part}^{total}(R)} = \frac{R_{backs} \delta_v (\delta_{mol} + 1) - \delta_{mol} (\delta_v + 1)}{(\delta_{mol} + 1)(\delta_v + 1)(R_{backs} - 1)}$$

Features:

- components: particles
- signals: cross and total
- retrieved backscatter coeff.
- overlap effects if K-F is used

... definitions of δ_{part} and δ_{part}^{total} :

$$\left. \begin{aligned} \delta_{part}(R) &= \frac{\beta_{part}^{\perp}(R)}{\beta_{part}^{\parallel}(R)} \\ \delta_{part}^{total}(R) &= \frac{\beta_{part}^{\perp}(R)}{\beta_{part}^{total}(R)} \end{aligned} \right\} \rightarrow \delta_{part}^{total}(R) = \frac{\delta_{part}(R)}{\delta_{part}(R) + 1}$$



LIDAR DEPOLARIZATION

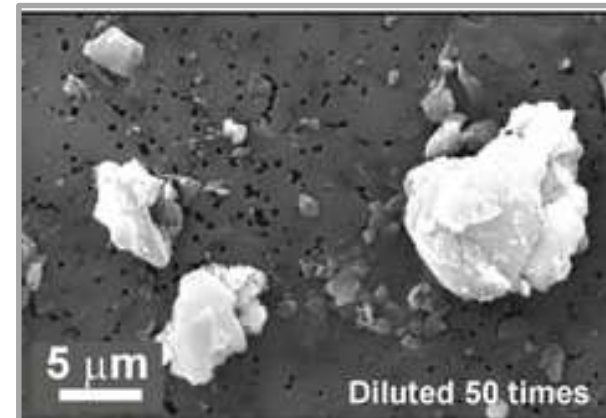
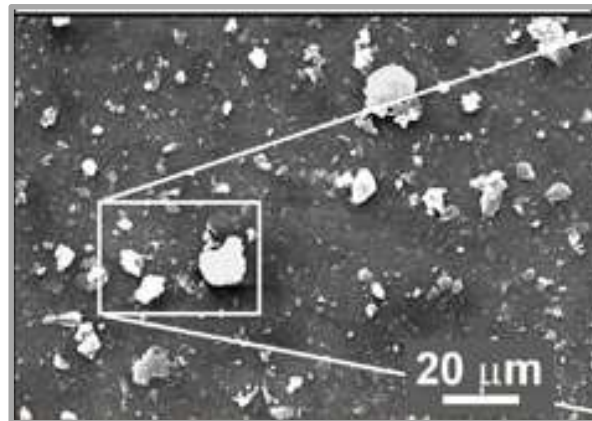
Summary of depolarization's parameters

Parameter	Symbol	Features	Formula
volume linear depolarization ratio	δ_v	Part.+mol; cross and parallel; raw data	-
volume linear depolarization ratio (total)	δ_v^{total}	Part.+mol ; cross and total; raw data	$\delta_v^{total} = \frac{\delta_v}{\delta_v + 1}$
particle linear depolarization ratio	δ_{part}	Part. ; cross and parallel; retrieved data	$\delta_{part} = \frac{R_{backs} \delta_v (\delta_{mol} + 1) - \delta_{mol} (\delta_v + 1)}{R_{backs} (\delta_{mol} + 1) - (\delta_v + 1)}$
particle linear depolarization ratio (total)	δ_{part}^{total}	Part. ; cross and total; retrieved data	$\delta_{part}^{total} = \frac{R_{backs} \delta_v (\delta_{mol} + 1) - \delta_{mol} (\delta_v + 1)}{(\delta_{mol} + 1)(\delta_v + 1)(R_{backs} - 1)}$



LIDAR DEPOLARIZATION

- great range of aerosol shapes
- many aerosols consist of spherical particles: very small aerosols (small size parameter), anthropogenic aerosols, volcanic acid sulfuric droplets, sea drops released by the action of wind on water waves... All shows low volume linear depolarization ratio
- irregularly shaped aerosols (particularly volcanic and desert dusts and partially crystallized acid droplets) show larger volume linear depolarization ratio



LIDAR DEPOLARIZATION



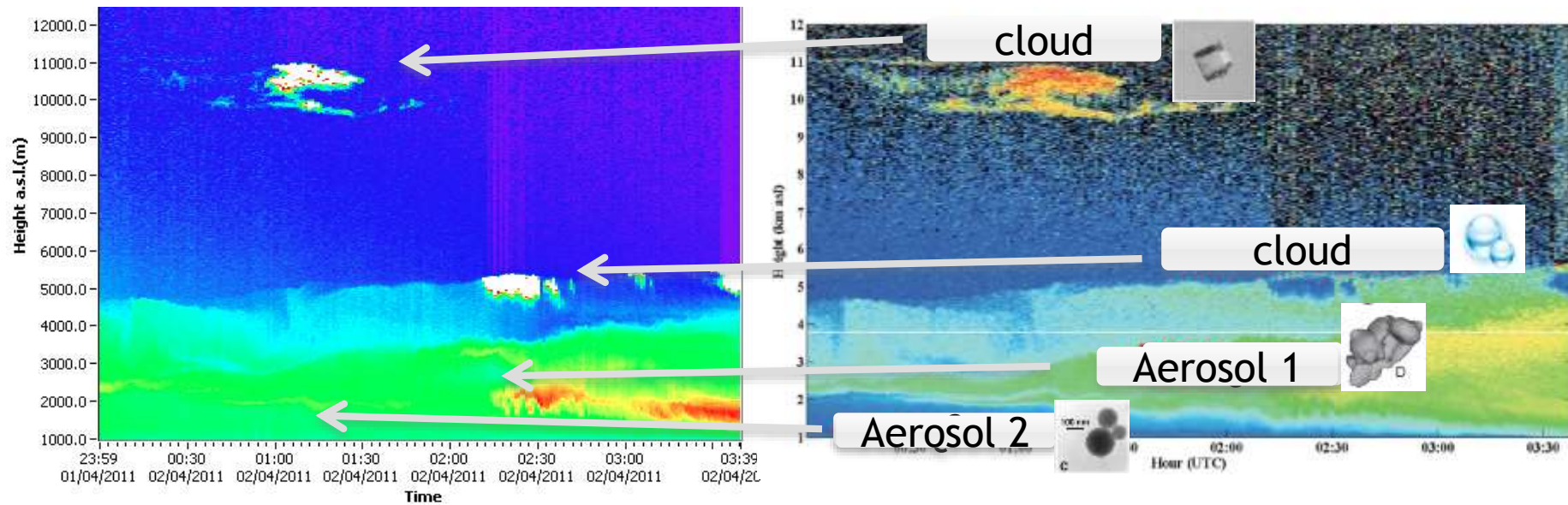
Aerosol type	Volume linear depol. ratio
arctic haze	~ 0.013
PBL (anthropogenic)	0.02-0.10
ammonium sulfate droplets	0.02
ammonium sulfate after crystallization	0.10-0.12
NaCl droplets partially crystallized	0.06-0.12
desert dust (Sahara)	~ 0.15-0.30
desert dust (Gobbi)	~ 0.18
desert dust (Taklamakan)	0.11-0.19

LIDAR DEPOLARIZATION



R.C.S. 532 nm

Volume linear depolarization ratio

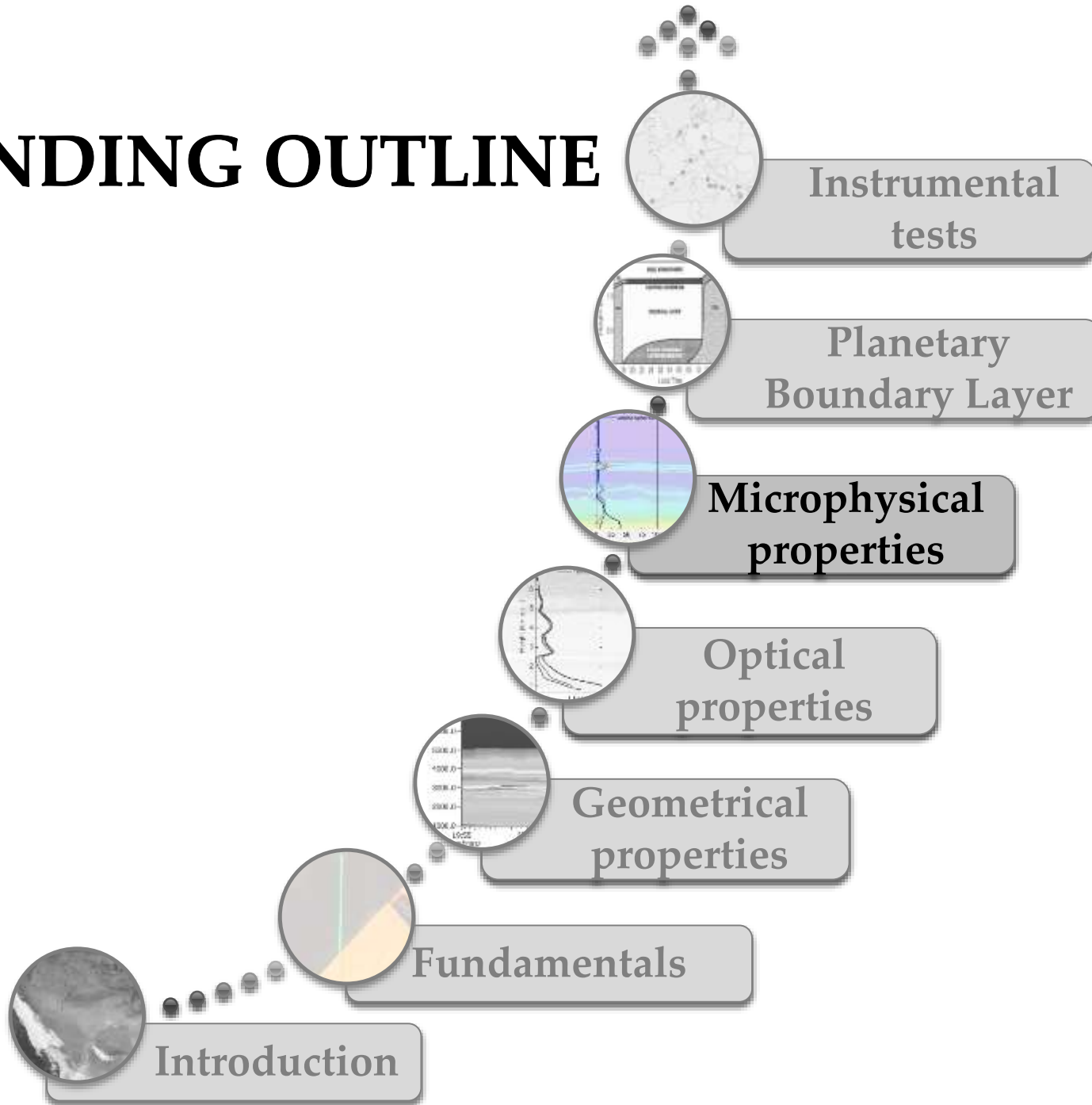


SUMMARY ON LIDAR DEPOLARIZATION

- The lidar depolarization technique is based on the fact that spherical particles always backscatter linearly polarized electromagnetic radiation in the same plane of polarization, whereas non-spherical particles introduce a depolarized component into the backscattered radiation
- Due to the different definitions for depolarization parameters, it's necessary to clarify what is used (parallel vs. total; particles vs. particles+molecules)
- Mainly, spherical particles show $\delta_v < 0.10$ and non-spherical particles show $\delta_v \sim 0.15-0.30$



ASCENDING OUTLINE



MICROPHYSICAL PROPERTIES

In nature, particle size distributions can be described rather well by analytic expressions such as logarithmic-normal distributions:

$$dn(r) = \frac{n_t}{\sqrt{2\pi} \ln \sigma} \exp \left[-\frac{(\ln r - \ln r_{\text{mod},N})^2}{2 (\ln \sigma)^2} \right] d \ln r$$

- $dn(r)$ number concentration of particles in the radius interval $[\ln r, \ln r + d \ln r]$
- n_t total number concentration
- $n_{\text{mod},N}$ mode radius with respect to the number concentration
- σ mode width (geometric standard deviation)

This is a monomodal distribution, however multimodal distributions (i.e. sum of ≥ 2 monomodal distributions) can be found



MICROPHYSICAL PROPERTIES

From the number concentration, other distributions can be obtained:

Number concentration distribution:

$$dn(r) = \frac{n_t}{\sqrt{2\pi} \ln \sigma} \exp \left[-\frac{(\ln r - \ln r_{\text{mod,N}})^2}{2 (\ln \sigma)^2} \right] d \ln r$$

Surface-area concentration distribution: $da(r) = 4\pi r^2 dn(r)$

Volume concentration distribution: $dv(r) = \frac{4}{3} \pi r^3 dn(r)$

Integrated properties of the particle ensemble determined from the inverted distributions are:

Effective radius:	Total surface-area concentration:	Total volume concentration:
$r_{\text{eff}} = \frac{\int n(r) r^3 dr}{\int n(r) r^2 dr}$	$a_t = 4\pi \int n(r) r^2 dr$	$v_t = \frac{4\pi}{3} \int n(r) r^3 dr$



MICROPHYSICAL PROPERTIES

A variety of methods have been proposed since the early 1970s. Examples:

Combined use of elastic lidar with other instruments

IF SUNPHOTOMETER IS USED:

- the drawback is that two colocated instruments are needed simultaneously to provide reliable data on the same particles
- different observational geometry of the instrumentation
- thus represents an additional source
- only daytime data

Inversion with regularization from Raman lidar

- uses the spectral information contained in the backscatter and extinction profiles at several wavelengths and its change with the particle size
- limitation in number of wavel.
- in most cases only night time data
- high data quality





METHOD OF INVERSION WITH REGULATIZATION

It is the standard method for the retrieval of particle microphysical properties from multiwavelength Raman lidar observations

Input: spectrally resolved particle backscatter and extinction coefficients

The optical data are related to the physical quantities by the Fredholm integral equations of the first kind:

$$g_i(\lambda_k) = \int_{r_{\min}}^{r_{\max}} K_i(r, m, \lambda_k, s) v(r) dr + \varepsilon_i^{\text{exp}}(\lambda_k)$$

$$i = \beta_{aer}, \alpha_{aer}, \quad k = 1, \dots, n$$



METHOD OF INVERSION WITH REGULATIZATION

$$g_i(\lambda_k) = \int_{r_{\min}}^{r_{\max}} K_i(r, m, \lambda_k, s) v(r) dr + \varepsilon_i^{\text{exp}}(\lambda_k)$$

$$i = \beta_{aer}, \alpha_{aer}, \quad k = 1, \dots, n$$

- $g_i(\lambda_k)$ optical data at wavelengths λ_k at a specific height R
- i kind of information, i.e., whether it is the particle backscatter or extinction coefficient
- k wavelength: 355, 532 and 1064 nm
- $\varepsilon_i^{\text{exp}}(\lambda_k)$ experimental error of backscatter or extinction coefficients



METHOD OF INVERSION WITH REGULATIZATION

$$g_i(\lambda_k) = \int_{r_{\min}}^{r_{\max}} K_i(r, m, \lambda_k, s) v(r) dr + \varepsilon_i^{\text{exp}}(\lambda_k)$$

$$i = \beta_{aer}, \alpha_{aer}, \quad k = 1, \dots, n$$

$K_i(r, m, \lambda_k, s)$ kernel functions of backscatter and extinction, depending on radius, complex refractive index, wavelength and shape of particles

For spherical particles, are calculated from the respective extinction and backscatter efficiencies for individual particles weighted with their geometrical cross section πr^2

$$K_i(r, m, \lambda, s) = \frac{3}{4r} Q_i(r, m, \lambda)$$

$v(r)$ volume concentration distribution of particles



METHOD OF INVERSION WITH REGULATIZATION

$$g_i(\lambda_k) = \int_{r_{\min}}^{r_{\max}} K_i(r, m, \lambda_k, s) v(r) dr + \varepsilon_i^{\text{exp}}(\lambda_k)$$
$$i = \beta_{aer}, \alpha_{aer}, \quad k = 1, \dots, n$$

r_{\min}

radius down to which particles are optically efficient. For measurements ≥ 355 nm (typical in lidars), the minimum particle size is 50 nm (in radius)

r_{\max}

radius at which concentrations are so low that particles no longer contribute significantly to the signal (typically ≤ 10 microns in troposphere)



METHOD OF INVERSION WITH REGULATIZATION

To simplify, the subscript p will be used summarizing the kind and wavelength of optical data:

$$g_p = \int_{r_{\min}}^{r_{\max}} K_p(r, m) v(r) dr + \varepsilon_p^{\text{exp}} \quad \text{where } p = (i, \lambda_k)$$

- it can not be solved analytically
- the microphysical retrieval from lidars is an ill-posed inverse problem
- incompleteness of the available information: small number of wavelengths and only backscatter and extinction information is available
- non-uniqueness of the solutions: highly complex structure of tropospheric aerosols (maybe multimodal, of variable shape, particle refractive index can be wavelength-dependent)



METHOD OF INVERSION WITH REGULATIZATION

- even uncertainties as small as round-off errors in the input data lead to disproportionately large changes in the final solution
- measurement errors are much larger than round-off errors
- different combinations of microphysical parameters may lead to similar optical properties within the measurement uncertainty
- many improvements have been done during the last decade. The most important: the reduction of measurement wavelengths to a realistic number
- the **minimum number of wavelengths is three** (355, 532 and 1064 nm) assuming simplifications for complex refractive index: the so-called 3+2 lidar systems (3 backscatters, 2 extinctions)
- the accuracy increases if backscatter up to six wavelengths are used

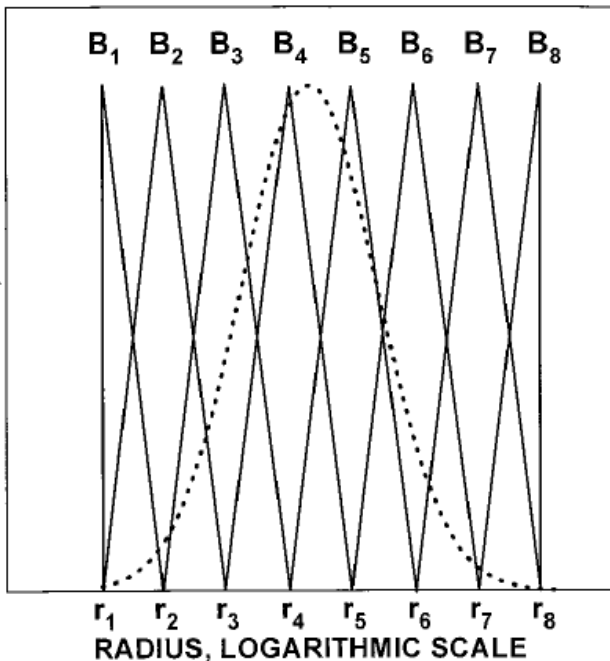


METHOD OF INVERSION WITH REGULATIZATION

To solve the equation:
$$g_p = \int_{r_{\min}}^{r_{\max}} K_p(r, m) v(r) dr + \varepsilon_p^{\text{exp}} \quad \text{where } p = (i, \lambda_k)$$

... $v(r)$ is discretized by a linear combination of triangular base functions $B_j(r)$ and weight factors w_j as ...

$$v(r) = \sum_j w_j B_j(r) + \varepsilon^{\text{math}}(r)$$



- $\varepsilon^{\text{math}}(r)$ is the mathematical residual error caused by the approximation with base functions
- $B_j(r)$ are distributed equidistantly on a logarithmic scale (to reproduce the high dynamic range of particle size distributions)
- minimum number of $B_j(r)$ is the number of input parameters
- typical number of $B_j(r)$ is 8



METHOD OF INVERSION WITH REGULATIZATION

In general the exact position of the investigated particle size distribution over the size range used is not known

To solve this: used of a inversion window of variable width and variable position over the investigated size range

No sensible solutions are obtained if the inversion window does not cover the position of the investigated particle size distribution

Currently 50 different inversion windows within the particle size range from 0.01 to 10 μm are used to obtain an estimate of the position of the particle size distribution



METHOD OF INVERSION WITH REGULATIZATION

Rewriting the equations into a vector-matrix equation:

$$\mathbf{g} = \mathbf{A}\mathbf{w} + \boldsymbol{\varepsilon}$$

$\mathbf{g} = [g_p]$
 optical data

$\mathbf{A} = [A_{pj}]$
 weight matrix

$$A_{pj}(m) = \int_{r_{\min}}^{r_{\max}} K_p(r, m) B_j(r) dr$$

$\mathbf{w} = [w_j]$
 weight factors

$\boldsymbol{\varepsilon} = [\varepsilon_p]$
 errors

$$\varepsilon_p = \varepsilon_p^{\text{exp}} + \varepsilon_p^{\text{math}}$$

The simple solution of this equation for the weight factors is:

$$\mathbf{w} = \mathbf{A}^{-1} \mathbf{g} + \boldsymbol{\varepsilon}'$$



METHOD OF INVERSION WITH REGULATIZATION

$$\mathbf{w} = \mathbf{A}^{-1} \mathbf{g} + \boldsymbol{\varepsilon}'$$

It fails to provide reasonable results although the optical data can be reproduced within the error limits $\boldsymbol{\varepsilon}$. Why?

High dynamic range of several orders of magnitude of the elements of \mathbf{A} and \mathbf{A}^{-1}

The term $\boldsymbol{\varepsilon}' = -\mathbf{A}^{-1} \boldsymbol{\varepsilon}$, which describes the respective errors, and \mathbf{A}^{-1} , which denotes the inverse of the matrix \mathbf{A} , lead to error amplification of the solutions

How to solve it? Application of a procedure called regularization



METHOD OF INVERSION WITH REGULATIZATION

Procedure of regularization: it is used to reduce the number of solutions by restricting the highest acceptable difference between the vector \mathbf{Aw} and \mathbf{g} :

$$e^2 \geq \|\varepsilon\|^2 = \|\mathbf{Aw} - \mathbf{g}\|^2$$

Only solutions that minimize ε are accepted

However, due to smoothed size distributions are expected, the penalty function $\Gamma(v)$ is introduced and the minimization problem is rewritten as:

$$e^2 \geq \|\varepsilon\|^2 = \|\mathbf{Aw} - \mathbf{g}\|^2 + \gamma\Gamma(v)$$

where $\Gamma(v) = \mathbf{w}^T \mathbf{H} \mathbf{w}$

transposed
vector \mathbf{w}

$$\mathbf{H} = \begin{bmatrix} 1 & -2 & 1 & 0 & 0 & 0 & 0 & 0 \\ -2 & 5 & -4 & 1 & 0 & 0 & 0 & 0 \\ 1 & -4 & 6 & -4 & 1 & 0 & 0 & 0 \\ 0 & 1 & -4 & 6 & -4 & 1 & 0 & 0 \\ 0 & 0 & 1 & -4 & 6 & -4 & 1 & 0 \\ 0 & 0 & 0 & 1 & -4 & 6 & -4 & 1 \\ 0 & 0 & 0 & 0 & 1 & -4 & 5 & -2 \\ 0 & 0 & 0 & 0 & 0 & 1 & -2 & 1 \end{bmatrix}$$



METHOD OF INVERSION WITH REGULATIZATION

Therefore...

$$\mathbf{w} = (\mathbf{A}^T \mathbf{A} + \gamma \mathbf{H})^{-1} \mathbf{A}^T \mathbf{g}$$

The final solution is:

$$v(r) = \sum_j w_j B_j(r)$$

Errors:

effective radius: ~20%

volume and surface-area concentrations: $\pm 50\%$

real part of the complex refractive index: ± 0.05 ,

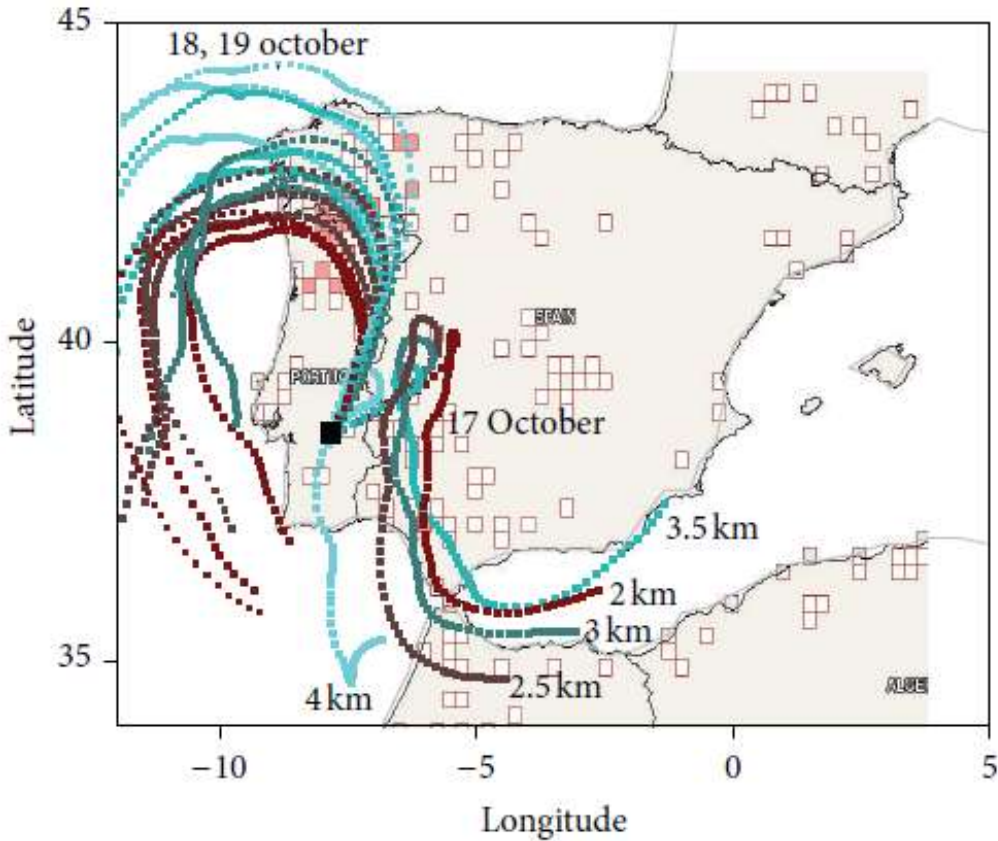
imaginary part: $\pm 50\%$

number concentrations $> \pm 50\%$



METHOD OF INVERSION WITH REGULATIZATION

An example of forest fire smoke (17/10/2011):



$\bar{R}_{\text{eff}} (\mu\text{m})$	0.15 ± 0.03	(20%)
$S (\mu\text{m}^2 \text{cm}^{-3})$	376 ± 130	(35%)
$V (\mu\text{m}^3 \text{cm}^{-3})$	18 ± 8	(44%)
CRI_{real}	1.61 ± 0.13	(8%)
CRI_{imag}	0.018 ± 0.012	(67%)

Pereira et al. (2014)



METHOD OF COMBINATION OF LIDAR AND SUNPHOTOMETER

- Sun-photometers: widespread tool to retrieve column integrated values of aerosol optical, microphysical and radiative properties



- ... for the vertical profiling of aerosols in the atmosphere. ... properties profiles are not easy to derive

- ... of European project ACTRIS ... Research InfraStructure Network

- ... combination of AERONET sun-photometer ... multiwavelength lidar data

profiles of aerosol microphysical properties, algorithm developed in the National Acad of Sciences of Belarus



LIRIC

LIDAR

- 3 elastic backscattered signals (355, 532 and 1064 nm)
- parallel and cross-polarized backscattered signal (532 nm)

SUN-PHOTOMETER

AERONET Retrieved properties:

- columnar particle size distribution
- volume concentrations
- refractive index
- radiative properties

LIRIC
(Lidar-Radiometer Inversion Code)

- **fine mode concentration profile**
- **coarse mode concentration profile:**
spherical/non-spherical if depolarization is available

- AOD
- column mode concentrations
- integrated backscatter



LIRIC

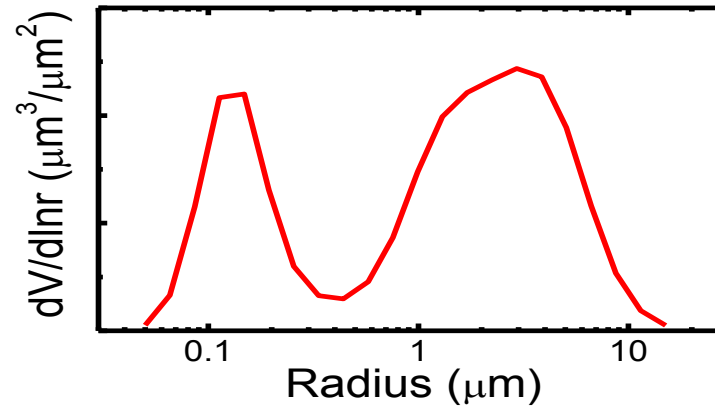
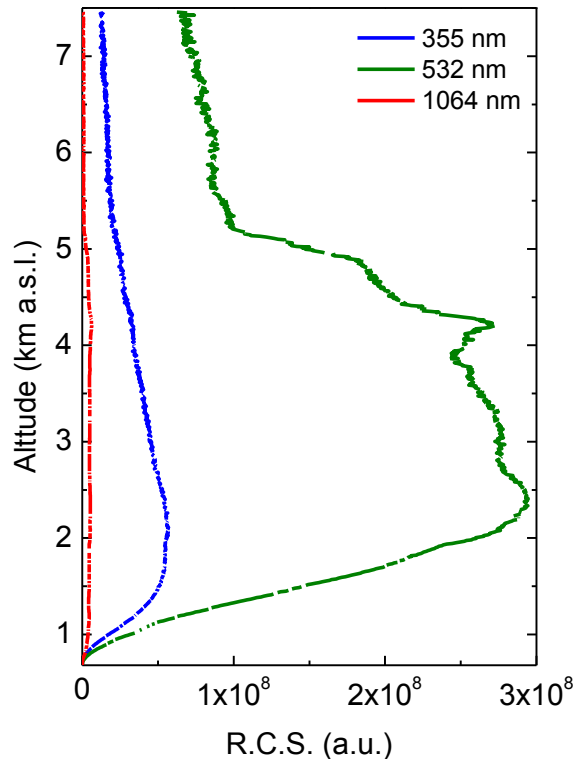
LIDAR

- 3 elastic backscattered signals (355, 532 and 1064 nm)
- parallel and cross-polarized backscattered signal (532 nm)

SUN-PHOTOMETER

AERONET Retrieved properties:

- columnar particle size distribution
- volume concentrations
- refractive index
- radiative properties



LIRIC

LIDAR

- 3 elastic backscattered signals (355, 532 and 1064 nm)
- parallel and cross-polarized backscattered signal (532 nm)

SUN-PHOTOMETER

AERONET retrieved properties:

- columnar particle size distribution
- volume concentrations
- refractive index
- radiative properties

LIRIC

(Lidar-Radiometer Inversion Code)

- the results of sun-photometric measurements represent the “truth” particle properties over the atmosphere
- the objective is to construct the particle vertical distribution matching both the integrated aerosol properties observed by ground-based radiometer and the vertically variable signal of multi-wavelength lidar



LIRIC

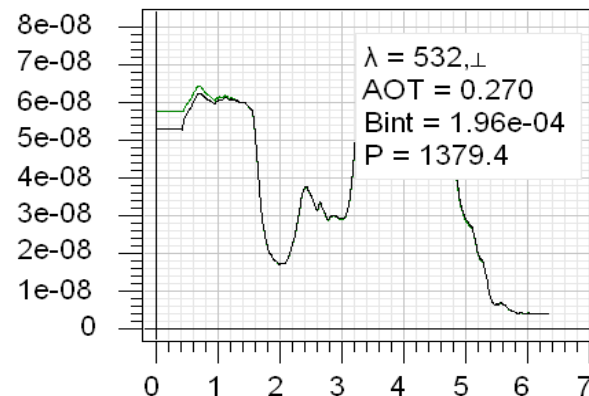
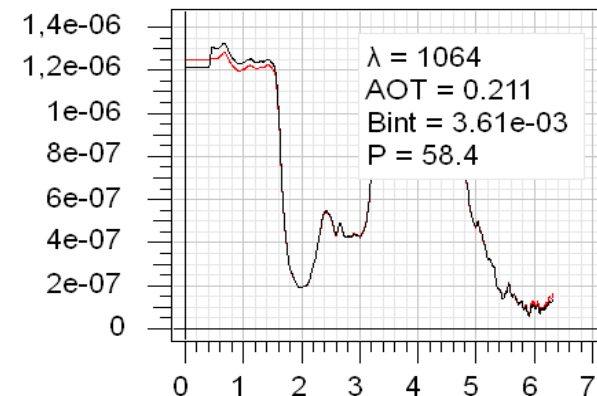
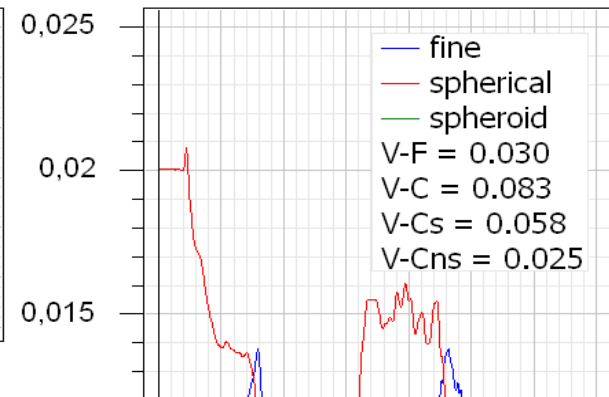
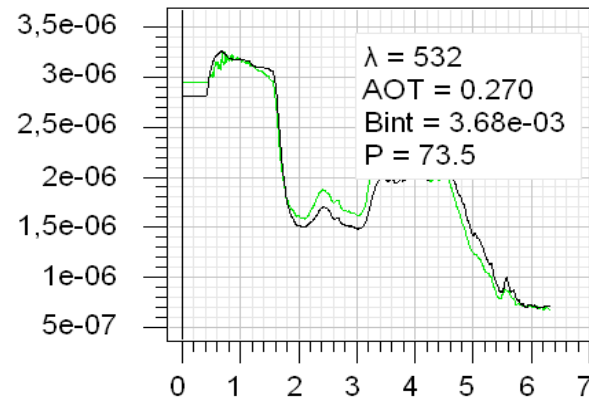
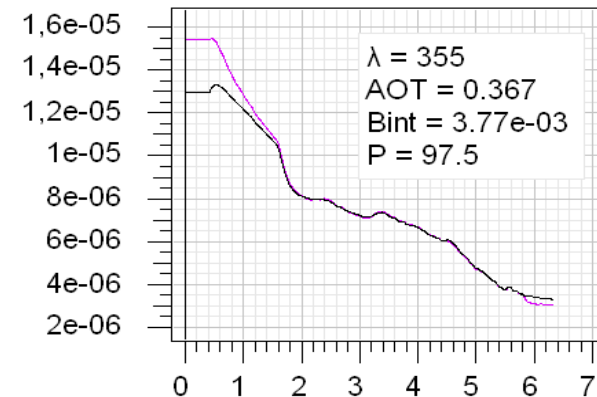
LIDAR

- 3 elastic backscattered signals (355, 532 and 1064 nm)
- parallel and cross-polarized backscattered signal (532 nm)

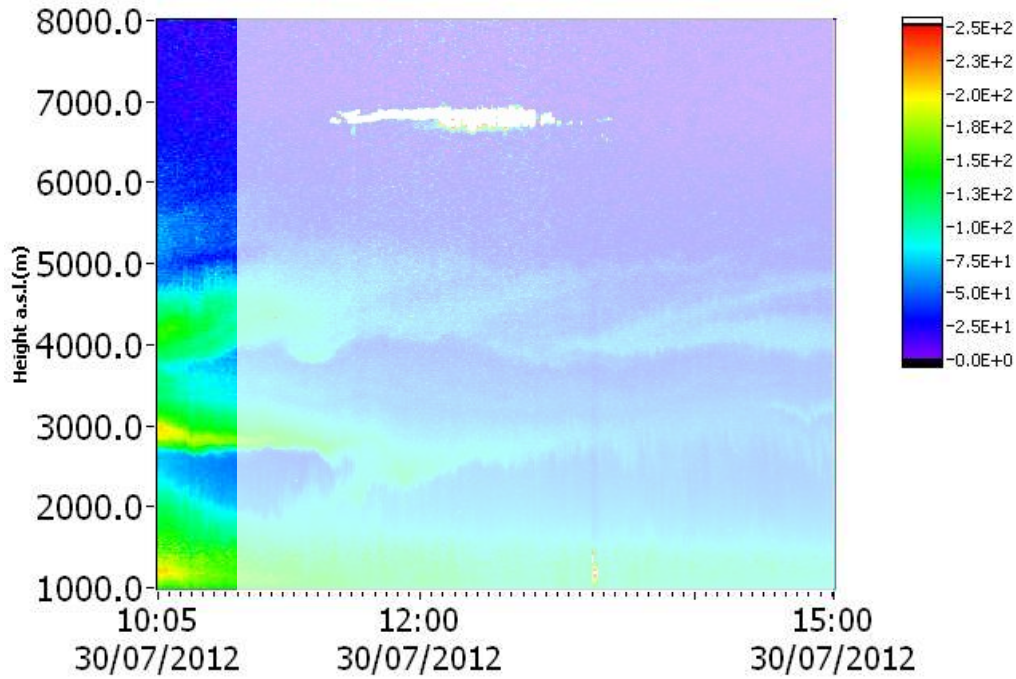
SUN-PHOTOMETER

AERONET Retrieved properties:

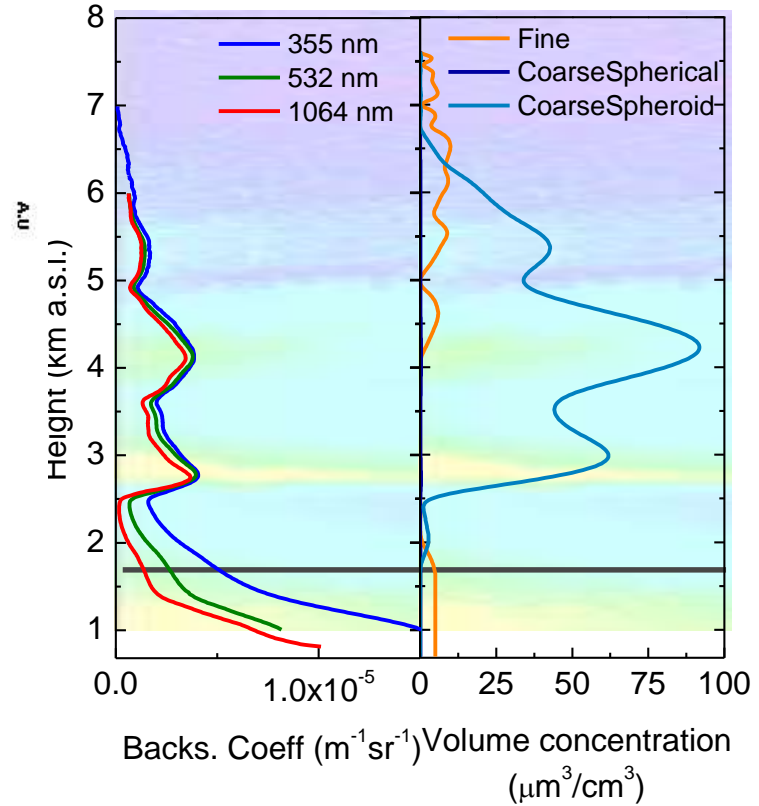
- columnar particle size distribution
- volume concentrations
- refractive index
- radiative properties



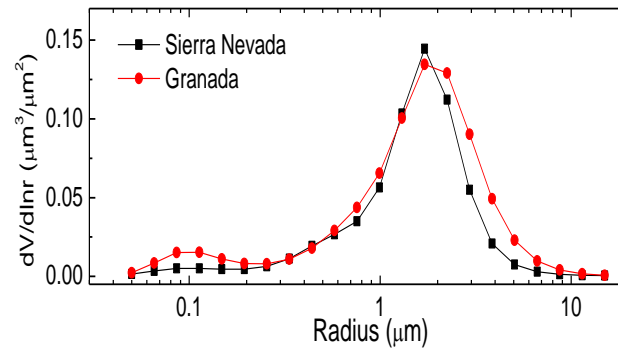
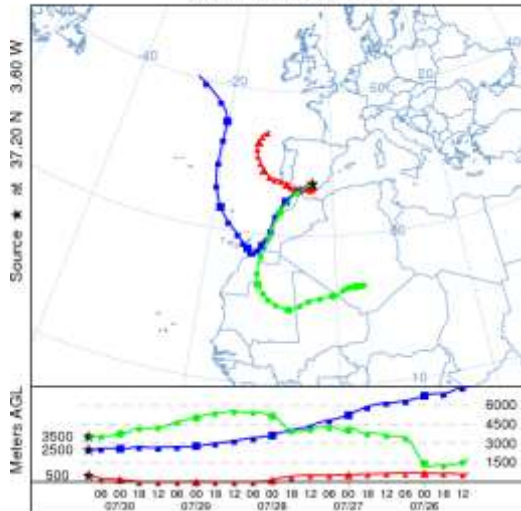
LIRIC



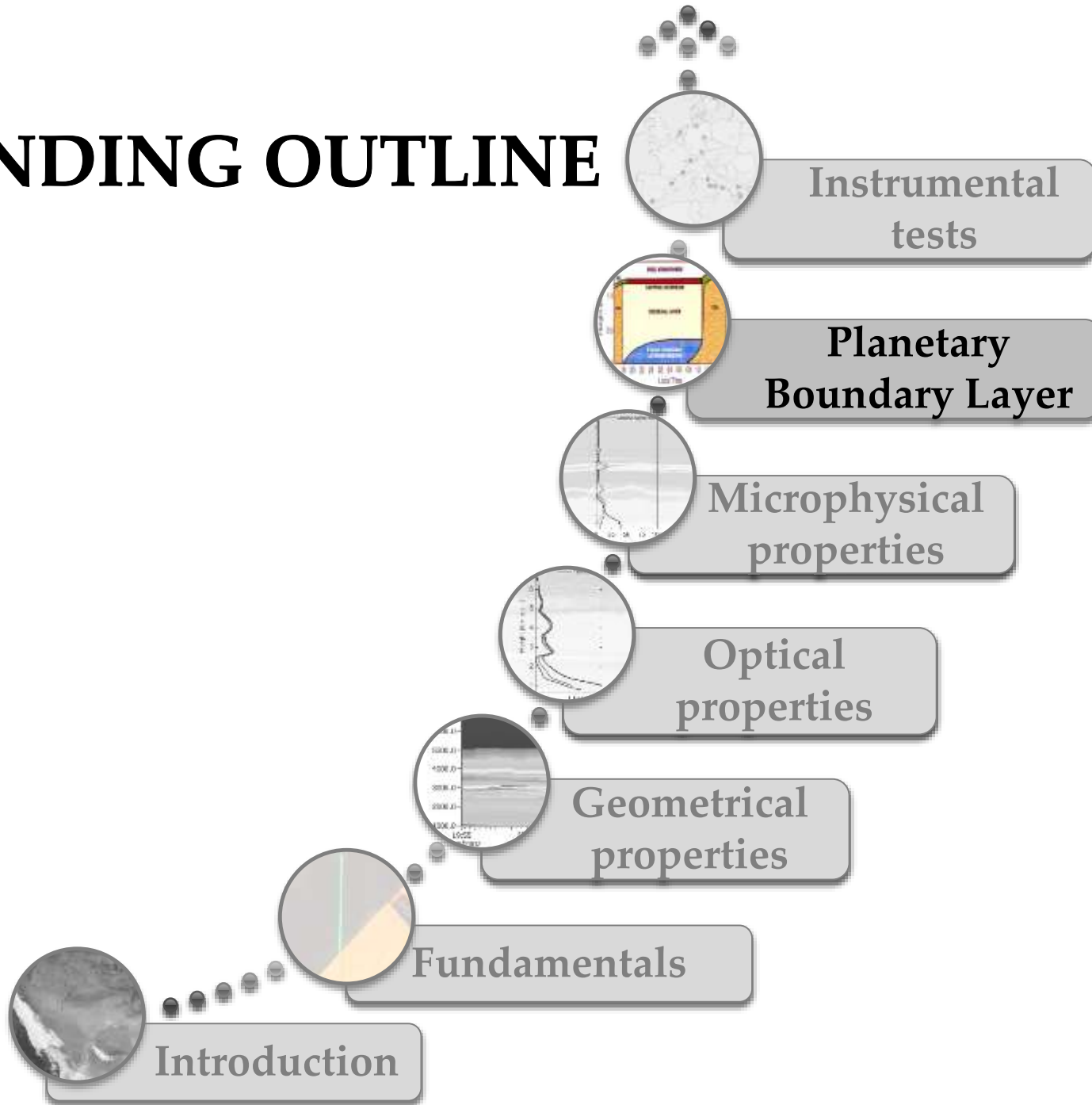
30/07/2012 10:00-10:30



NOAA HYSPLIT MODEL
Backward trajectories ending at 1000 UTC 30 Jul 12
GDAS Meteorological Data



ASCENDING OUTLINE

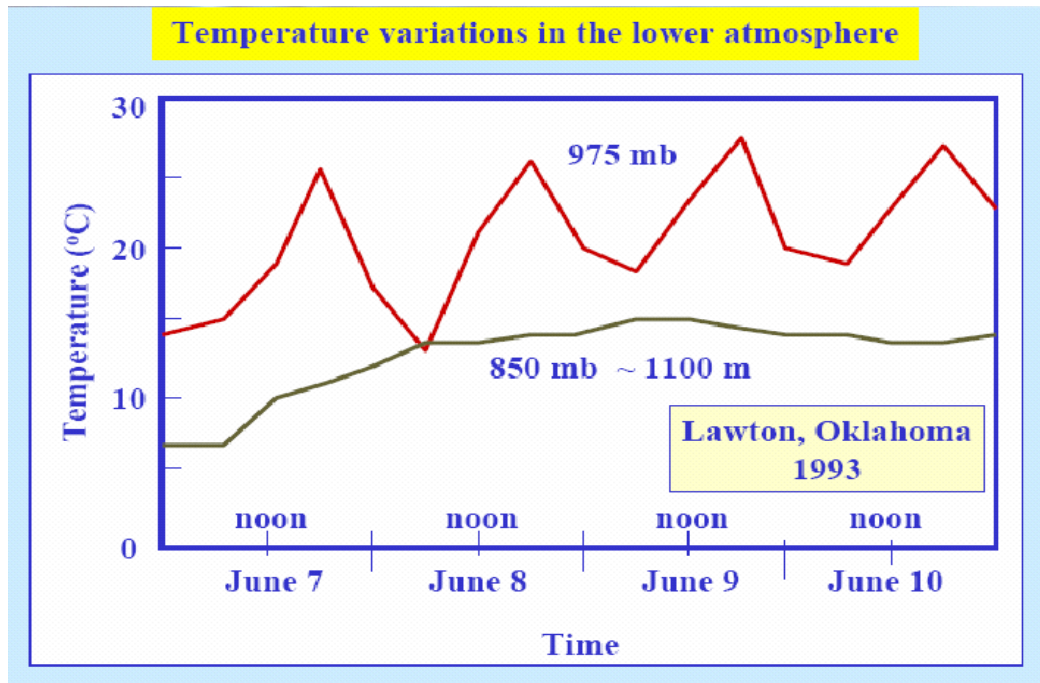


WHAT IS THE PLANETARY BOUNDARY LAYER?

“The planetary boundary layer is the part of the troposphere that is directly **or indirectly** influenced by the presence of the Earth’s surface (**ground or sea**), and responds to surface forcings with a time scale of **a few hours** or less. These forcings include heat transfer, frictional drag, atmospheric **aerosol particles emission, gases emission** and terrain induced flow modification”. (based on Stull 1998 and **Cost Action 1303 ToProf**)

Features:

- time scale: a few hours or less
- affected by diurnal surface changes
- Its height varies from hundred of meters to a few kilometer



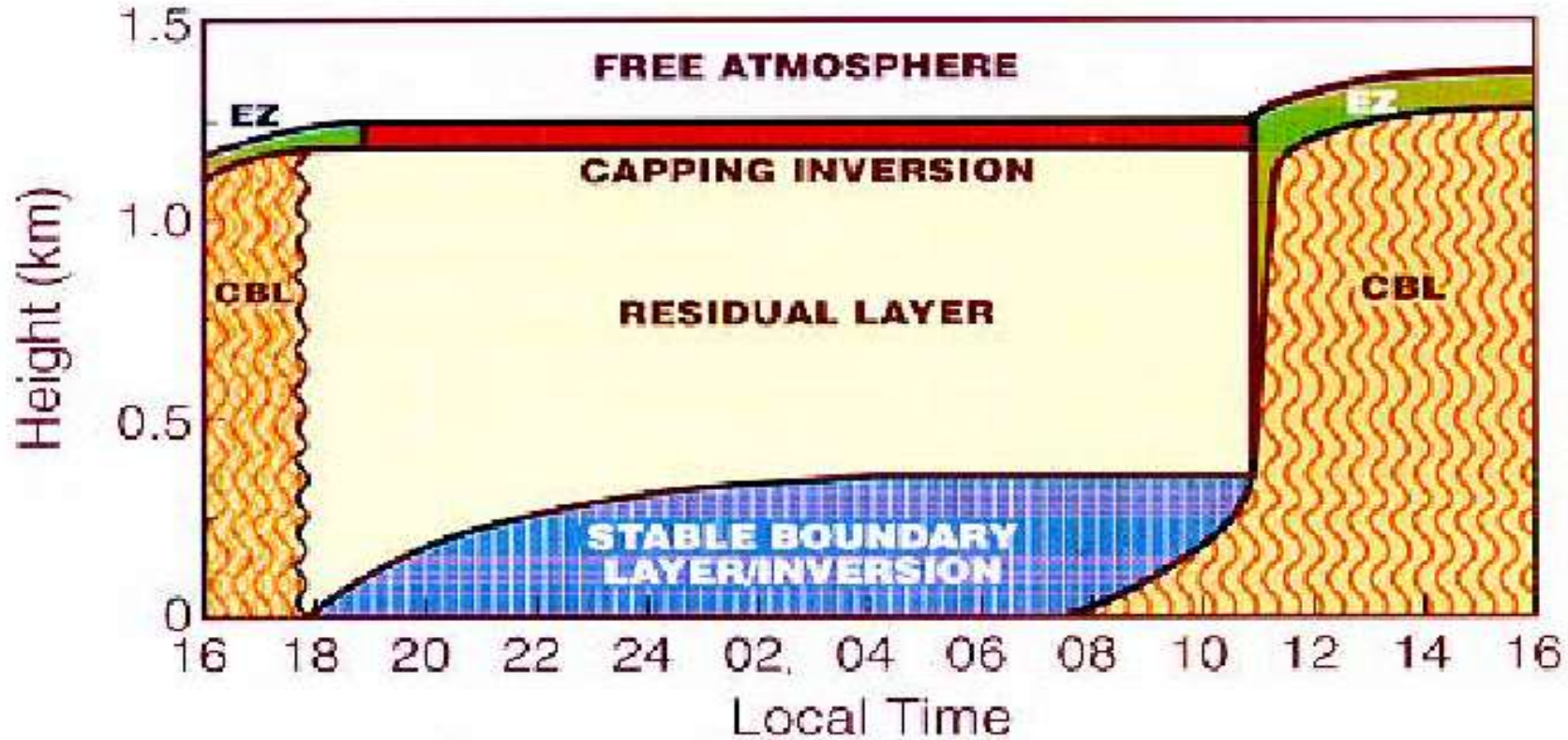
WHAT IS THE PLANETARY BOUNDARY LAYER?

Importance of determining the PBL height:

- forecast of pollutant concentration
- forecast of surface temperatures
- turbulence measurements
- assimilation in numerical models for weather and climate forecast

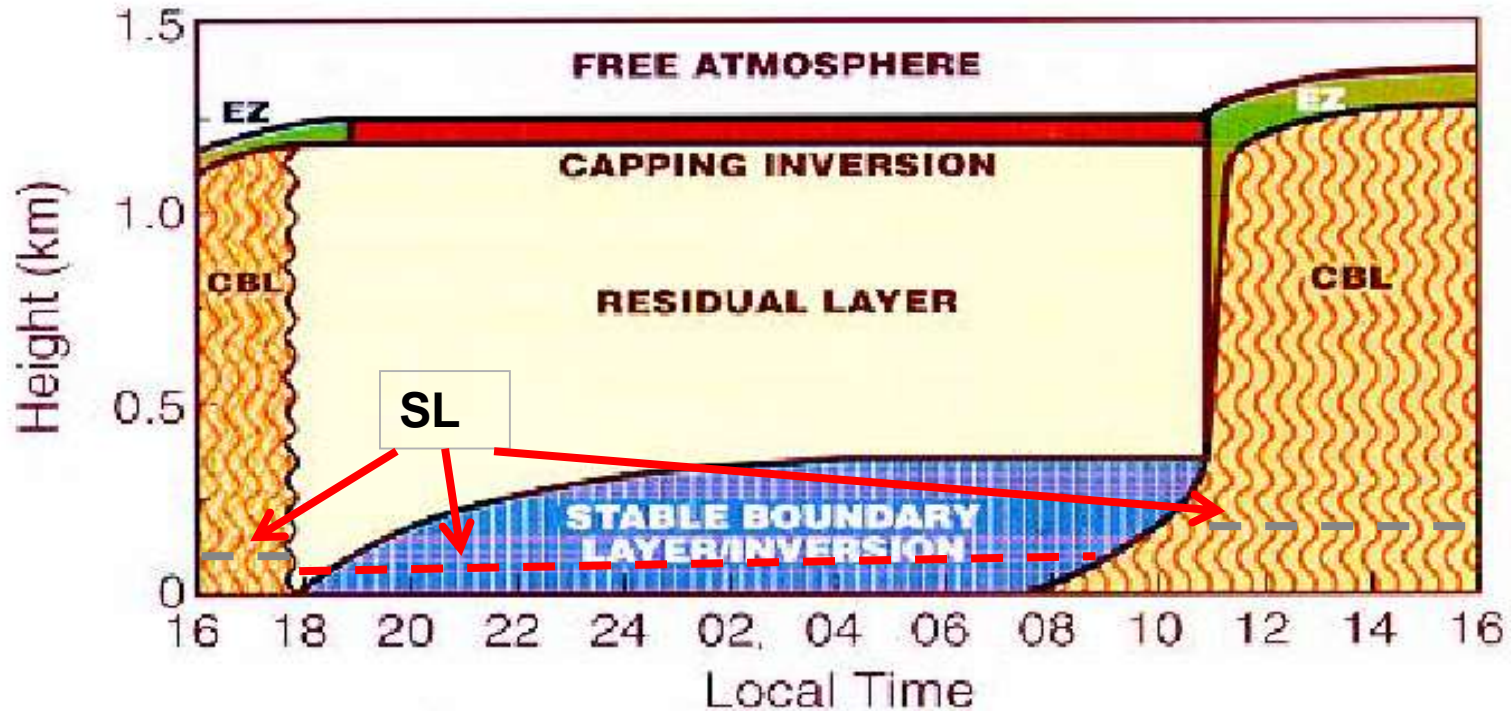


STRUCTURE OF THE PLANETARY BOUNDARY LAYER



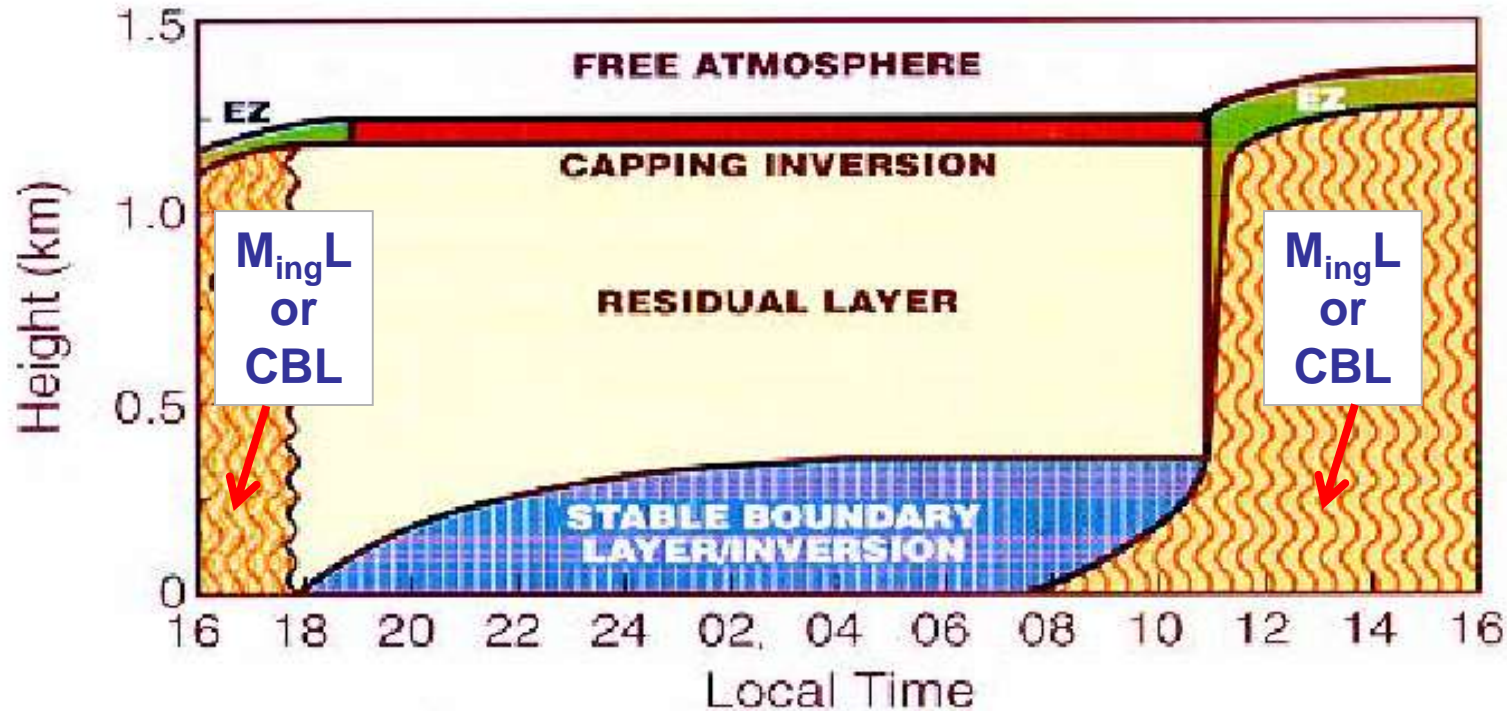
(Stull 1998)

STRUCTURE OF THE PLANETARY BOUNDARY LAYER



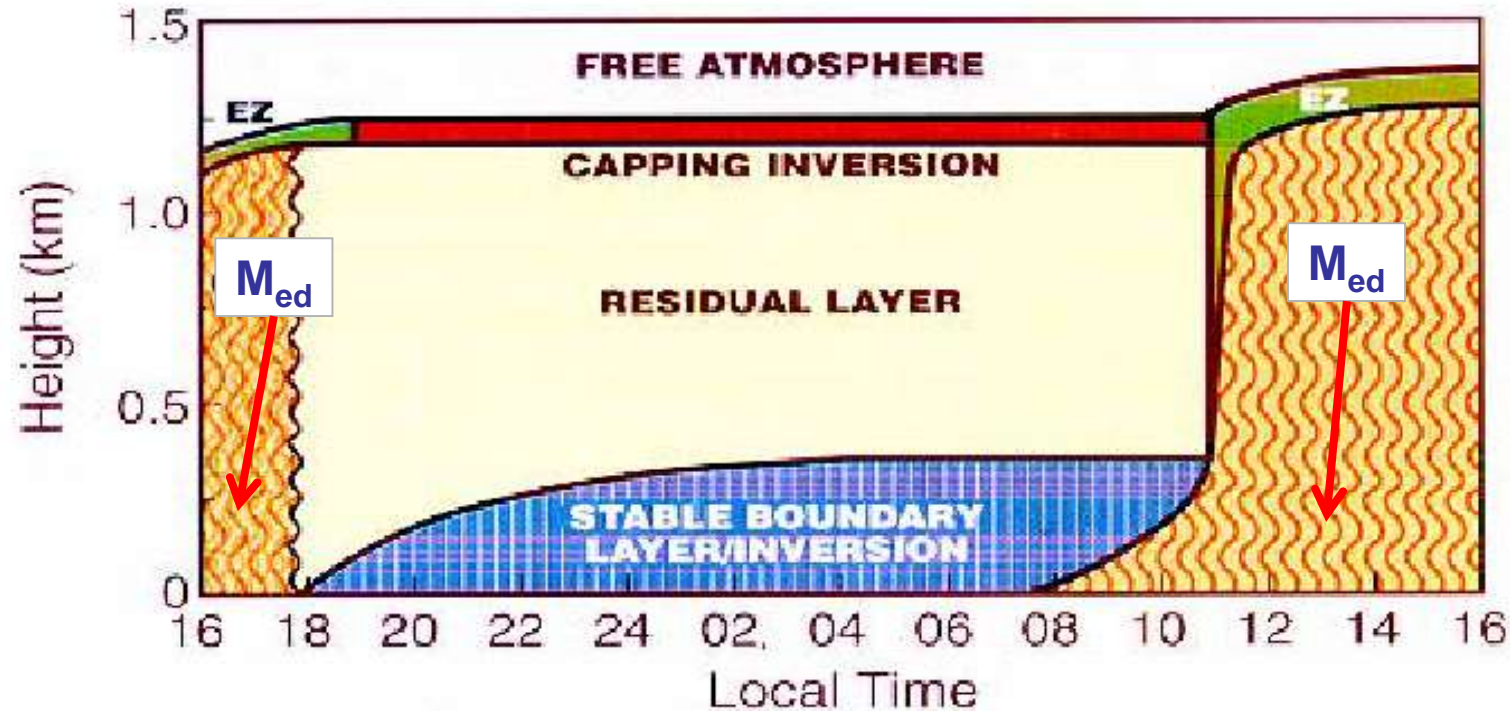
Surface layer (SL): region at the bottom of the PBL where heat conduction, evaporation and frictional drag from the surface cause substantial changes of temperature, humidity and wind speed with height. Arbitrarily, the bottom 10% of the PBL is called the surface layer, regardless of whether it is part of a $M_{ing}L$ (typically day), $M_{ed}L$ (typically day) or SBL (typically night). Thus, SL depth is higher during day than night. During daytime the surface layer is statically unstable and during nighttime is stable

STRUCTURE OF THE PLANETARY BOUNDARY LAYER



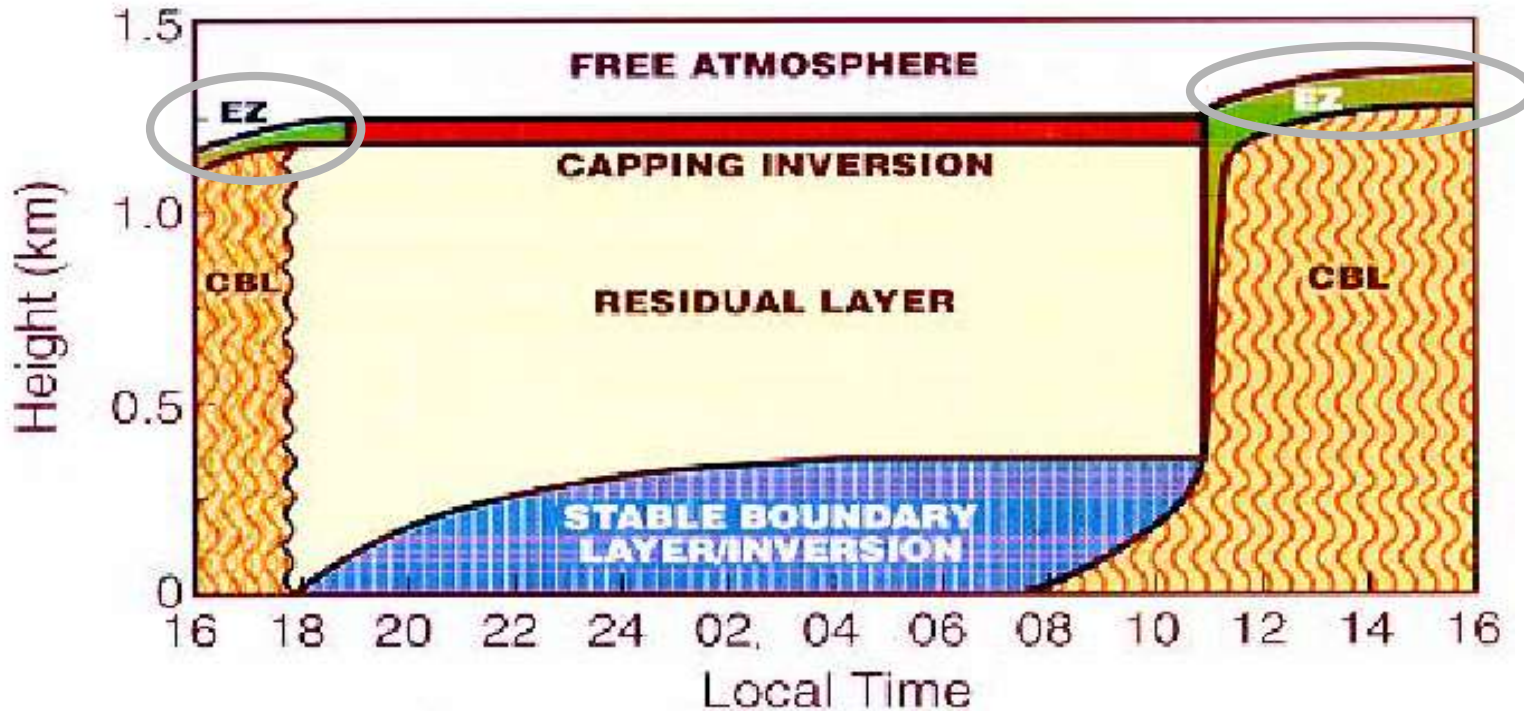
Mixing layer ($M_{ing}L$) (also known as **convective boundary layer, CBL**): layer where the turbulence is predominant as a result of convection. Its growth is linked to solar heating of the surface. After sunrise, warm parcels of air rise from the surface layer through the mixing layer, creating strong turbulence and causing potential temperature, humidity and pollutants to mix. This layer is statically unstable, with potential temperature decreasing with height and tends to be nearly constant (but not constant), that means this atmospheric region is being homogenized

STRUCTURE OF THE PLANETARY BOUNDARY LAYER



Mixed layer ($M_{ed}L$): Only during situations when turbulence is particularly vigorous, i.e., under strong convective situations, the $M_{ing}L$ is re-called **mixed layer ($M_{ed}L$)**, and it is characterized by potential temperature (or virtual potential temperature) constant with height, which means the portion of atmosphere becomes completely homogenized (statically neutral)

STRUCTURE OF THE PLANETARY BOUNDARY LAYER

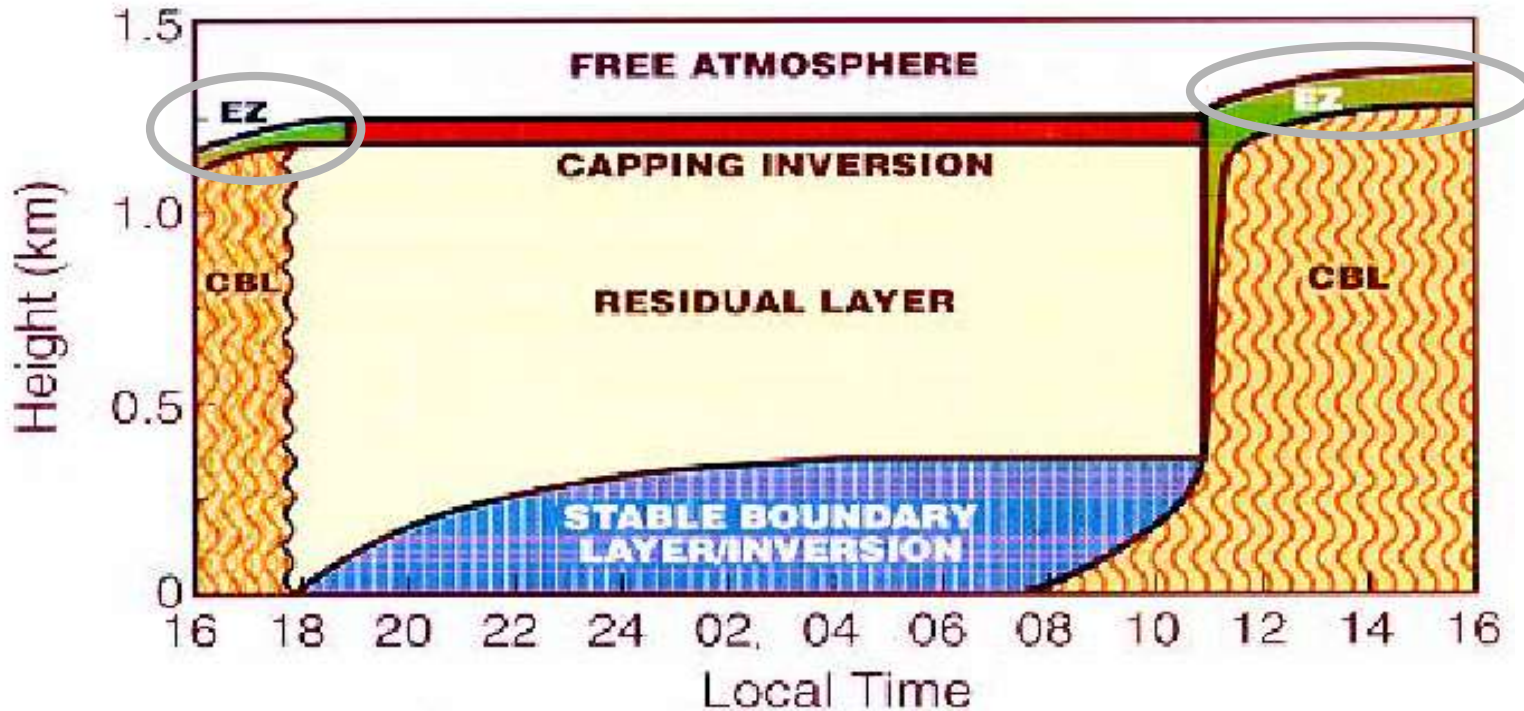


Entrainment zone (EZ): stable layer at the top of the $M_{ing}L$ (or $M_{ed}L$ if exists) acting as a cap to the rising warm parcels of air. In the EZ, free troposphere air is incorporated (i.e. entrained) into the $M_{ing}L$ (or $M_{ed}L$ if exists), causing the layer depth to increase during the day (EZ can be understood as a one-way valve)

Évora
4th July 2016

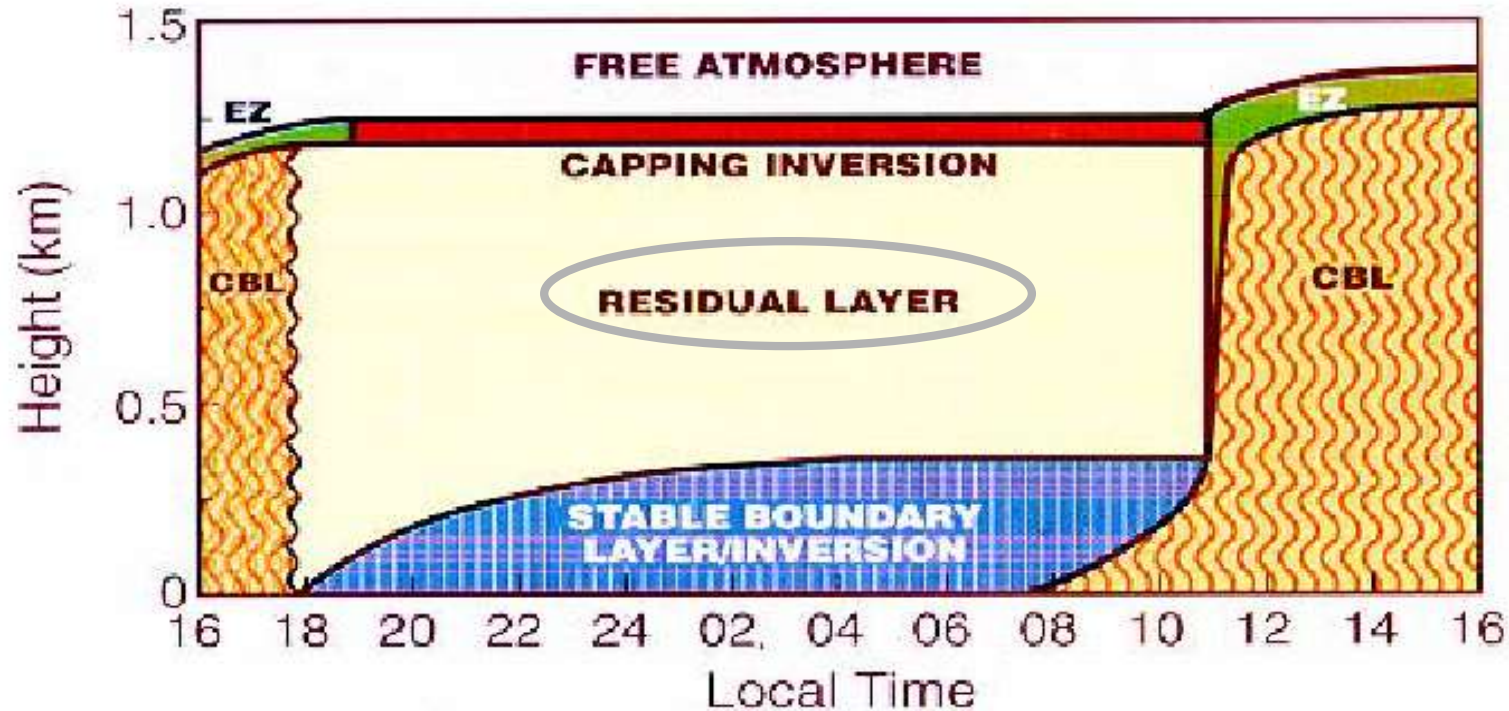


STRUCTURE OF THE PLANETARY BOUNDARY LAYER



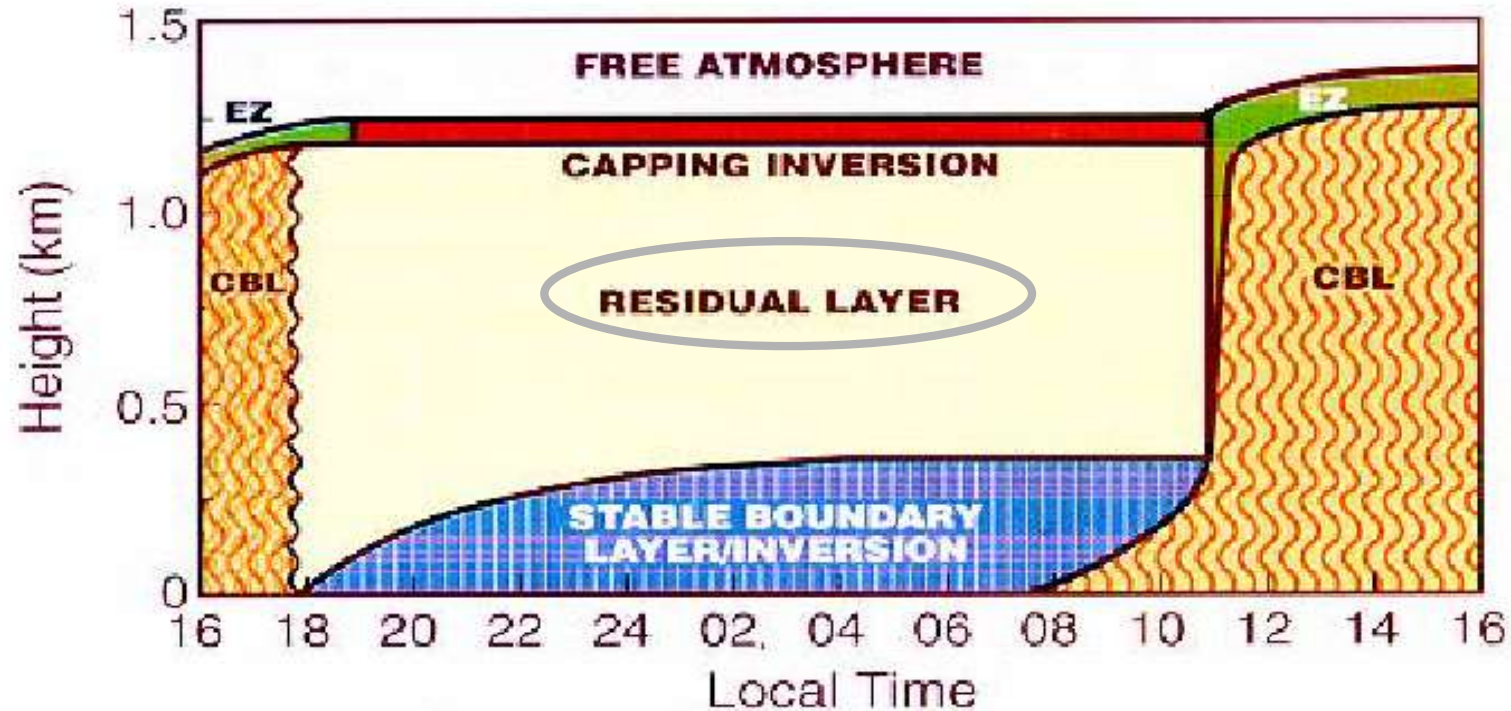
Entrainment zone (EZ) (continuation): sometimes this capping stable layer is really a temperature inversion, i.e. temperature increases with altitude, and therefore this layer can be called **inversion layer**. The latter name is strictly only valid when temperature increases with height. However, in many cases literature collects studies wrongly denoting inversion layer to this stable layer independently on the temperature behavior

STRUCTURE OF THE PLANETARY BOUNDARY LAYER



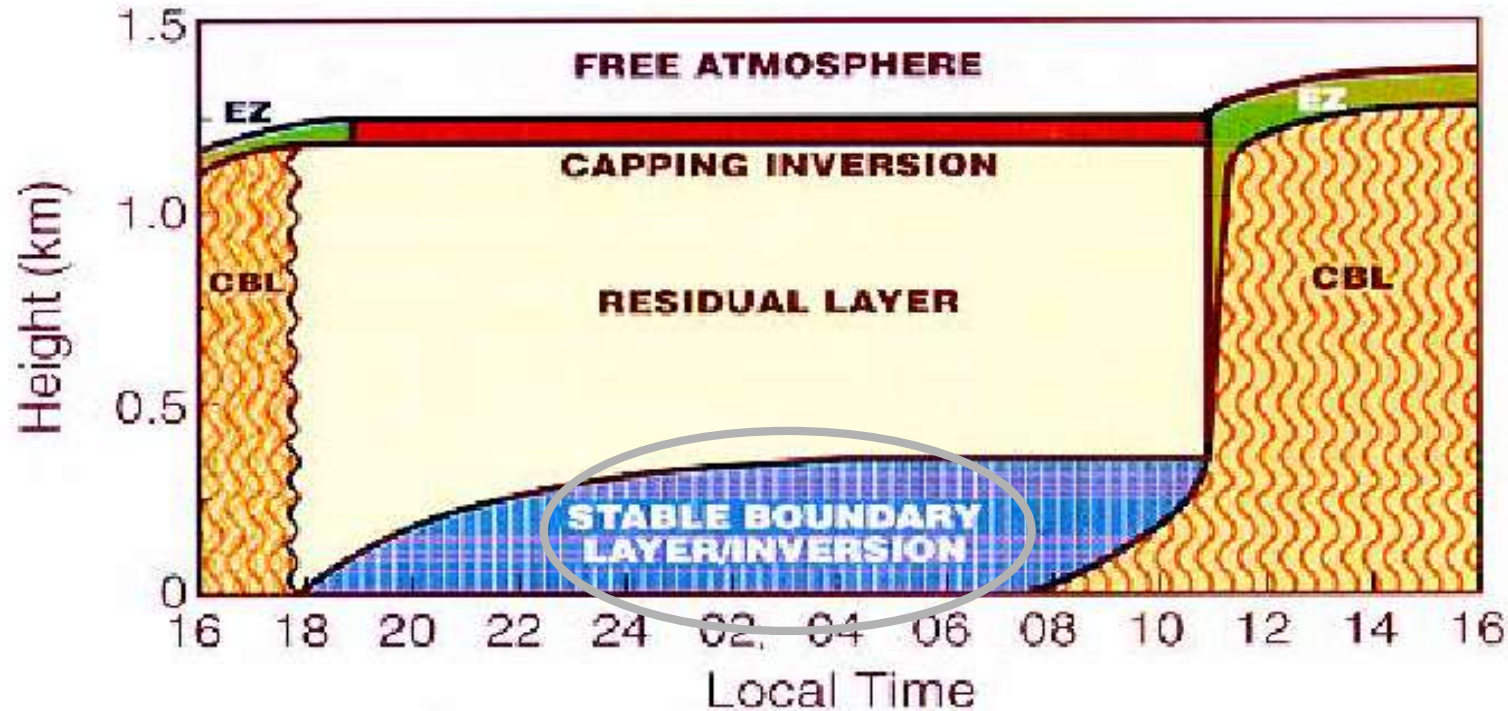
Residual layer (RL): a layer containing characteristics from the previous $M_{\text{ing}}L$ (or $M_{\text{ed}}L$ if exists) (thermodynamic variables or aerosol particles and gases). It is formed around sunset when the turbulence decays. This layer is statically nearly neutral, causing aerosol particles and gases emitted into tend to disperse at equal rates in the vertical and horizontal directions. Variables such as virtual potential temp. are nearly uniform through the RL (not exactly constant). RL is statically neutral only when the boundary layer of the previous layer is mixed

STRUCTURE OF THE PLANETARY BOUNDARY LAYER



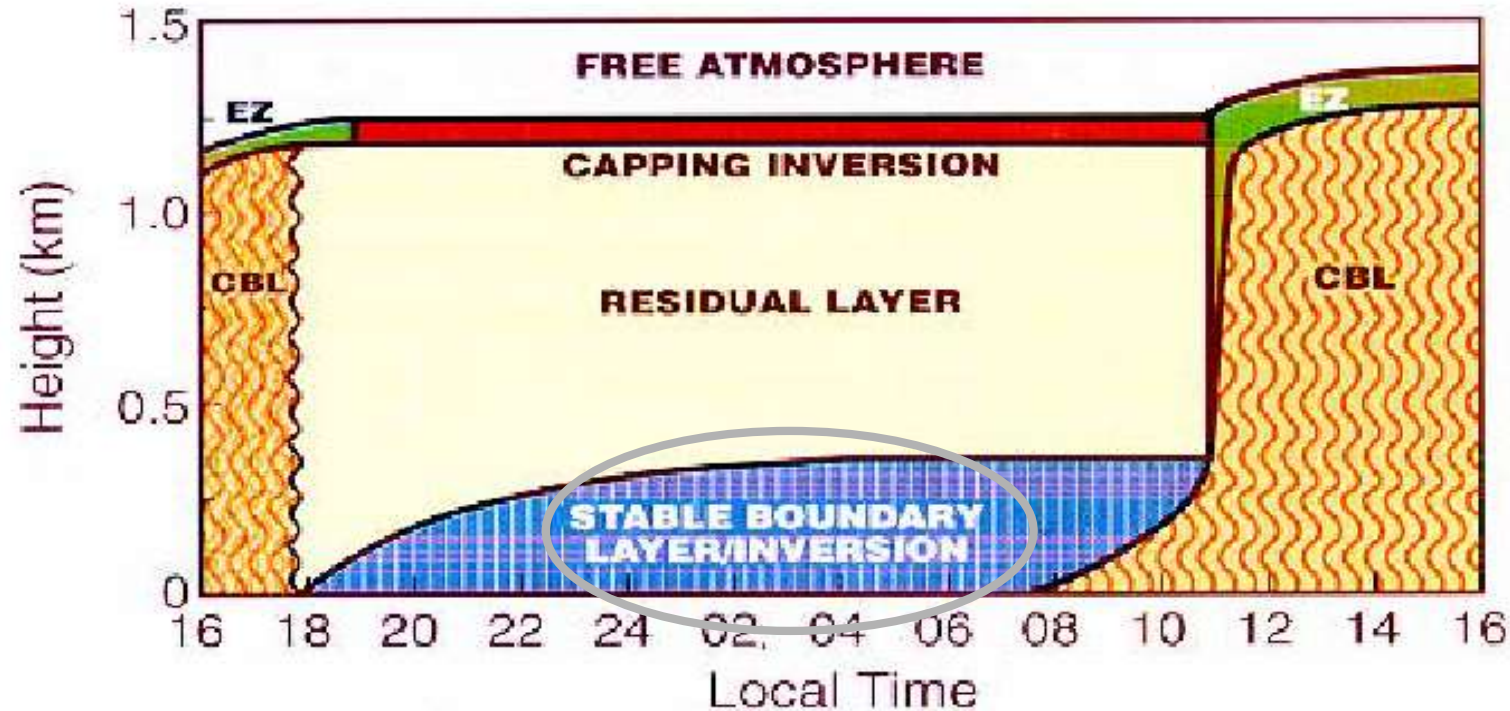
Residual layer (RL) (continuation): When the top of the mixing layer of the next day reaches the base of the RL, the mixing layer grows very fast. Because this layer has not direct contact with the surface and therefore RL is not affected by turbulent transport, many authors (such as Stull, 1988) do not consider it as part of the PBL, but at present ToProf includes it as part of the PBL due to RL affects the characteristics of the PBL of the next day.

STRUCTURE OF THE PLANETARY BOUNDARY LAYER



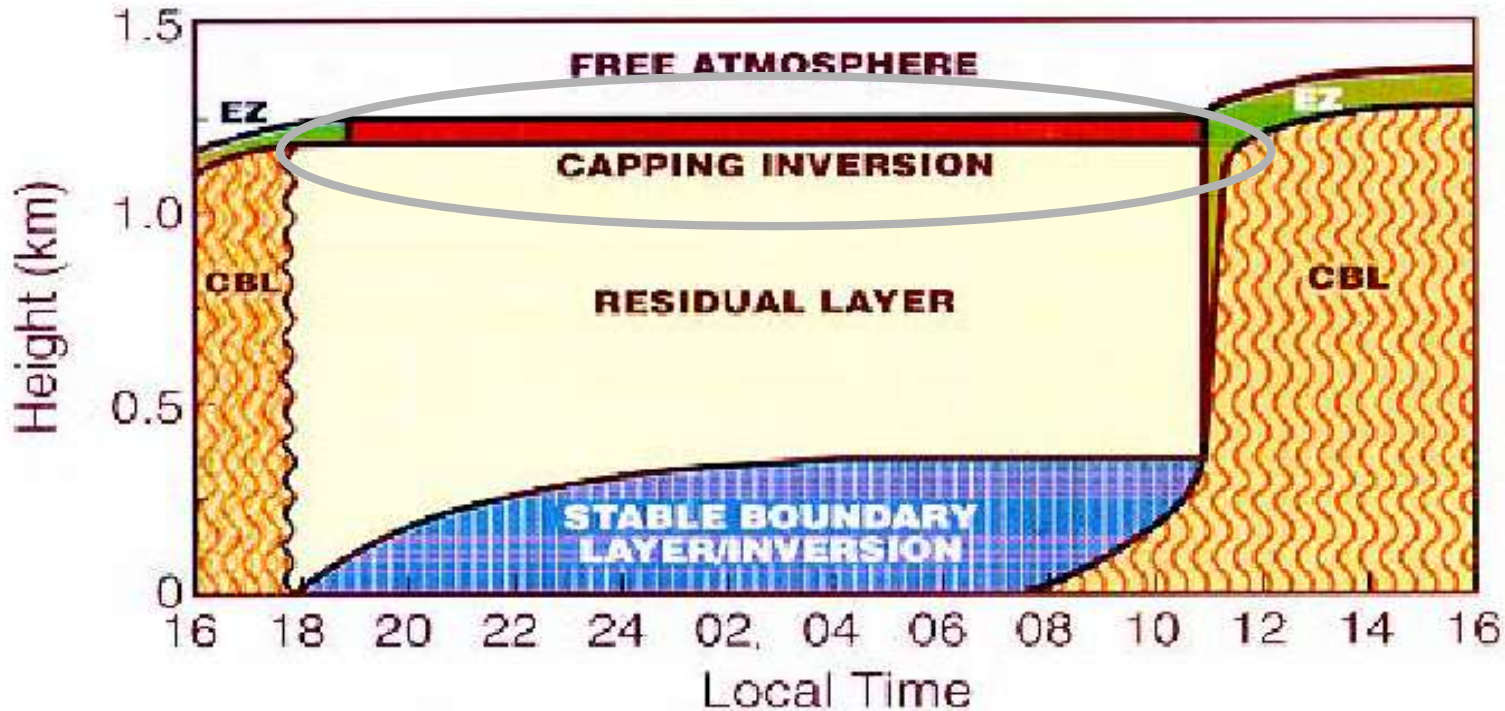
Stable boundary layer (SBL) (also known as **nocturnal boundary layer**, NBL): this layer is formed when the radiative heating of Earth's surface ends and the radiative cooling, together with the surface friction, transforms the lowest part of the $M_{\text{ing}}L$ (or $M_{\text{ed}}L$ if exists) and stabilize this layer. The statically stable air tends to suppress turbulence, but the wind shears tend to generate turbulence. This results in sporadic (and weaker turbulence), which may cause mix throughout the stable boundary layer.

STRUCTURE OF THE PLANETARY BOUNDARY LAYER



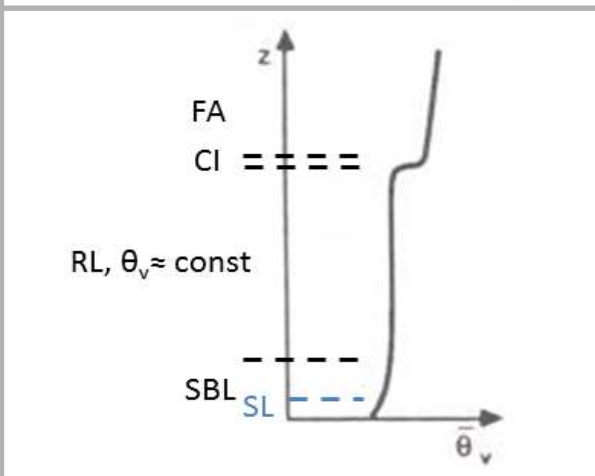
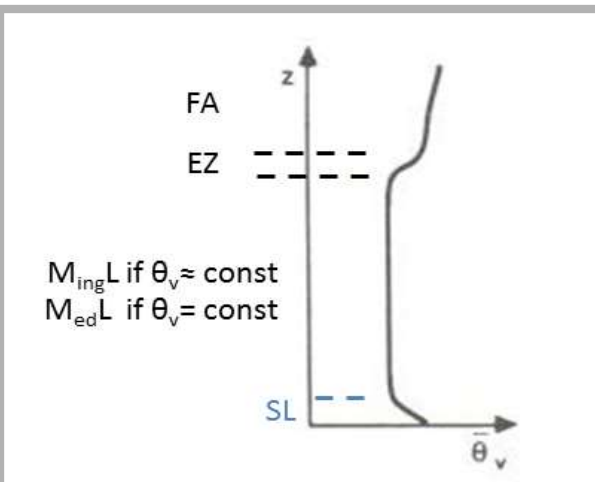
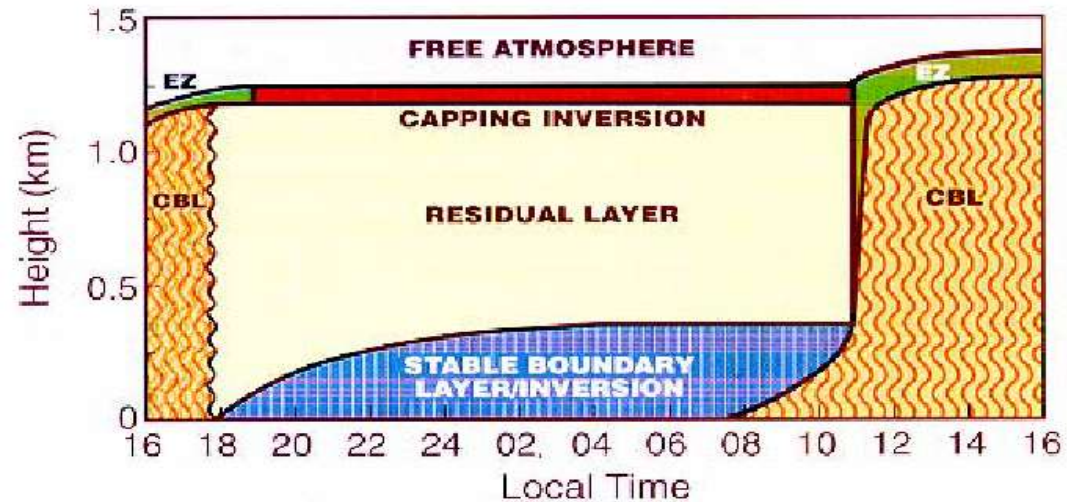
Stable boundary layer (SBL) (continuation): Aerosol particles and gases emitted in the SBL disperse relatively little in the vertical and disperse more efficiently in the horizontal. Stable boundary layers can be formed during daytime if the underlying surface is colder than the air (for example when warm air is advected over a colder surface)

STRUCTURE OF THE PLANETARY BOUNDARY LAYER



Capping inversion (CI): strongly stable layer at the top of the residual layer, leaving a separation between the residual layer and the free troposphere. Because absolute temperature increases with altitude, it can be defined as inversion and plays a similar role (in the sense of acting as a cap) than the entrainment zone during daytime

EVOLUTION OF THE PLANETARY BOUNDARY LAYER



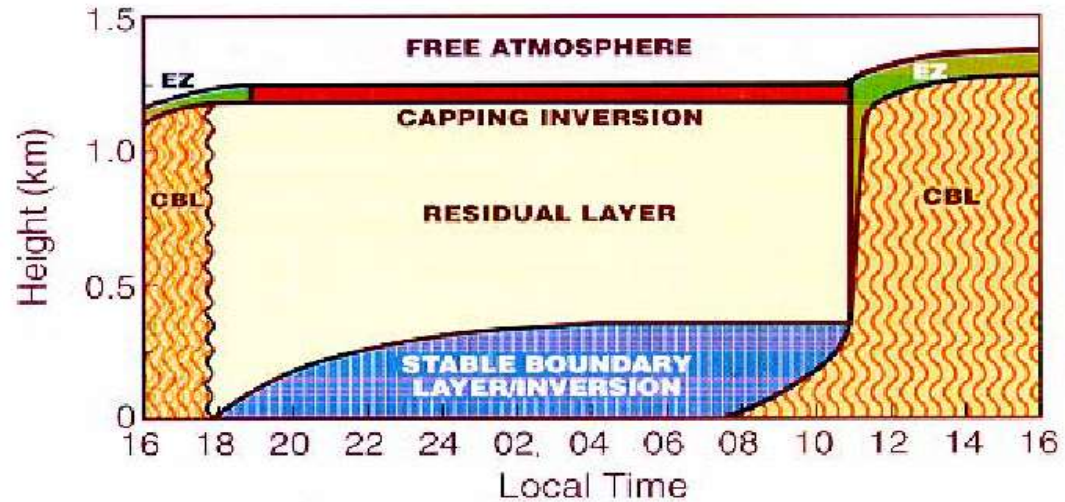
Scenario 1:

PBL layering during daytime. In mixing layer θ_v is nearly constant in height, in mixed layer θ_v is constant in height

Scenario 2:

PBL layering during night time, just after sunset. In residual layer θ_v is nearly constant in height

EVOLUTION OF THE PLANETARY BOUNDARY LAYER

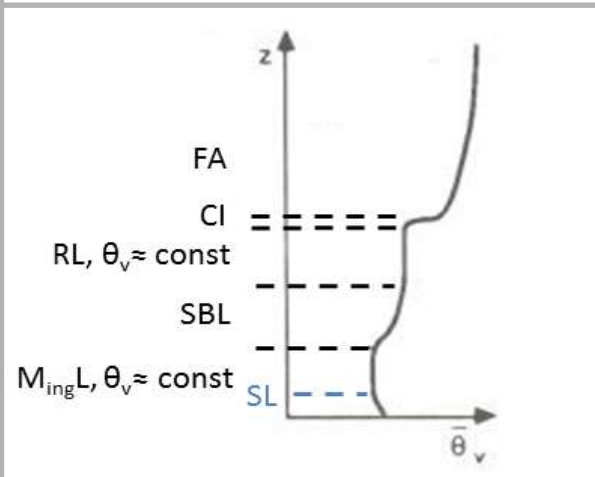
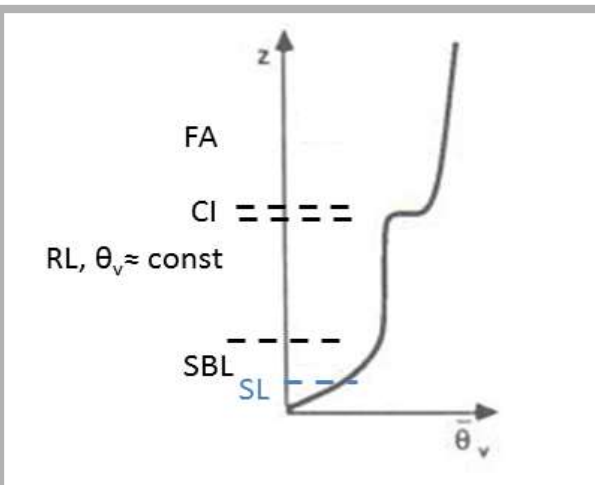


Scenario 3:

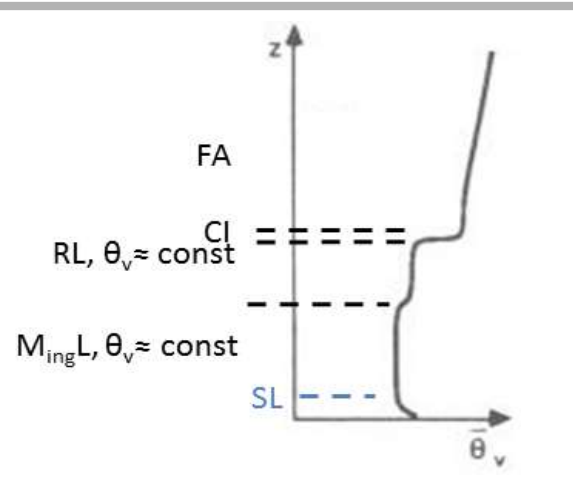
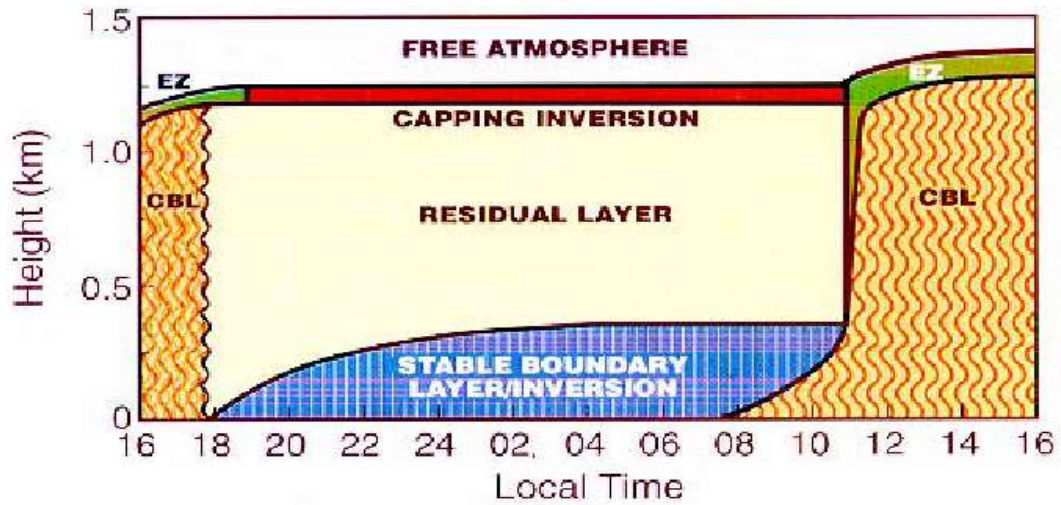
PBL layering during night time, in the middle of the night. In residual layer θ_v is nearly constant in height. SBL is more pronounced

Scenario 4:

PBL layering during daytime, just after sunrise. Solar heating starts to develop a mixing layer, but still a SBL and RL remains above

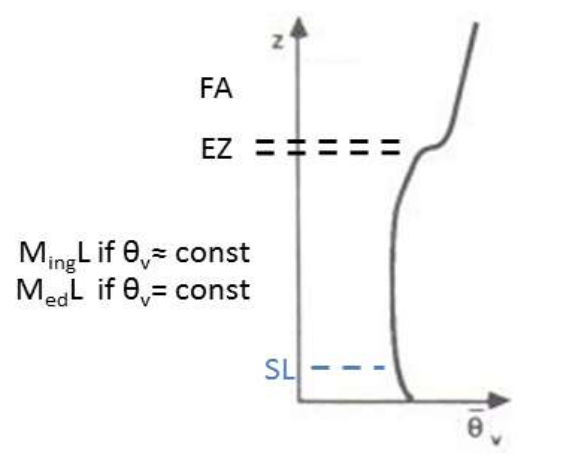


EVOLUTION OF THE PLANETARY BOUNDARY LAYER



Scenario 5:

PBL layering during daytime, along the morning. Turbulence is increasing but still not strong enough and RL remains

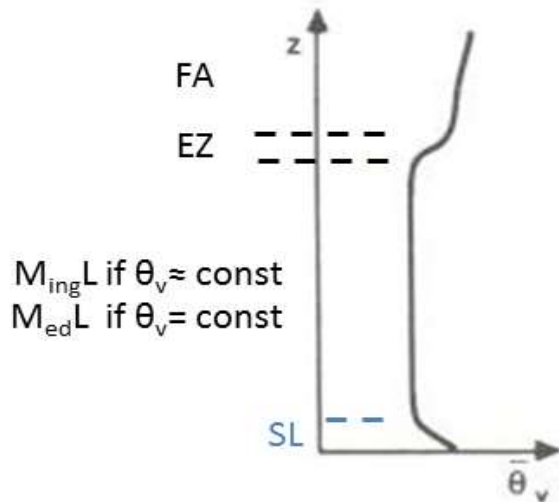


Scenario 6:

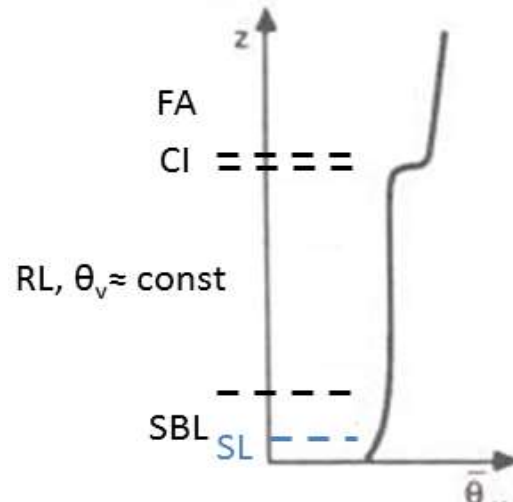
PBL layering during daytime. Mixing layer catches the RL and grows very fast. In mixing layer θ_v is nearly constant in height, in mixed layer θ_v is constant in height



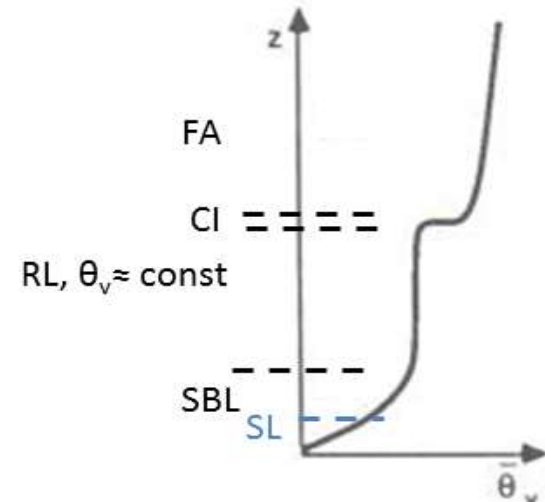
EVOLUTION OF THE PLANETARY BOUNDARY LAYER



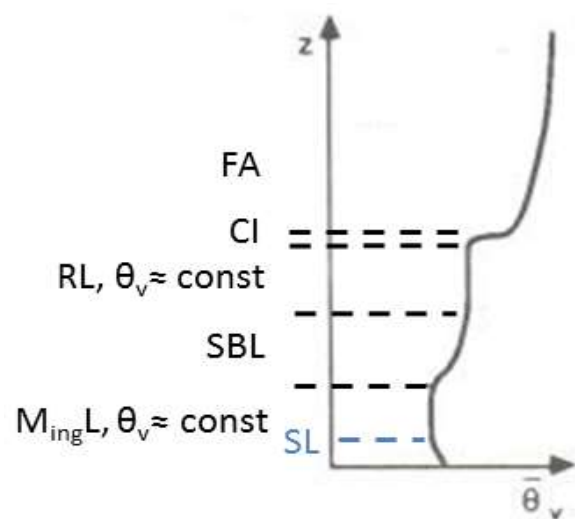
Scenario 1: afternoon



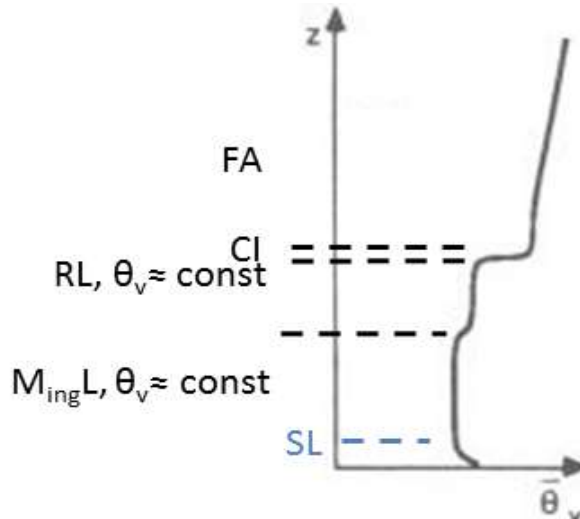
Scenario 2: Sunset



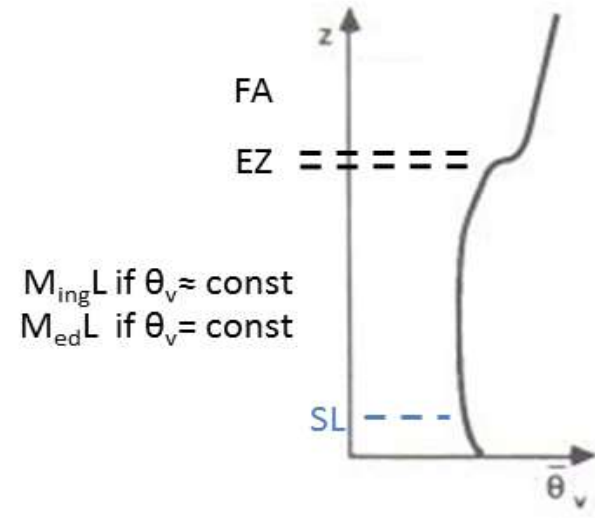
Scenario 3: night



Scenario 4: after Sunrise



Scenario 5: morning



Scenario 6: day

SOME METHODS TO DETERMINE THE PLANETARY BOUNDARY LAYER HEIGHT

- **Radiosoundings:**

-*Richardson's number method:*

based on wind, temperature and pressure profiles

Richardson's number method is used under convective conditions to determine the PBL height from radiosounding data. The Richardson's number, R_{ib} , is computed as function of altitude as:

$$R_{ib}(z) = \frac{g(z - z_0) [\theta(z) - \theta(z_0)]}{\theta(z) [u(z)^2 + v(z)^2]}$$

$M_{ing}L$ height is the altitude where the Richardson's number profile matches a threshold ($R_{ib} = R_{ibc}$). Previous studies (e.g. Vogelezang et al., 1996) suggested $R_{ibc} = 0.21$



SOME METHODS TO DETERMINE THE PLANETARY BOUNDARY LAYER HEIGHT

- **Radiosoundings:**

- *Potential temperature method:*

based on temperature and pressure profiles

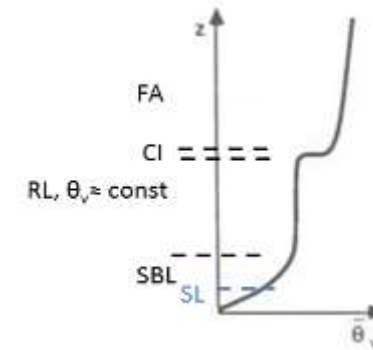
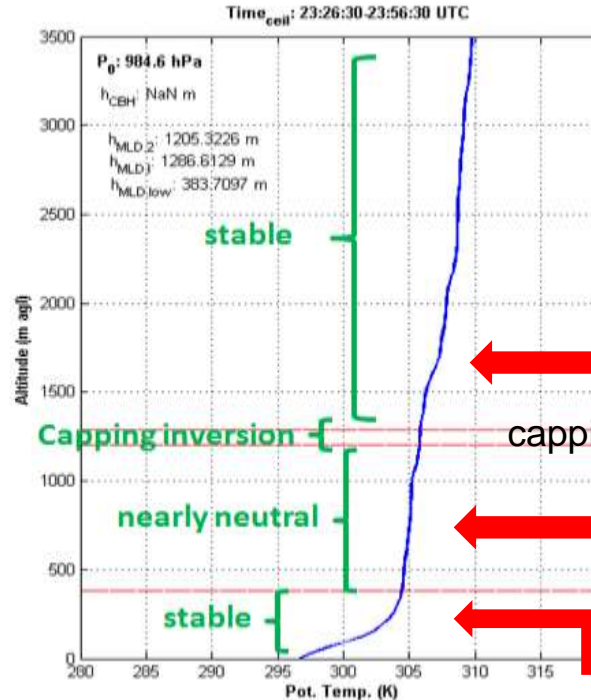
Potential temperature method studies the atmospheric stability and instability conditions



$$\frac{\partial \theta}{\partial z} > 0 \quad \text{stability}$$

$$\frac{\partial \theta}{\partial z} = 0 \quad \text{neutrality}$$

$$\frac{\partial \theta}{\partial z} < 0 \quad \text{unstability}$$



Free atmosphere (FA)

capping inversion

Residual Layer with $\theta \sim \text{const.}$ [1.4K (RS)]

Stable boundary layer (SBL) very pronounced



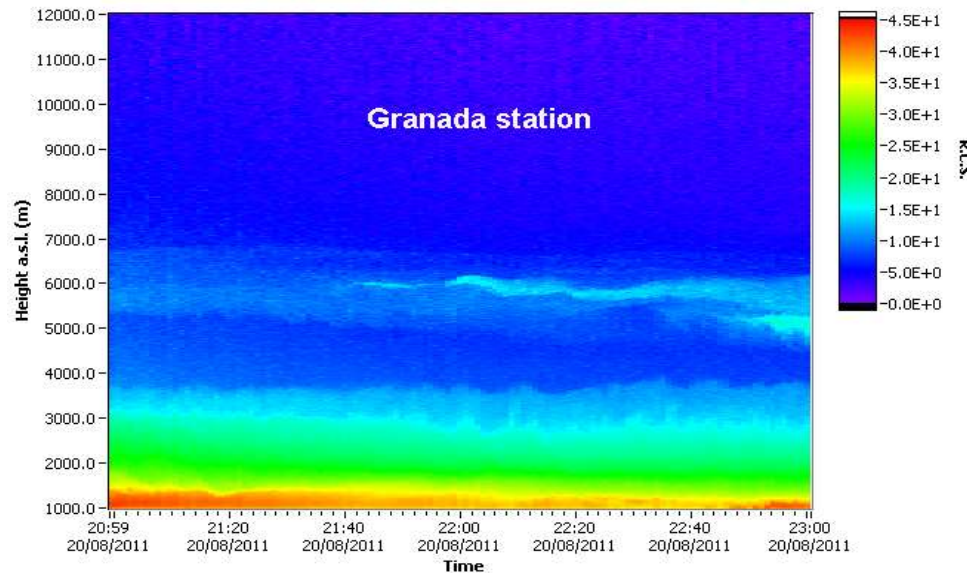
SOME METHODS TO DETERMINE THE PLANETARY BOUNDARY LAYER HEIGHT

- **Active remote sensing (lidar):**

Radiosounding: low temporal frequency of launches

lidar: high temporal frequency

methods based on aerosol profiling



$$R.C.S.(z, \lambda) \equiv P(z, \lambda) \cdot R^2 = P_o(z) \cdot C \cdot O(z) \cdot \beta(z, \lambda) \cdot e^{-2 \int_0^z \alpha(x, \lambda) dx}$$

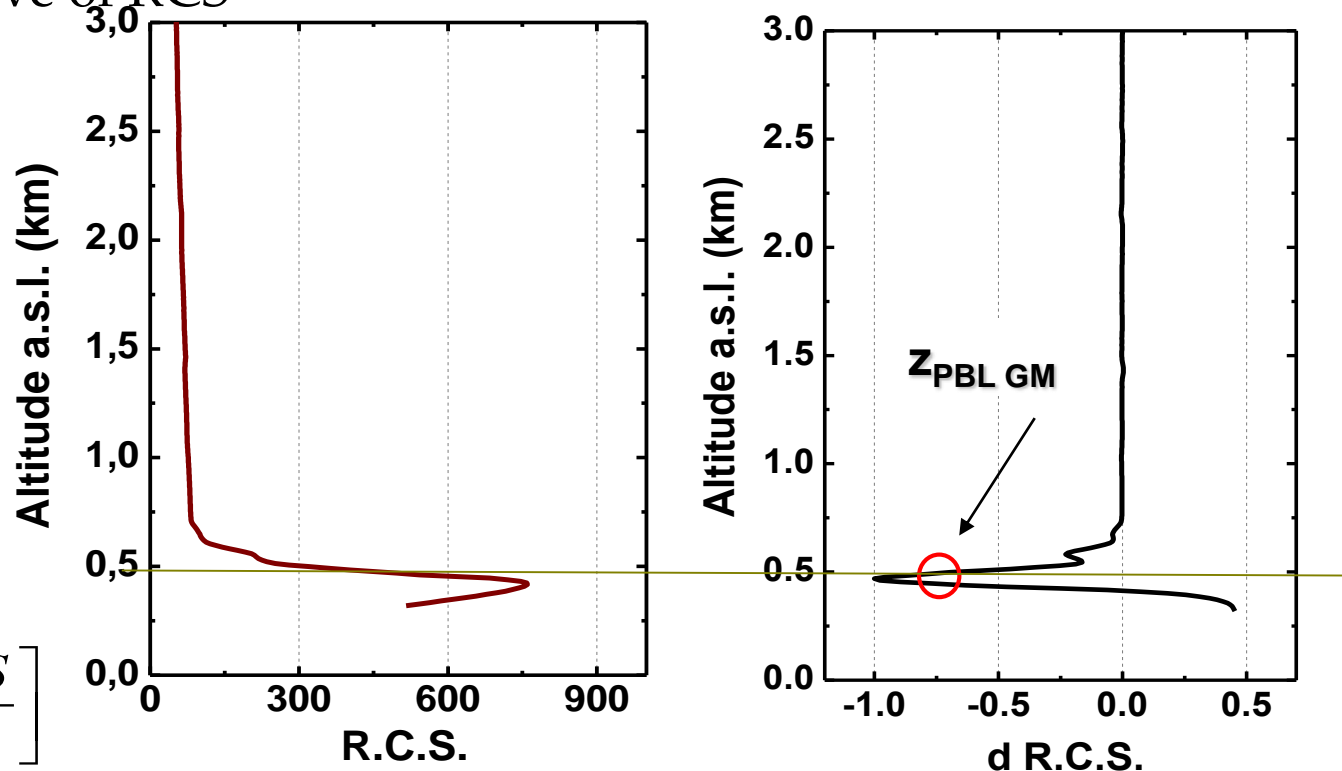
$$R.C.S.(z, \lambda) \propto \beta(z, \lambda) \cdot T(z, \lambda)^2$$

SOME METHODS TO DETERMINE THE PLANETARY BOUNDARY LAYER HEIGHT

- **Active remote sensing (lidar):**

- *Gradient method (GM):*

based on the sharp change of the RCS derivative at the transition between the $M_{ed}L$ or ($M_{ing}L$) and the free troposphere. This method attributes the PBL height ($z_{PBL GM}$) as the height with the absolute negative minimum of the first derivative of RCS



$$z_{PBL GM} = \min \left[\frac{\partial RCS}{\partial z} \right]$$

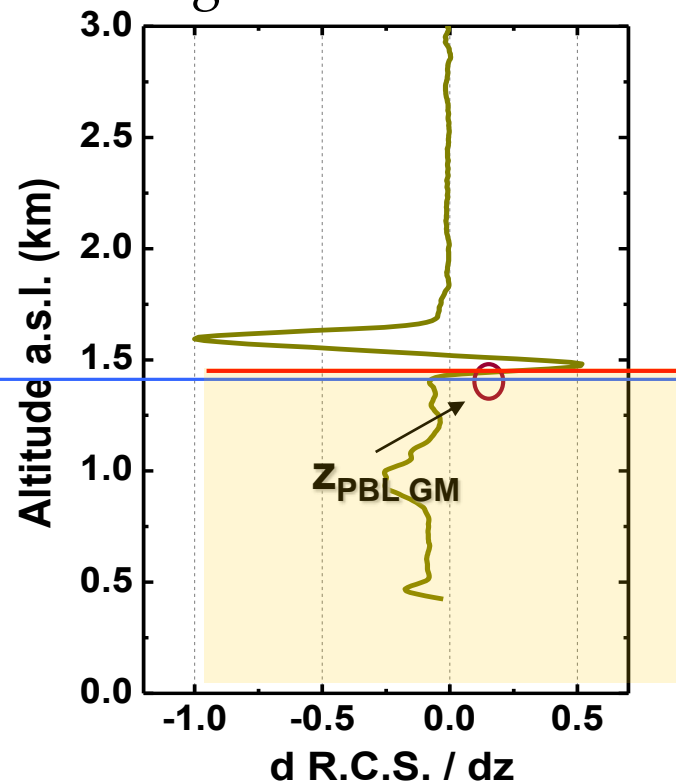
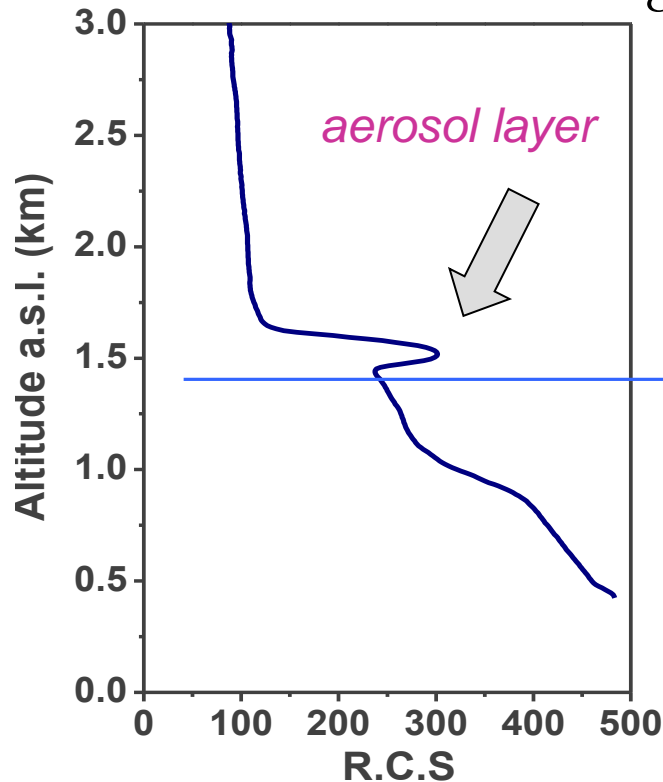
SOME METHODS TO DETERMINE THE PLANETARY BOUNDARY LAYER HEIGHT

- **Active remote sensing (lidar):**

-*Gradient method (GM) with several layers:*

several local negative minima on the first derivative of RCS

PBL height ($z_{\text{PBL GM}}$) is the height with the negative minimum located at the highest altitude inside the first region with negative derivative of RCS



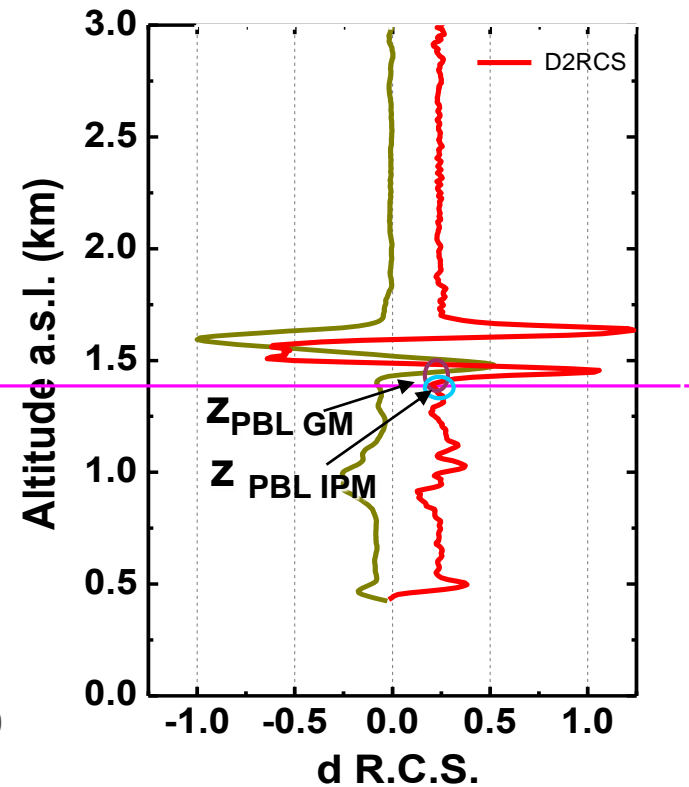
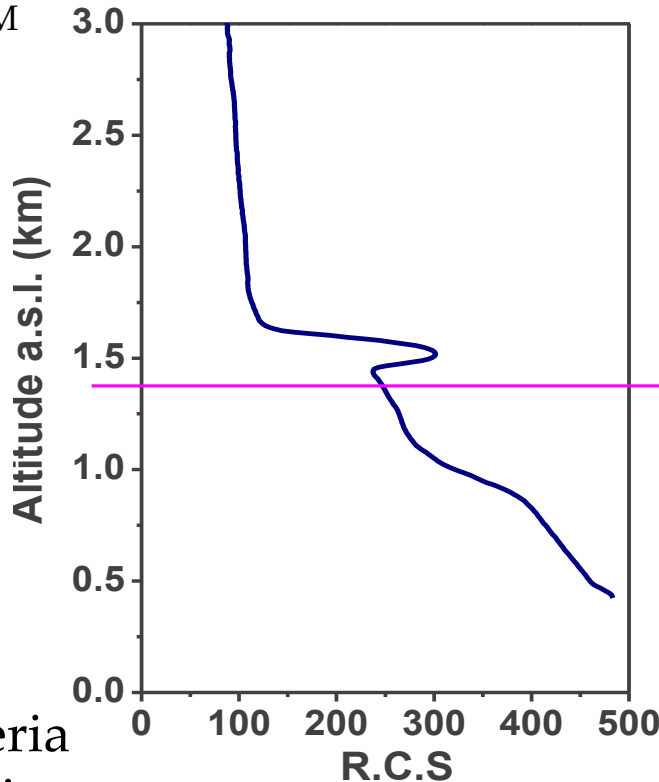
SOME METHODS TO DETERMINE THE PLANETARY BOUNDARY LAYER HEIGHT

- **Active remote sensing (lidar):**

-*Inflexion point method (IPM):*

This method attributes the PBL height ($z_{PBL\ IPM}$) as the height of the inflexion point of the first derivative of RCS. Therefore, $z_{PBL\ IPM}$ is the altitude of the local minimum of the second derivative of the RCS just below the $z_{PBL\ GM}$

$$z_{PBL\ IPM} = \min \left[\frac{\partial^2 RCS}{\partial z^2} \right]$$



The same criteria if several layers exist

SOME METHODS TO DETERMINE THE PLANETARY BOUNDARY LAYER HEIGHT

- **Active remote sensing (lidar):**

- *Logarithm gradient method (LGM):*

This method attributes the PBL height ($z_{PBL\ LGM}$) as the height with the absolute negative minimum of the first logarithmic derivative of RCS

$$z_{PBL\ LGM} = \min \left[\frac{\partial \ln(RCS)}{\partial z} \right]$$

- *Logarithm gradient method (LGM) with several layers:*

several local negative minima on the first logarithmic derivative of RCS

PBL height ($z_{PBL\ LGM}$) is the height with the negative minimum located at the highest altitude inside the first region with negative logarithmic derivative of RCS



SOME METHODS TO DETERMINE THE PLANETARY BOUNDARY LAYER HEIGHT

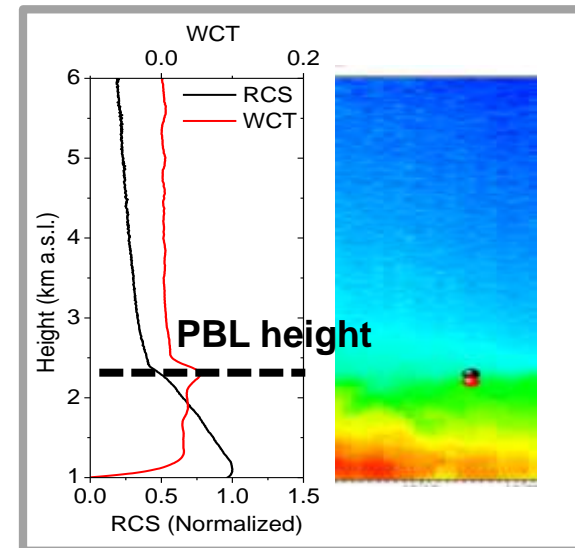
Assumption: aerosol particles are much more abundant within the PBL than in the Free Troposphere (FT)

Wavelet Covariance Transform (WCT) has the advantage of being less affected by noise than any other method and it can be easily automated

$$W_f(a, b) = \frac{1}{a} \int_{z_b}^{z_t} RCS(z) h\left(\frac{z-b}{a}\right) dz$$

with the Haar function:

$$h\left(\frac{z-b}{a}\right) = \begin{cases} +1, & b - \frac{a}{2} \leq z \leq b \\ -1, & b \leq z \leq b + \frac{a}{2} \\ 0, & \text{elsewhere} \end{cases}$$



SOME METHODS TO DETERMINE THE PLANETARY BOUNDARY LAYER HEIGHT

Optimization of the WCT-based algorithm for PBL height detection

- Selecting an appropriate dilation parameter (a) is critical
- To distinguish among strong and weak gradients Baars *et al.* (2008) proposed introducing a threshold value for the W_f profile

These parameters were optimized by comparison with radiosondes (Richardson method and parcel method) and microwave radiometer (parcel method)

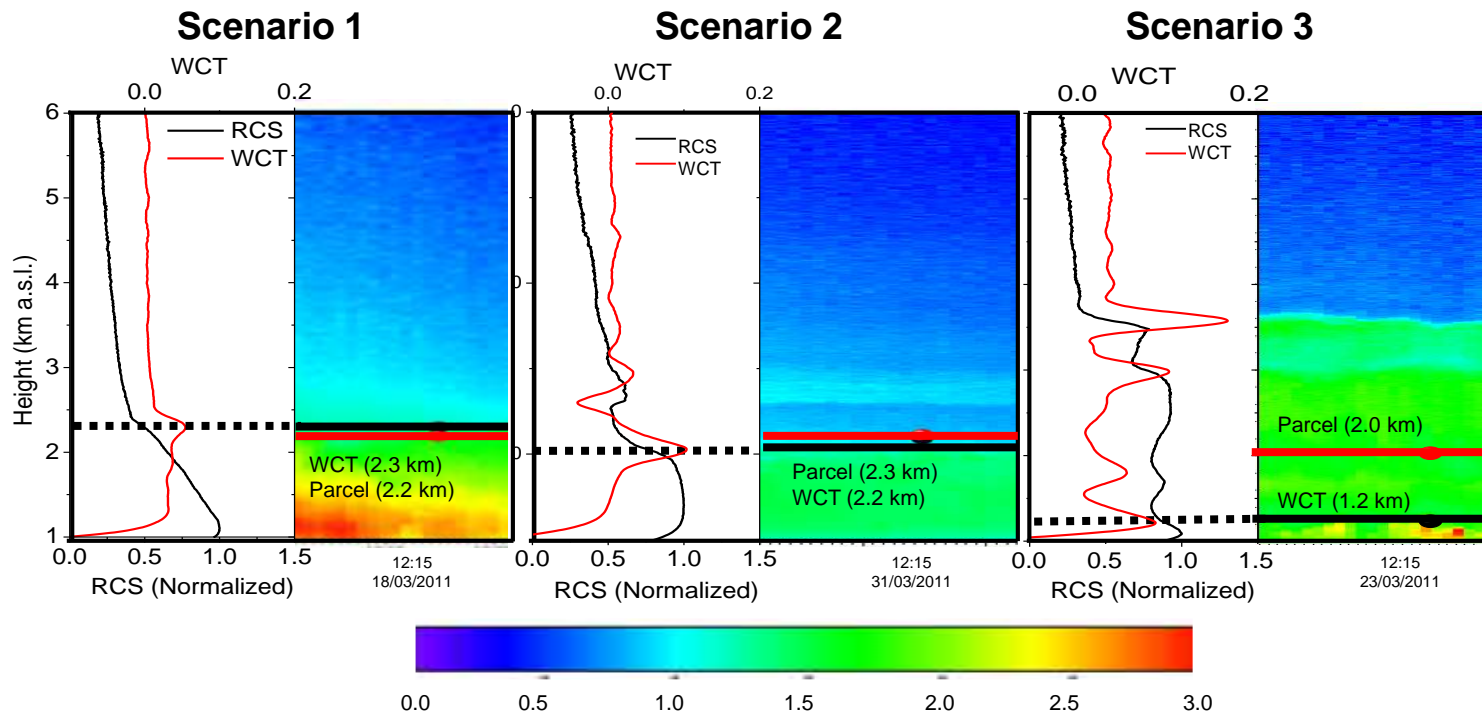
Optimum values

$a = 300 \text{ m}$
WCT-threshold value = 0.05



SOME METHODS TO DETERMINE THE PLANETARY BOUNDARY LAYER HEIGHT

From 3-month comparison between lidar and MWR, 3 scenarios are clearly identified [Granados-Muñoz et al., 2012]:



aerosol well-mixed
PBL without
stratification

aerosol decoupled
from the PBL with a
well-mixed PBL

PBL presents
stratification

PBL height detection ✓

Fail to detect
the PBL height ✗



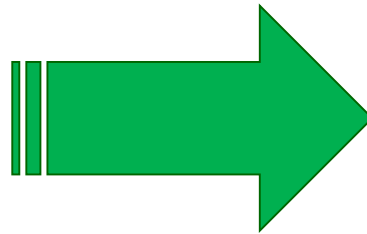
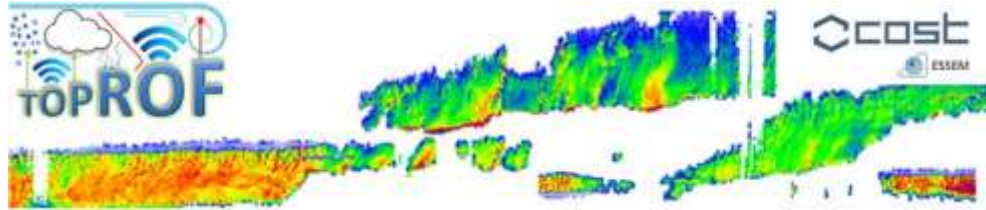
SOME METHODS TO DETERMINE THE PLANETARY BOUNDARY LAYER HEIGHT

Radiosoundings:

- low launch frequency
- spot-like detection

MWRs:

- continuously monitoring
- low vertical resolution (10-200 m < 3 km agl)



**Hybrid method
ALCs + MWRs**

Automatic Lidars/ceilometers (ALCs):

- better resolution (typically <15 m)
- ambiguous layer attribution
- STRAT software (STRucture of ATmosphere)

[Morille et al., 2007; Haeffelin et al., 2012]

SOME METHODS TO DETERMINE THE PLANETARY BOUNDARY LAYER HEIGHT

Hybrid method ALCs + MWRs:

➤ 1. *STRAT candidates (ALC):*

All candidates obtained from STRAT (applied to ceilometer data) are potentially considered as boundaries of some sub-layers

➤ 2. *Atmospheric stability (MWR):*

Established in terms of potential temp. (θ)

$$\frac{\partial \theta}{\partial z} > 0$$

stable

$$\frac{\partial \theta}{\partial z} = 0$$

neutral

$$\frac{\partial \theta}{\partial z} < 0$$

unstable

➤ 3. *Layer attribution:*

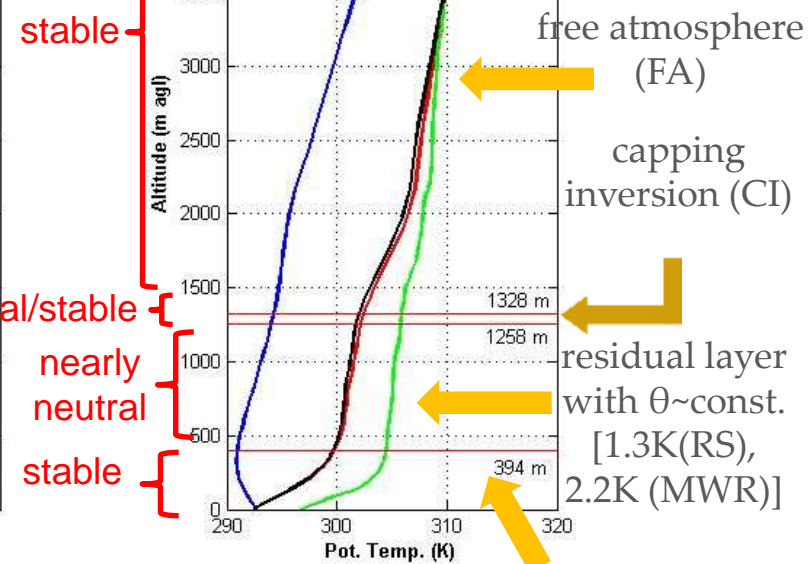
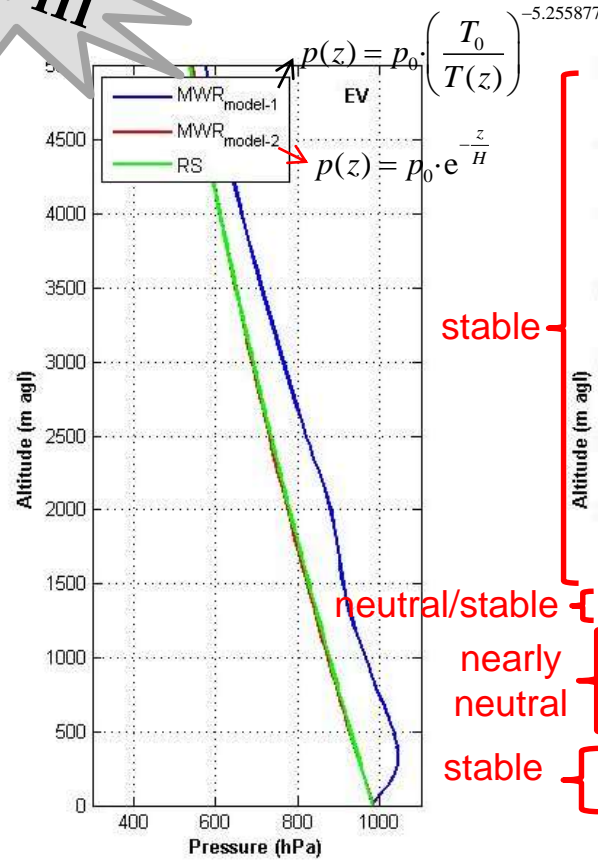
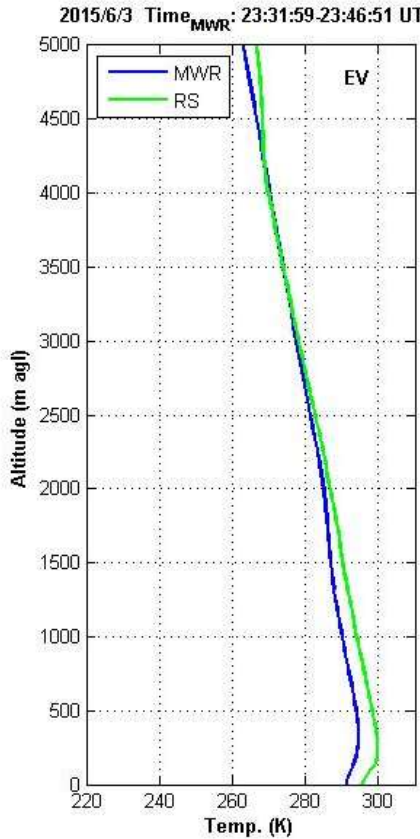
STRAT candidates (ceilometer) are attributed considering the atmospheric stability (assessed by MWR) compared to the expected theoretical value



SOME METHODS TO DETERMINE THE PLANETARY BOUNDARY LAYER HEIGHT

Scenario III

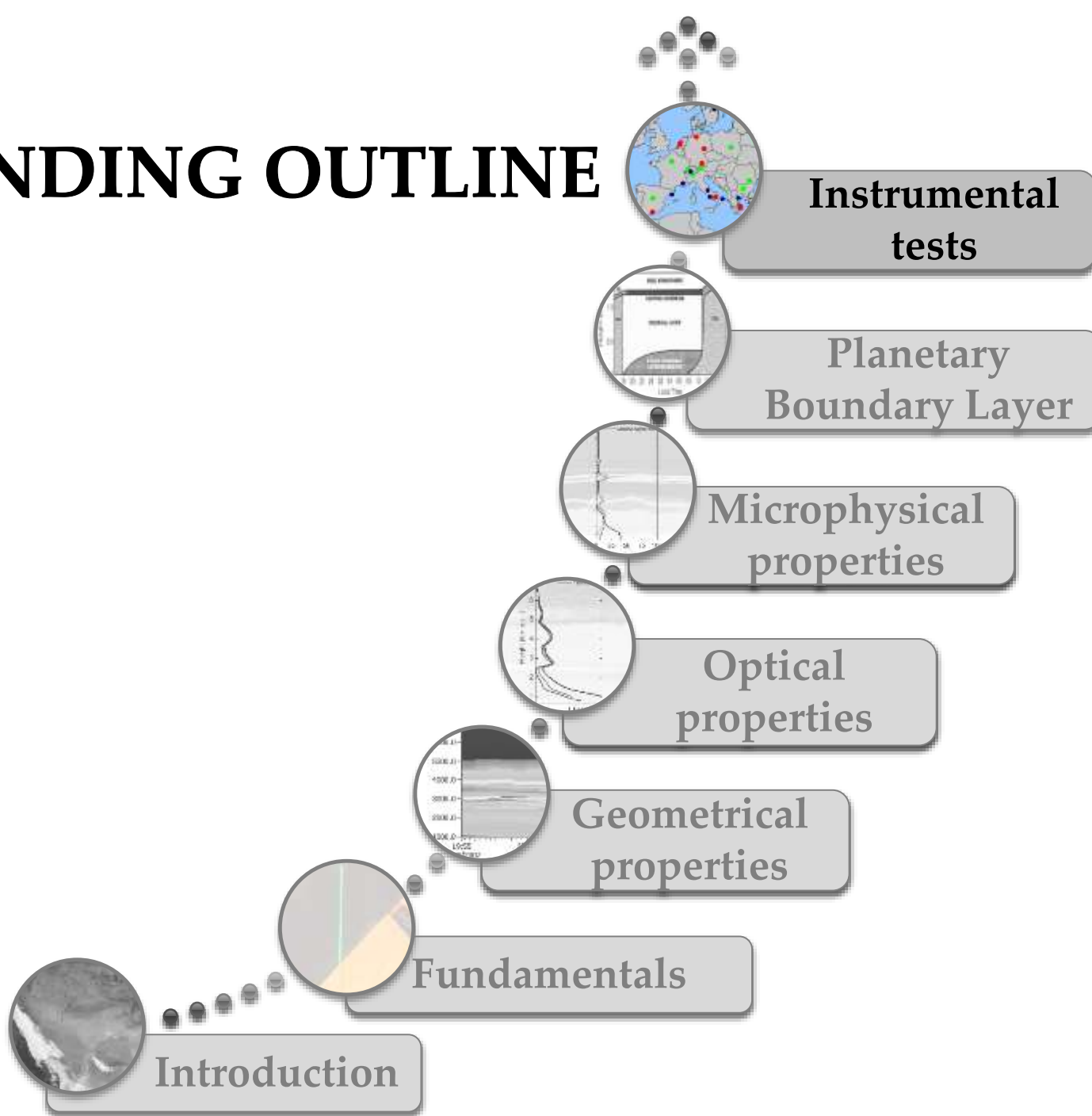
Red horizontal lines: candidates obtained from STRAT (ceilometer data)



The hybrid method alone resolves PBL layering, clearly identifying the SBL, RL, CI and FA

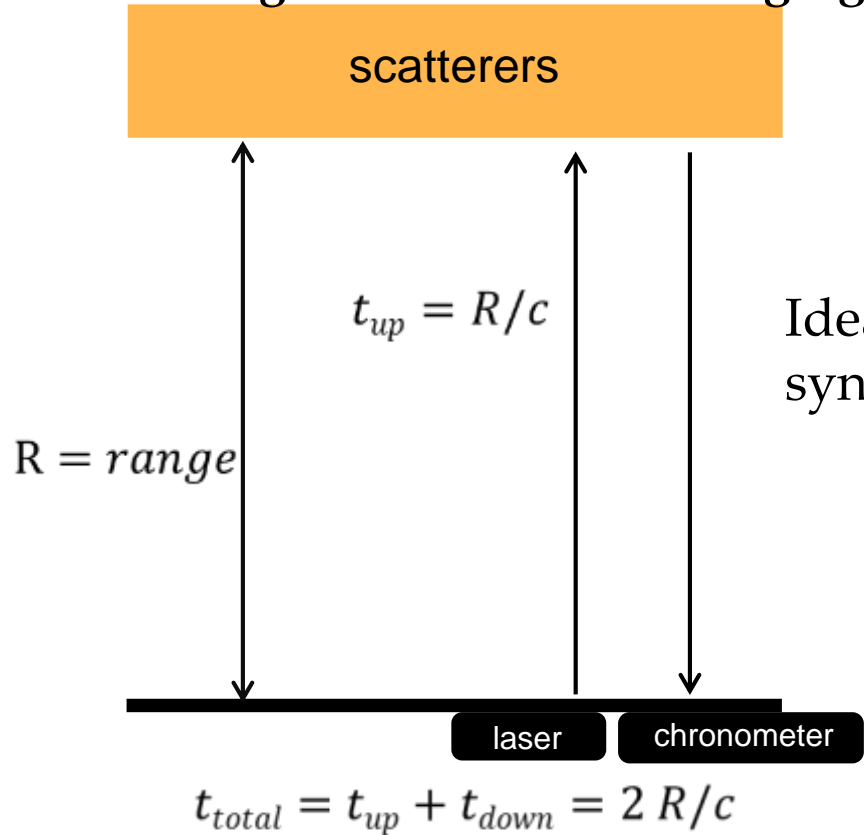


ASCENDING OUTLINE



TEST #1: ZERO-BIN AND BIN-SHIFT

Lidar (*light detection and ranging*) ... but ranging based on timing



Ideally laser and chronometer are synchronized

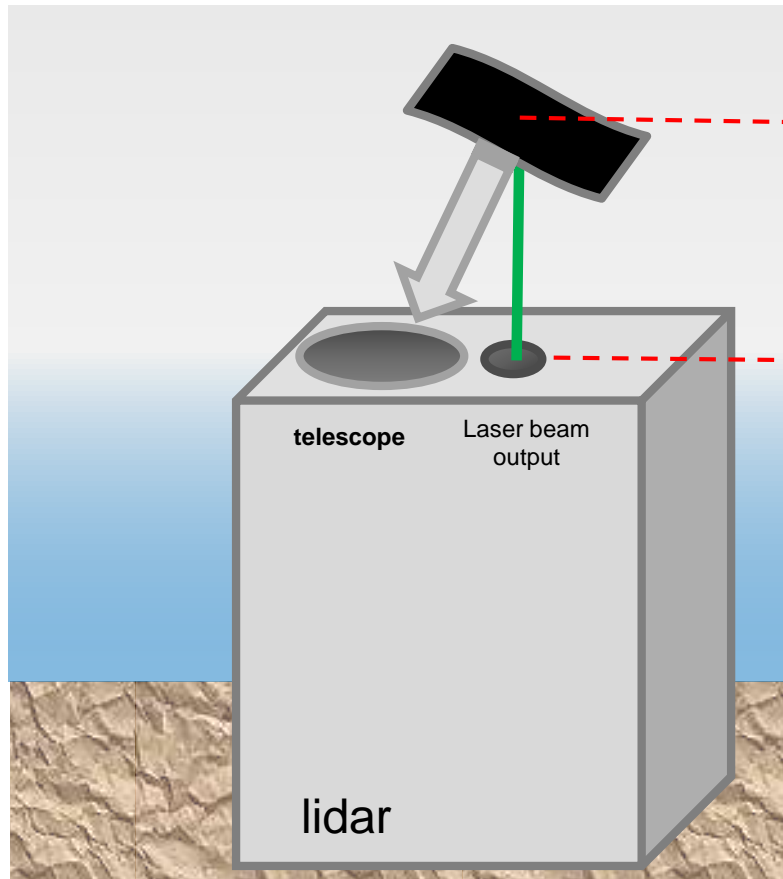
In practise... not



wrong range determination!!!

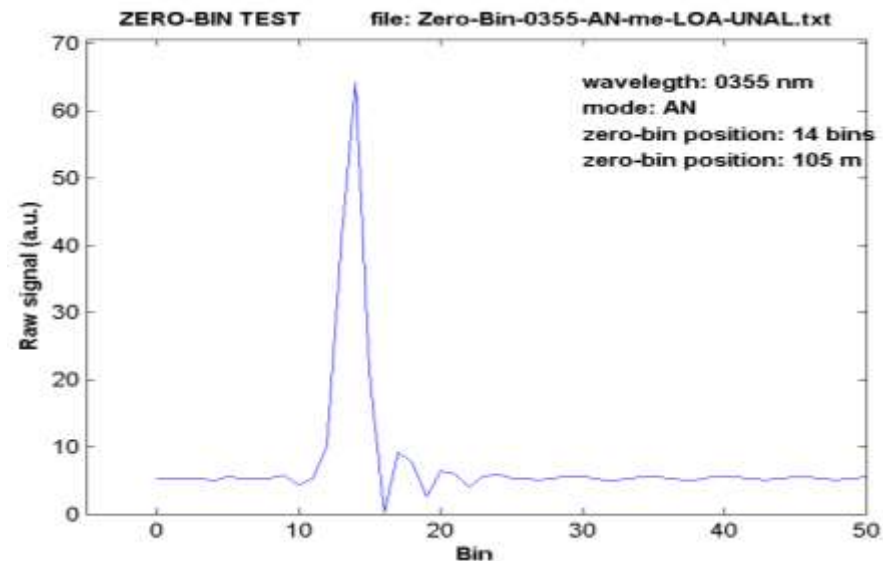
TEST #1: ZERO-BIN AND BIN-SHIFT

Zero-bin test: a target is placed at the output of the laser window in order to produce strong backscattered radiation. Thus, the first intense peak observed by the detector system should correspond to the zero position of our measurements



$$R < \Delta z$$

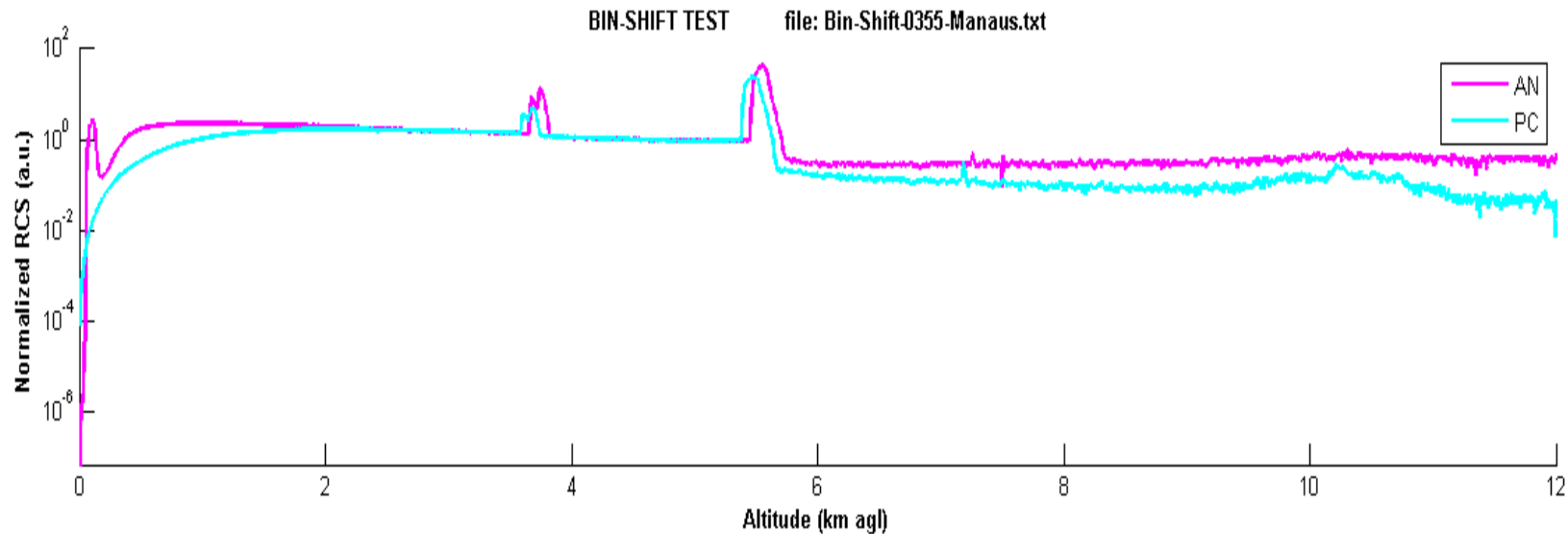
Our target is placed at zero-bin, however...



TEST #1: ZERO-BIN AND BIN-SHIFT

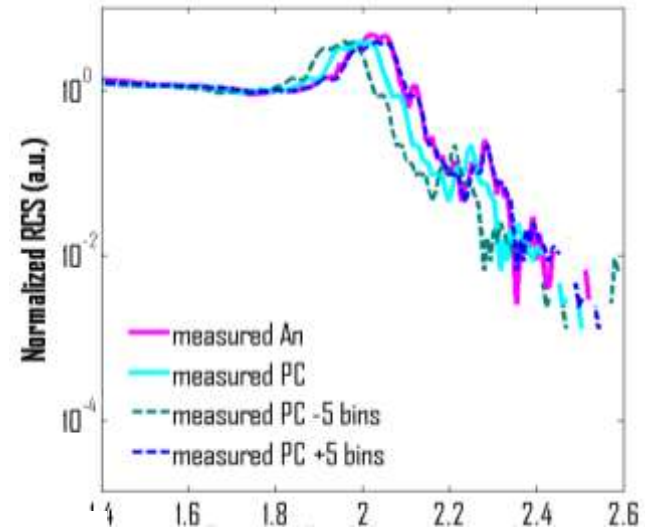
This test was only carried out for AN signals, since the saturation suffered in PC mode at close height range could lead to wrong results

For measuring a possible delay between AN and PC signals (bin-shift), target as clouds or aerosol layers are used

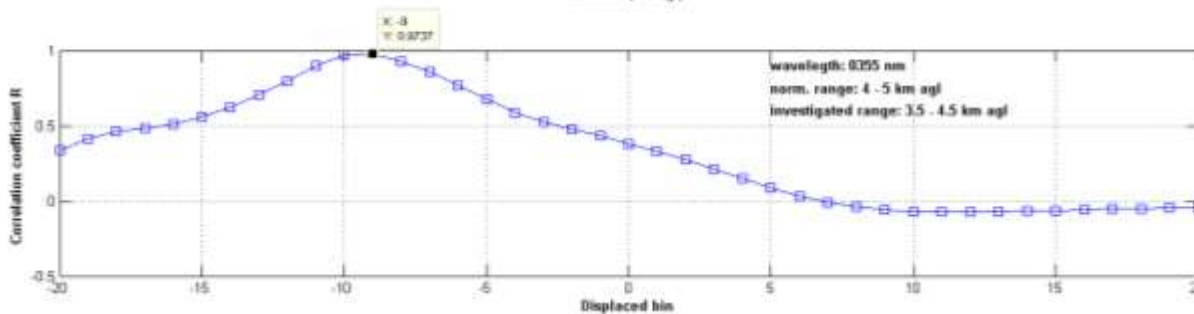
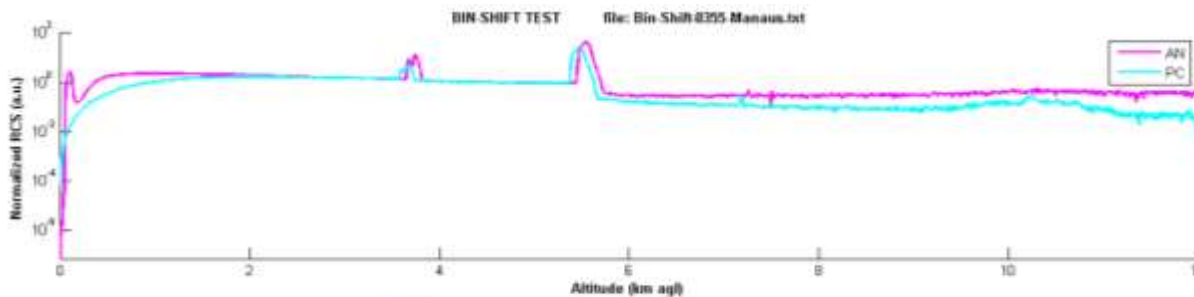


TEST #1: ZERO-BIN AND BIN-SHIFT

Bin-shift is determined by the best linear fit between AN and PC signals fixing the AN signal and displacing the PC signal from -20 to +20 bins



In this case,
Bin-shift = - 9bins



$$bin_0^{PC} = bin_0^{AN} + \Delta bin_{AN-PC}$$



TEST #1: ZERO-BIN AND BIN-SHIFT

Example of results for system sp-CLA-IPEN-MSP-LIDAR-I (São Paulo)

$$bin_0^{PC} = bin_0^{AN} + \Delta bin_{AN-PC}$$

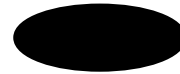
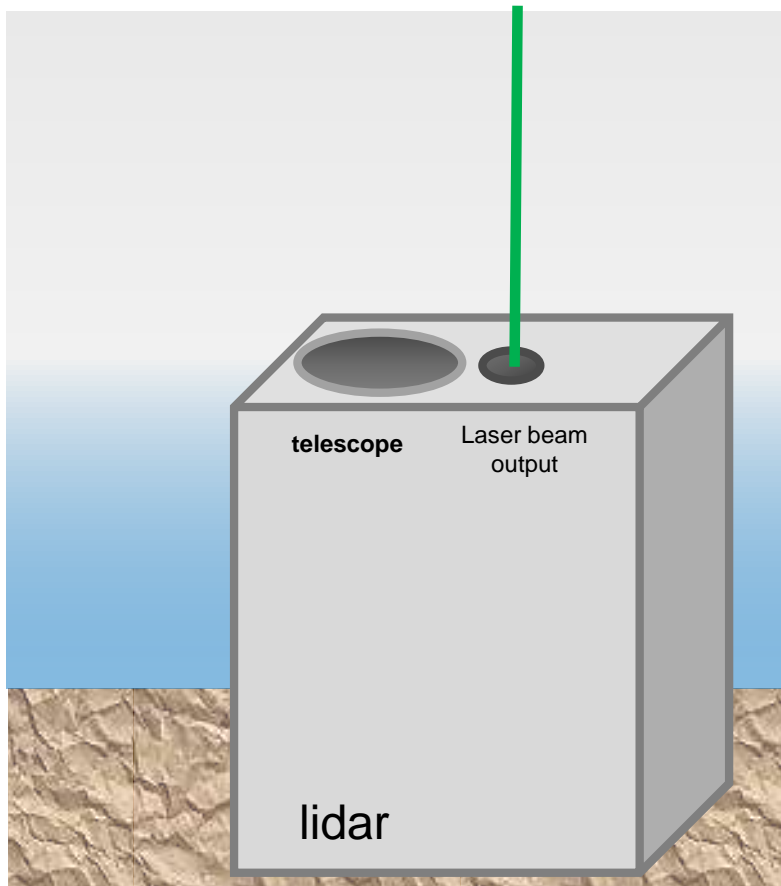
Channel (nm)	Zero-bin AN (bins)	Bin-shift (bins)	Zero-bin PC (bins)
355	8	-10	-2
387	8	-10	-2
408	8	-10	-2
532	1	-2	-1
607	6	-9	-3
660	7	-9	-2

To properly use the lidar signals, the some bins of the AN signals must be removed and several blank bins must be introduced in the PC signals following this table



TEST #2: DARK CURRENT

Dark current (DC) is the response exhibited by a receptor of radiation even during periods when it is not actively illuminated

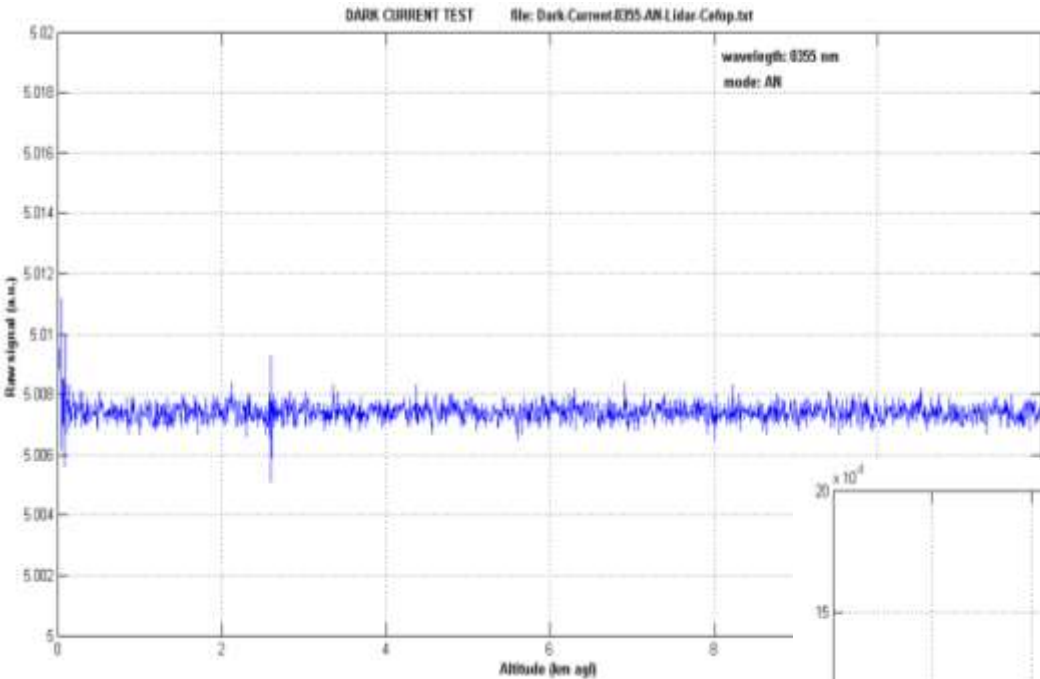


-measurement taken by covering totally the telescope or detectors performed with enough averaging time (~10 min)

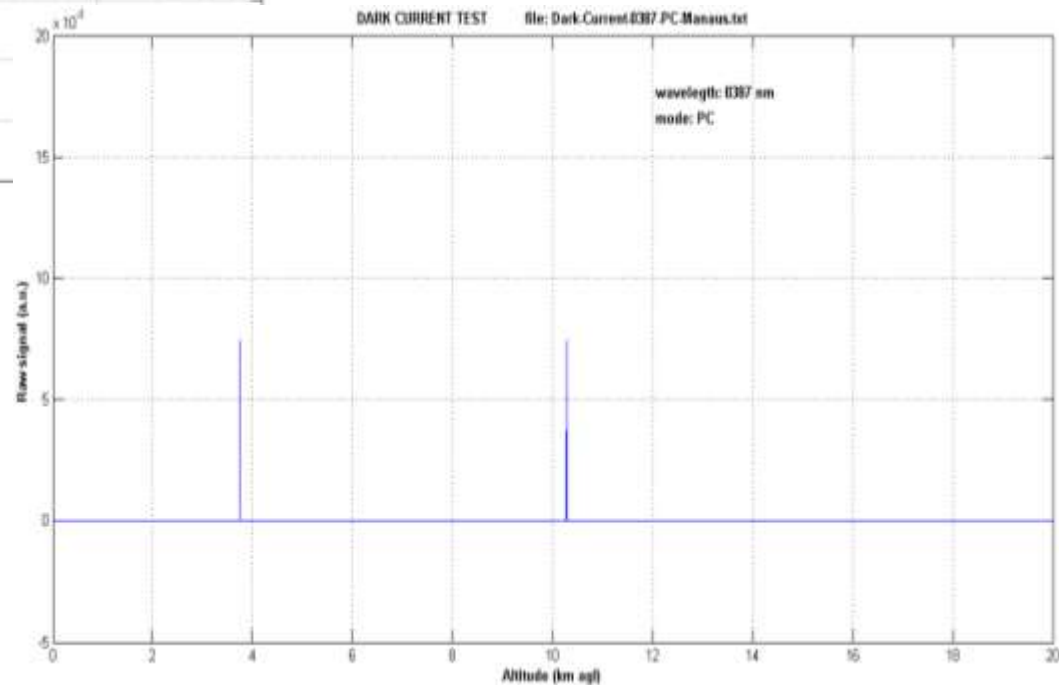
-all parameters (voltages, pulse repetition frequency ...) are configured as a usual measurement

TEST #2: DARK CURRENT

Example of results for systems co_CEFOP-UDEC (Medellín) and ma-MA (Manaus)



Important to know during preprocessing step

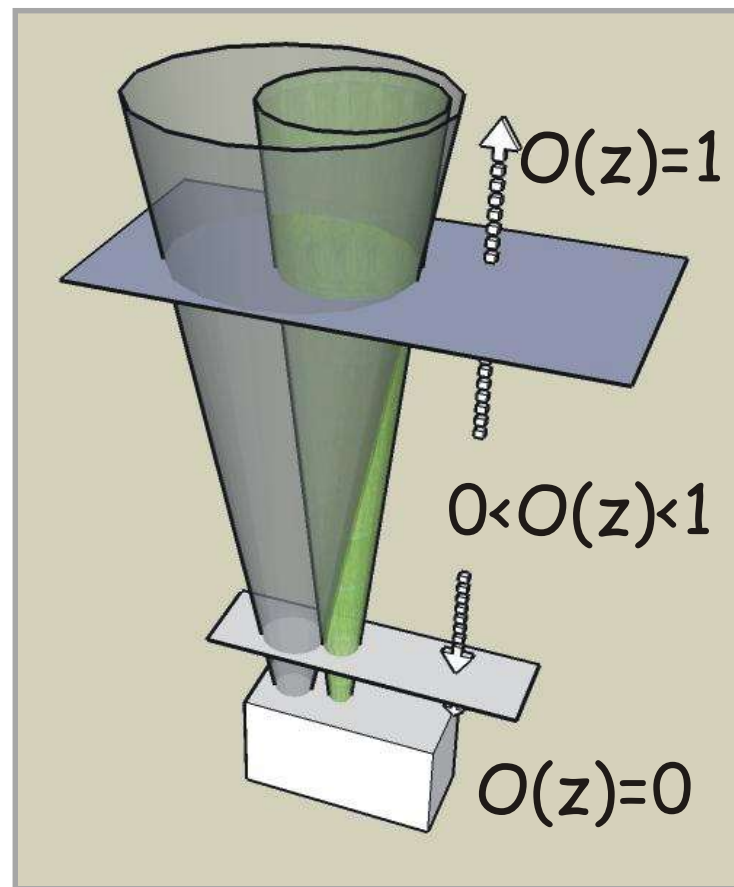


TEST #3: TELECOVER TEST

Overlap function $O(R)$:
geometrical overlap between laser
beam and telescope field of view

$O(R)$ accounts for the partial
overlap in the near height-range
and tends to stabilize (ideally to 1)
in the far height-range

$O(R)$ depends, among other factors,
on the alignment

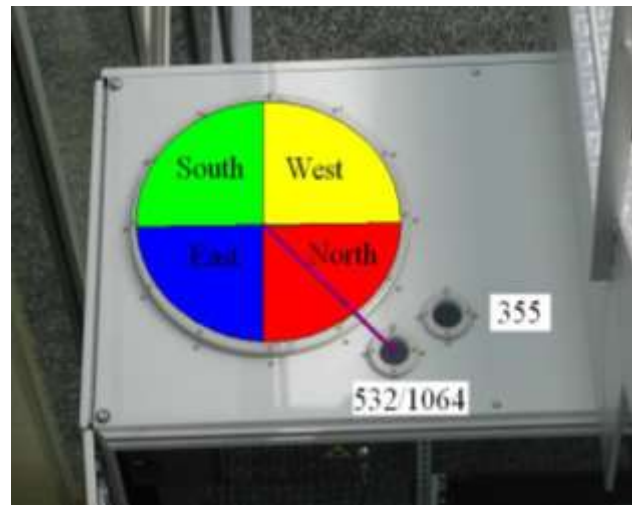
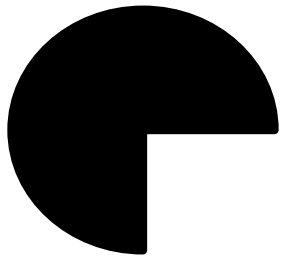


Guerrero-Rascado et al., OPA, 2011

TEST #3: TELECOVER TEST (QUADRANTS)

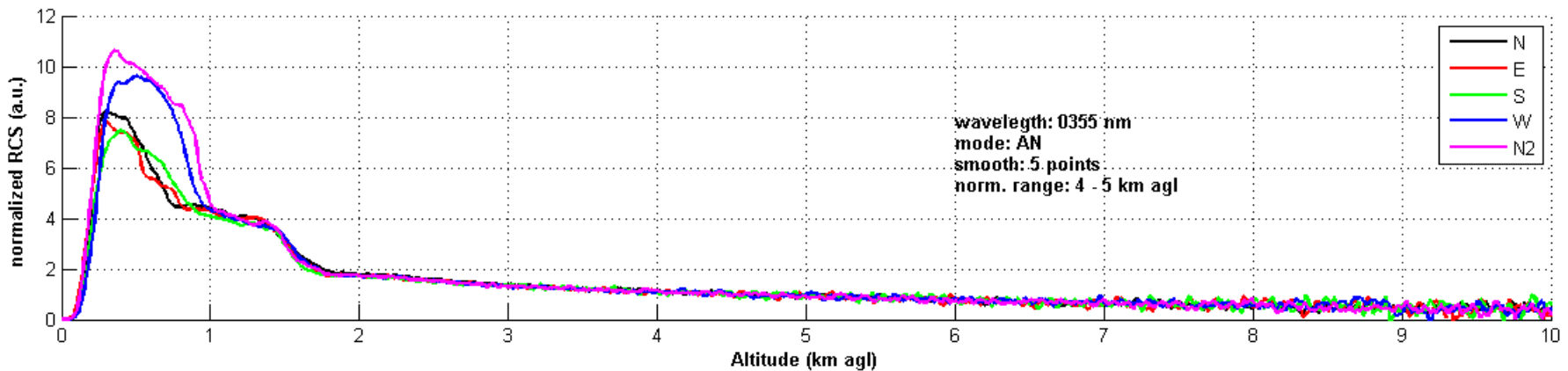
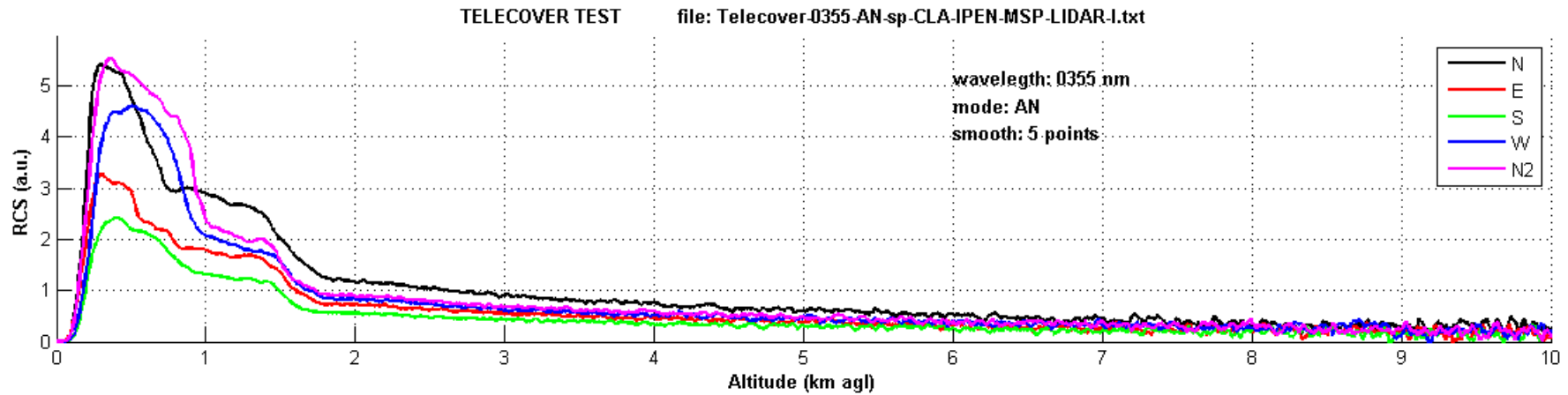
Telecover test (quadrants):

- based on the comparison of signals measured using different quadrants of the telescope
- named as N, E, S and W, where N is the quadrant nearest to the laser beam axis and the others named following the clockwise sense
- N measurement is performed at the end of the telecover test (N2) to check the atmospheric stability
- Measurements ~2 min



TEST #3: TELECOVER TEST (QUADRANTS)

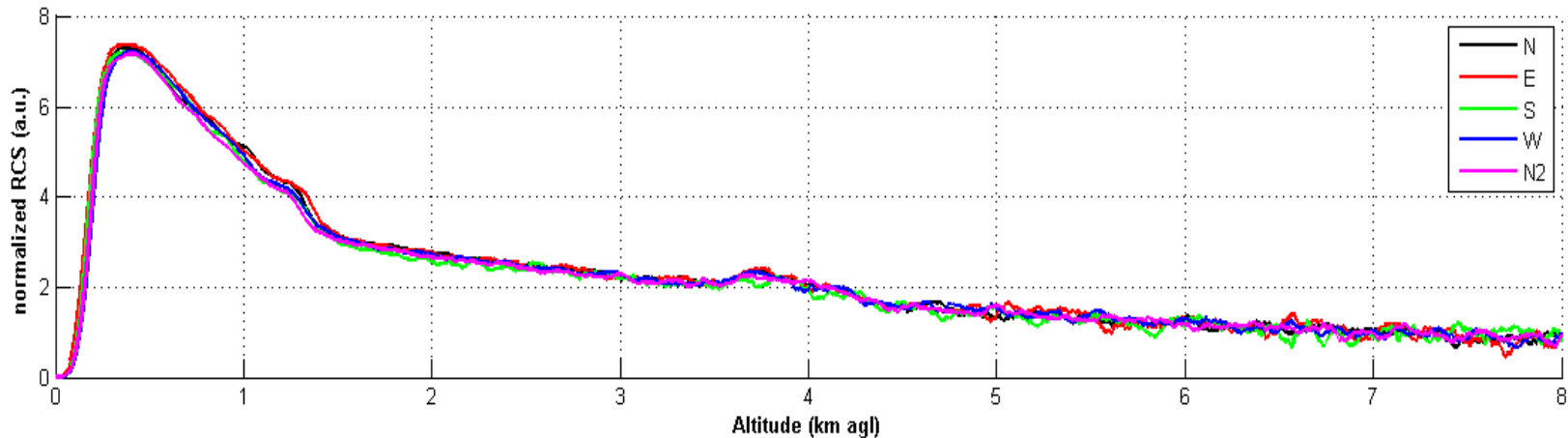
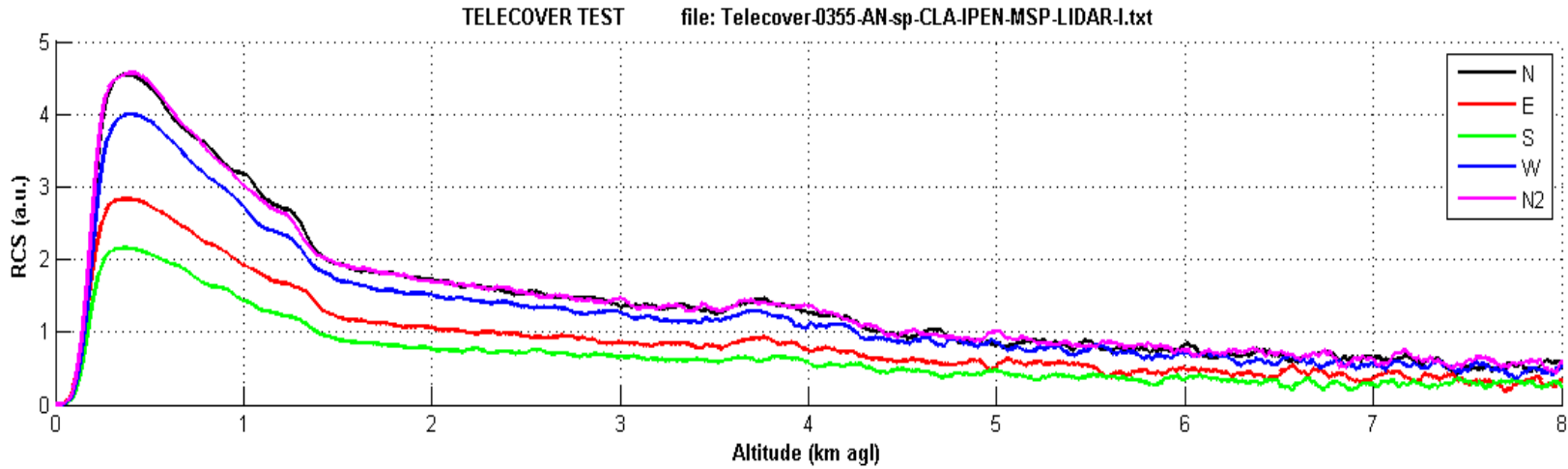
Atmospheric variability: Bad telecover!!!



TEST #3: TELECOVER TEST (QUADRANTS)

Biaxial systems: $N=N2 < E = W < S$

Coaxial systems: $N=N2 = E = W = S$



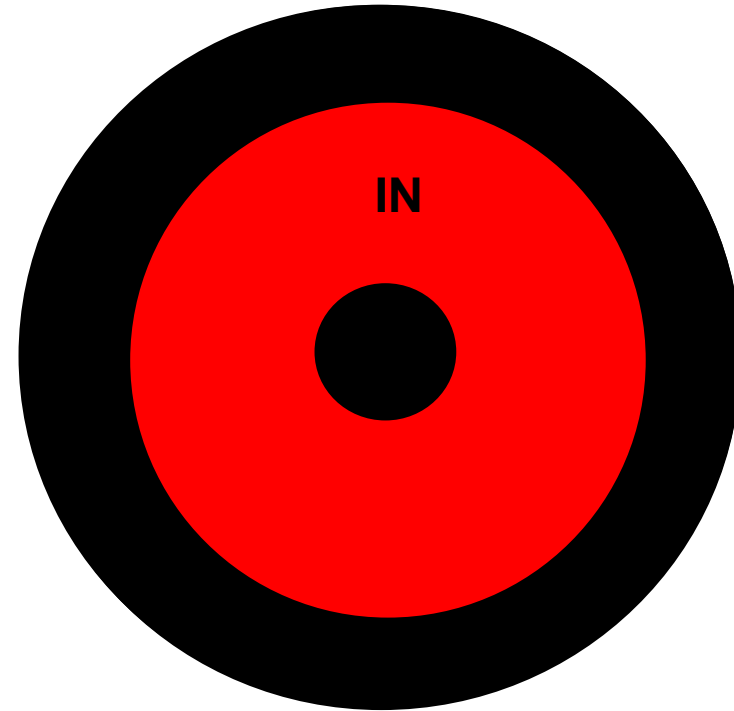
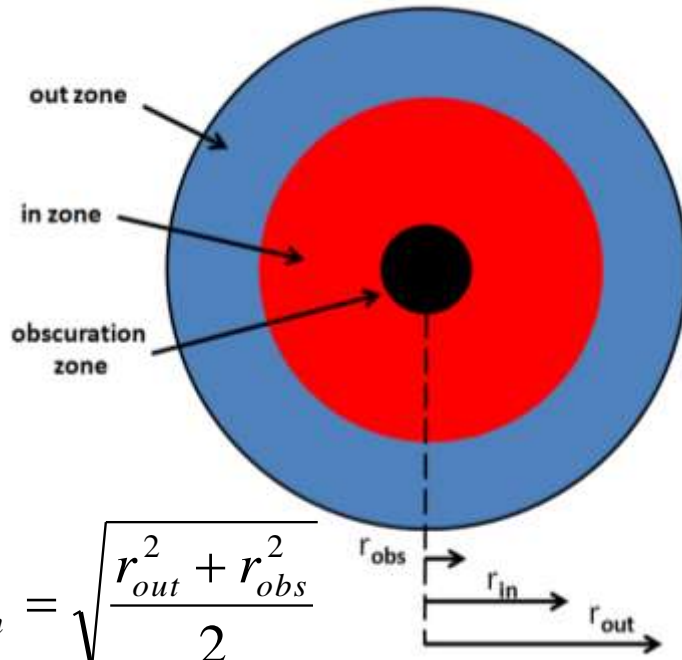
TEST #3: TELECOVER TEST (IN-OUT)

Telecover test (in-out):

-based on the comparison of signals measured using different rings of the telescope, named as IN and OUT

-IN measurement is performed at the end of the telecover test (IN2) to check the atmospheric stability

-Measurements ~2 min

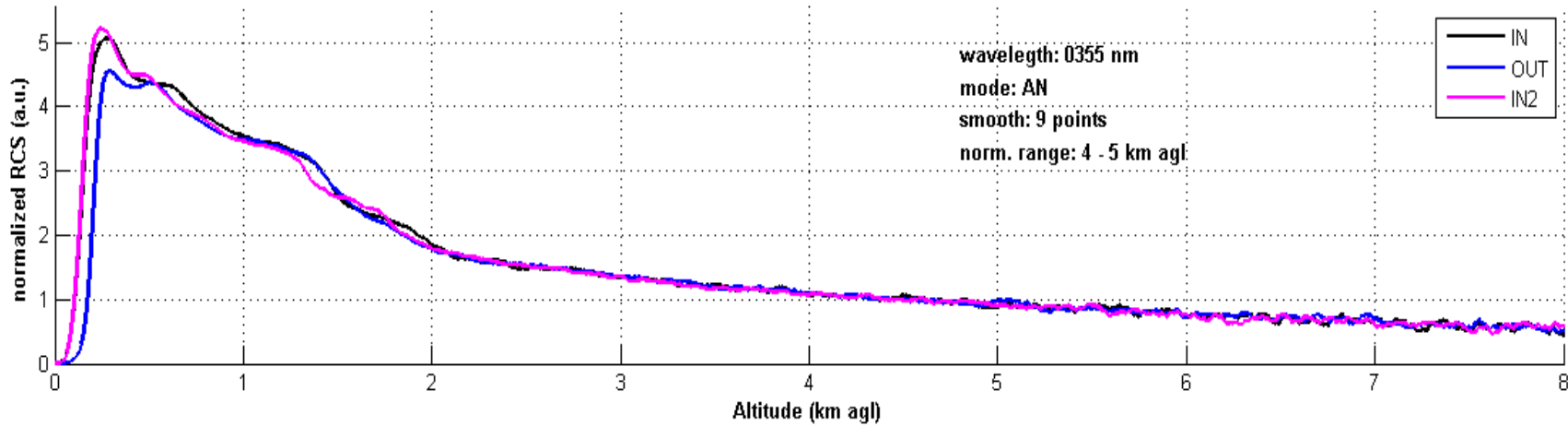
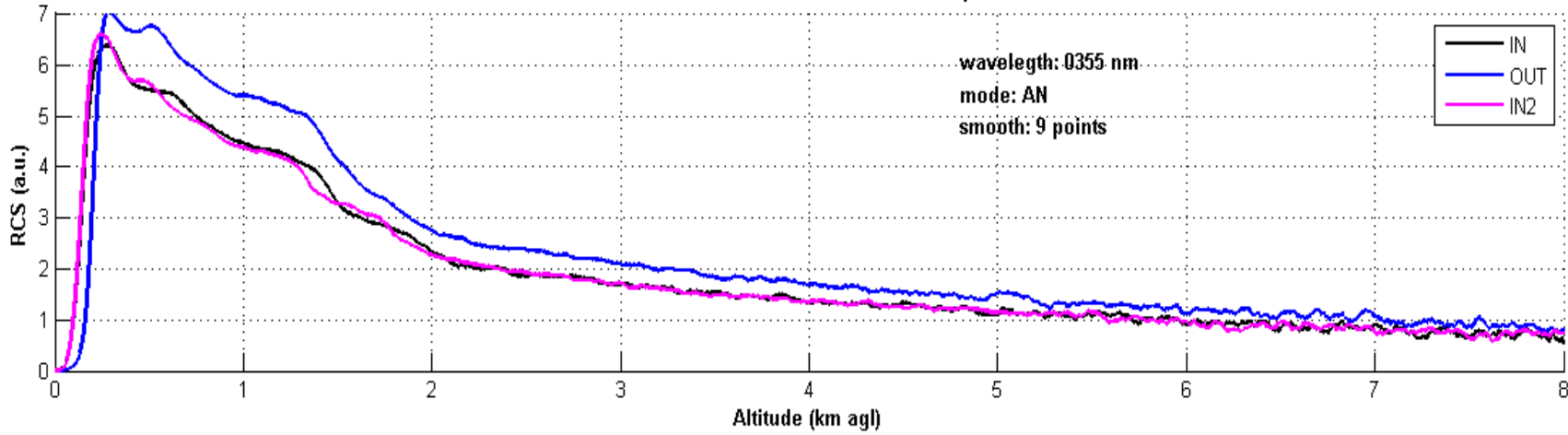


$$r_{in} = \sqrt{\frac{r_{out}^2 + r_{obs}^2}{2}}$$

TEST #3: TELECOVER TEST (IN-OUT)

Coaxial systems: $IN=IN2 < OUT$

TELECOVER TEST IN-OUT file: Telecover-in-out-0355-AN-sp-CLA-IPEN-MSP-LIDAR.I.txt



TEST #4: RAYLEIGH FIT

The Rayleigh (or molecular) fit is a tool to analyze the quality of far range lidar signal:

-the range corrected signal measured by the lidar system is compared to the expected molecular range corrected signal

$$R.C.S._{mol}(z) = \beta_{mol}(z) \cdot \exp \left\{ -2 \int_0^z \alpha_{mol}(\xi) d\xi \right\} \equiv \beta_{mol}^{att}(z)$$

$$R.C.S.(z) = K \cdot \beta(z) \cdot \exp \left\{ -2 \int_0^z \alpha(\xi) d\xi \right\} \propto \beta^{att}(z)$$

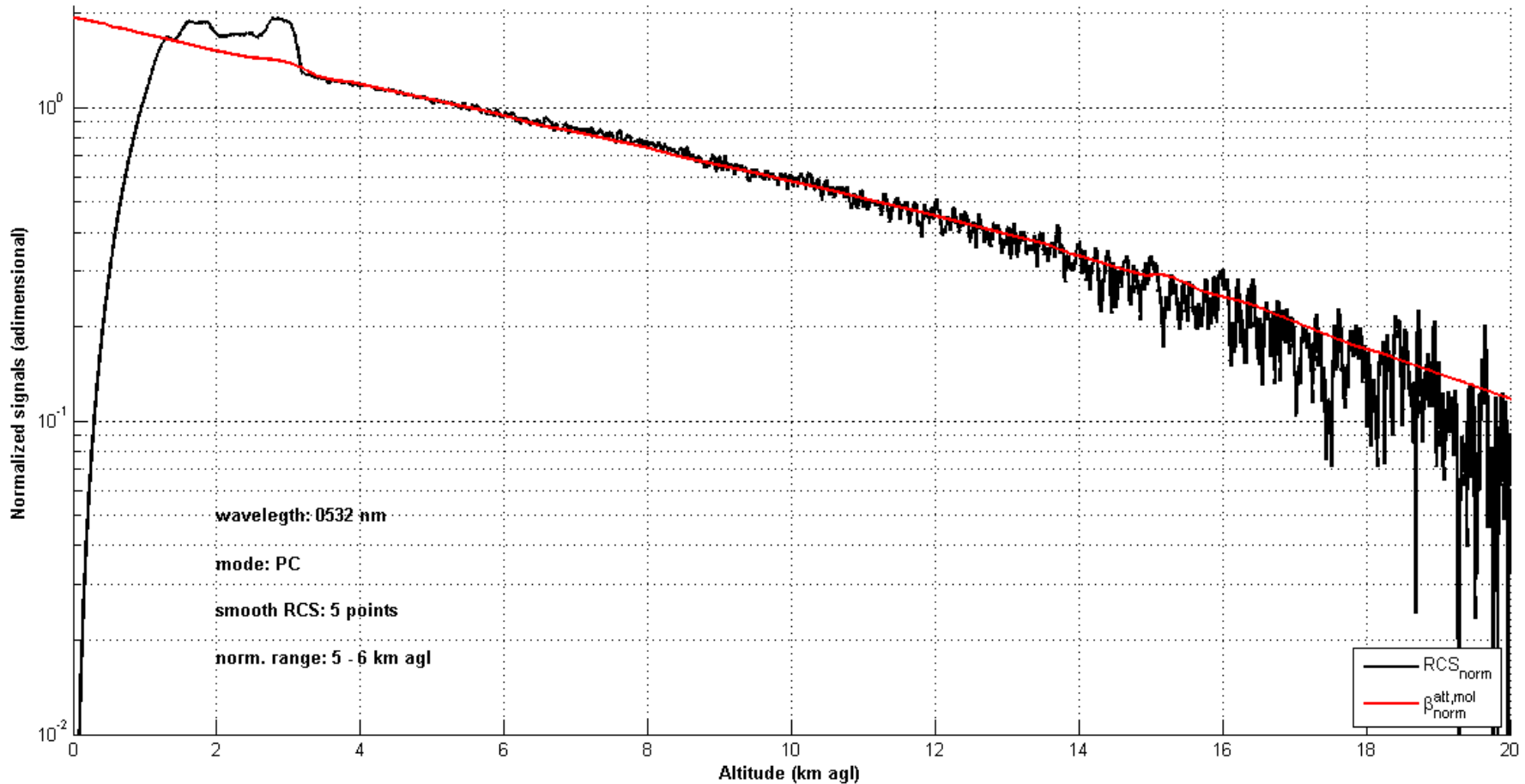
-measurement ~30 min



TEST #4: RAYLEIGH FIT

RAYLEIGH FIT

file: Rayleigh-0532-PC-sp-CLA-IPEN-MSP-LIDAR-I.txt



Similar trend above 3 km agl up to 15 km agl (approx.)
This height range can be used as z_{ref} for Klett-Fernald and Raman methods





*European Aerosol
Research Lidar
Network*



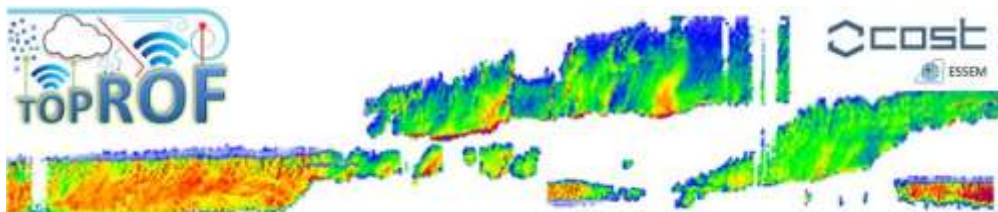
*Spanish and
Portuguese Aerosol
Lidar Network*



*Aerosols, Clouds, and Trace
gases Research InfraStructure Network*



*Latin American
Lidar Network*



*Towards operational ground based
profiling with ceilometers, Doppler
lidars and microwave radiometers
for improving weather forecasts
(COST ACTION ToProf ES1303)*



SHORT SUMMER SCHOOL ON
ATMOSPHERIC PHYSICS

Évora
4th July 2016



Barcelona

Granada

Potenza

Madrid

Évora

Courtesy of J.A. Bravo -Aranda